Synthesis of Fc peptides and glycopeptides to be used as internal standards for absolute quantitation of glycoforms of two human IgG subclasses by MALDI-MS analysis

by

Rini Roy

A Thesis submitted to the Faculty of Graduate Studies of the

University of Manitoba

In partial fulfilment of the requirements for the degree of

Master of Science

Department of Chemistry

Abstract

Immunoglobulins (IgGs) play a central role in the immune system of living organisms. Human IgG comprises of 4 subclasses, ranging from IgG1 to IgG4, of which IgG1 and IgG2 are the most abundant in healthy individuals. Every IgG subclass has a different amino acid sequence in the Fc (Fragment crystallizable) region, which can influence the biological character of the antibodies. In an effort to develop an absolute MALDI-ToF-MS (Matrix Assisted Laser Desorption Ionization) quantitation method for these subclasses and their Fc *N*-glycoforms, peptides and (glyco)peptides were synthesized using a solid phase approach and used as internal standards for enriched fractions from human IgG tryptic digests. Mass spectrometry (MS), which is a powerful analytical tool capable to analyze the biomolecules quantitatively was used throughout the experiment. Tryptic digest glycopeptides from monoclonal IgG1 and IgG2 samples were first quantified using EEQYN(GlcNAc)STYR and EEQFN(GlcNAc)STFR, respectively. For IgG1, a similar glycopeptide where tyrosine (Y) was isotopically labelled was used to quantify monoclonal IgG1 that had been treated with the enzyme Endo-F2, i.e. yielding tryptic glycopeptide EEQYN(GlcNAc)STYR. The next step was to quantify single subclasses within polyclonal human IgG samples, without knowing if the presence of other subclass peptides would cause interference or not. Although the ion abundances in MALDI (Matrix Assisted Laser Desorption Ionization) spectra often showed higher signals for IgG2 than IgG1 depending on the spotting solvent used, the newly developed method allowed to calculate relative concentrations where IgG species were predominant. It was observed that simultaneous quantitation of IgG1 and IgG2 yielded non-quantitative results, and more success was obtained when subclasses were quantified one by one. The study also explored the relative sensitivities of the two synthetic Fc tryptic peptides of IgG1 and IgG2 under MALDI conditions. More experiments would serve to access the ionization efficiencies of EEQYNSTYR/EEQFNSTFR, EEQYN(GlcNAc)STYR and EEQFN(GlcNAc)STFR mixtures under different solvent and concentration conditions.

Acknowledgements

I would first like to thank my advisor Hélène Perreault of the Department of Chemistry at the University of Manitoba, Canada for providing me this wonderful opportunity to work with her in exploring areas of mass spectrometry and analytical research techniques. Dr Perreault had consistently and patiently guided me throughout my research work with invaluable knowledge and steered me in the right direction.

I would like to specially acknowledge my committee experts, Frank Schweizer and Silvia Cardona for their precious feedback during the research progress meetings. Without their passionate participation and input, this work could not have been successfully conducted.

I would like to thank the members of my laboratory, Emy, Evelyn and Claudia for providing me unfailing support as well as my friend Ron for his conversation and suggestions.

Finally, I must express my profound gratitude to my parents and to my husband Banibrata Roy and my son Rayan Roy for providing me continuous encouragement throughout my years of study and through the process of writing this thesis. This accomplishment would not have been possible without them.

Table of Contents

Abbreviations

ACN	Acetonitrile
Boc	tert-butyloxy-carbonyl
CHCA	α-cyano-4-hydroxycinamic acid
CHO	Chinese hamster ovary cells (CHO) cells
Da	Dalton
DCM	Dichloromethane
DHB	2,5-dihydroxy benzoic acid
DMF	Dimethyl formamide
DNA	Deoxyribonucleic acid
Eg2-hFc	Chimeric heavy chain monoclonal antibody
EI	Electron impact
ESI	Electrospray ionization
ER	Endoplasmic reticulum
Endo H	Endo-β-*N*-acetylglucosaminidase
FAB-MS	First atom bombardment MS
Fab	Fragment, antigen-binding
Fc	Fragment crystallizable
Fmoc	9-Fluorenyl methyloxy carbonyl

Fuc	Fucose
Gal	Galactose
GalNAc	*N*-acetyl galactosamine
GC-MS	Gas chromatography mass spectrometry
Glc	Glucose
GlcNAc	*N*-acetylglucosamine
HPLC	High performance liquid chromatography
HCAb	Heavy chain antibodies
IgG	Immunoglobulin G
kDa	kilo Dalton
KE	Kinetic energy
L	Liter
LC	Liquid chromatography
µ	Micro; $x10^{-6}$
M	Molar
mAb	monoclonal antibody
MALDI	Matrix-assisted laser desorption ionization
Man	Mannose
Man-6-P	Mannose -6-phosphate
MeOH	methanol
MGUS	Monoclonal gammopathy of unknown significance
MRM	Magnetic resonance microscopy
mRNA	messenger ribonucleic acid
MS	Mass spectrometry

MS/MS	tandem mass spectrometry
m/z	mass to charge ratio
Nd: YAG	Neodymium-yttrium aluminium garnet
Neu5AC	*N*-Acetylneuraminic acid
OST	Oligosaccharyl transferase
PNGaseF	peptide *N*-glycosidase F
PTM	post translational modification
Q	quadrupole
QqTOF	quadrupole-quadrupole time-of-flight
RP	reverse phase
SA	3,5-dimethoxy-4-hydroxycinnamic acid; Sinapinic acid
ScFv	Single-chain fragment variable
SPPS	Solid phase peptide synthesis
TFA	trifluoracetic acid
TOF	time-of-flight
TOF/TOF	tandom time-of-flight
UV	ultraviolet
X	any amino acid
ZP3	Zona pellicida

Amino acids	1-letter code	3-letter code	Chemical formula	Monoisotopic (Da)	Average (Da)
Alanine	A	Ala	$C_3H_7NO_2$	71.03711	71.0788
Arginine	R	Arg	$C_6H_{14}N_4O_2$	156.10111	156.1875
Asparagine	N	Asn	$C_4H_8N_2O_3$	114.04293	114.1038
Aspartic acid	D	Asp	$C_4H_7NO_4$	115.02694	115.0886
Cysteine	C	Cys	$C_3H_7NO_2S$	103.00919	103.1388
Glutamine	Q	Gln	$C_5H_{10}N_2O_3$	128.05858	128.1307
Glutamic acid	E	Glu	$C_5H_9NO_4$	129.04259	129.1155
Glycine	G	Gly	$C_2H_5NO_2$	57.02146	57.0519
Histidine	H	His	$C_6H_9N_3O_2$	137.05891	137.1411
Isoleucine	I	lle	$C_6H_{13}NO_2$	113.08406	113.1594
Leucine	L	Leu	$C_6H_{13}NO_2$	113.08406	113.1594
Lysine	K	Lys	$C_6H_{14}N_2O_2$	128.09496	128.1741
Methionine	M	Met	$C_5H_{11}NO_2S$	131.04049	131.1926
Phenylalanine	F	Phe	$C_9H_{11}NO_2$	147.06841	147.1766
Proline	P	Pro	$C_5H_9NO_2$	97.05276	97.1167
Serine	S	Ser	$C_3H_7NO_3$	87.03203	87.0782
Threonine	T	Thr	$C_4H_9NO_3$	101.04768	101.1051
Tryptophan	W	Trp	$C_{11}H_{12}N_2O_2$	186.07931	186.2132
Tyrosine	Y	Tyr	$C_9H_{11}NO_3$	163.06333	163.1760
Valine	V	Val	$C_5H_{11}NO_2$	99.06841	99.1326

Standard Abbreviations and Masses of the 20-common amino acids' Residues

Taken from the Expert Protein Analysis System (ExPASY.org)

List of Tables

List of Figures

Chapter-1 Introduction

1.1. Glycosylation and its importance

Glycosylation is one of the common forms of post translational modification in proteins. It regulates many biological processes including protein folding, stability and host-pathogen interactions which involve many enzymes, resulting in a great diversity of carbohydrate protein bonding and glycan structures.[1,2] Glycosylation also plays a critical function in the biosynthetic-secretary pathway in the endoplasmic reticulum (ER) and Golgi apparatus. Glycosylation can occur on several amino acid residues in the protein sequence. A large number of cell membrane proteins and serum proteins contain carbohydrates or glycans. Glycosylated proteins perform diverse biological functions like enzymatic catalysis, hormonal control, immunological protection, cell adhesion, intercellular interaction and most importantly cell recognition.[3] It is also known that glycans influence the physiochemical properties of proteins such as isoelectric pH, viscosity, solubility and thermal stability. The removal of glycans from glycosylated hormones such as lutropin (LH) and thyrotropin (TSH) results in drastically reduced biological response relative to that of native hormones.[4] Glycans generally play two major roles: to confer certain physicochemical properties and to act as signals for cell-surface recognition phenomena. In research, the interest of functional significance of carbohydrate moieties in glycoprotein has increased significantly over the past two decades, which has brought the need for rapid, reliable and sensitive methods for determining glycosylation, qualitatively and quantitatively.

1.1.1. Types of glycosylation

Glycans are classified according to the type of linkage to a protein. They can be linked to two different types of amino acids. Most common and widely studied forms are *N*-linked and *O*-linked glycosylation. *N*-glycans are attached to the amide nitrogen atom on the side chain of the

asparagine (Asn) residue(s) of a polypeptide with consensus sequence Asn-X-Ser/Thr, in which X could be any residue except proline. More specifically, *N*-glycans have a reducing terminal *N*-acetyl glucosamine (GlcNAc) attached to the amide group of the Asn through an aspartylglycosylamine linkage (Figure 1.1). They encompass a common trimannosyl core to which different types of carbohydrate chains, as will be described a little further in this section.[5] In contrast, *O*-glycans are extremely diverse in nature. They are most commonly linked to an hydroxyl group of a serine (Ser) or threonine (Thr) residue through an *N*-acetylgalactosamine (GalNAc) by an *O*-glycosidic bond and are called mucin *O*-glycans or *O*-GalNAc glycans as shown in Figure 1.1. Examples are α-*O*-glyosidic bond formation (membrane and secreted proteins) and β-*O*-linked (cytoplasmic and nuclear proteins).[3] *N*-linked sugars are more commonly found than *O*-linked sugars in mammalian glycoproteins. A single glycoprotein may have multiple sugar chains, some of which are *N*-linked and some of which are *O*-linked.[6]

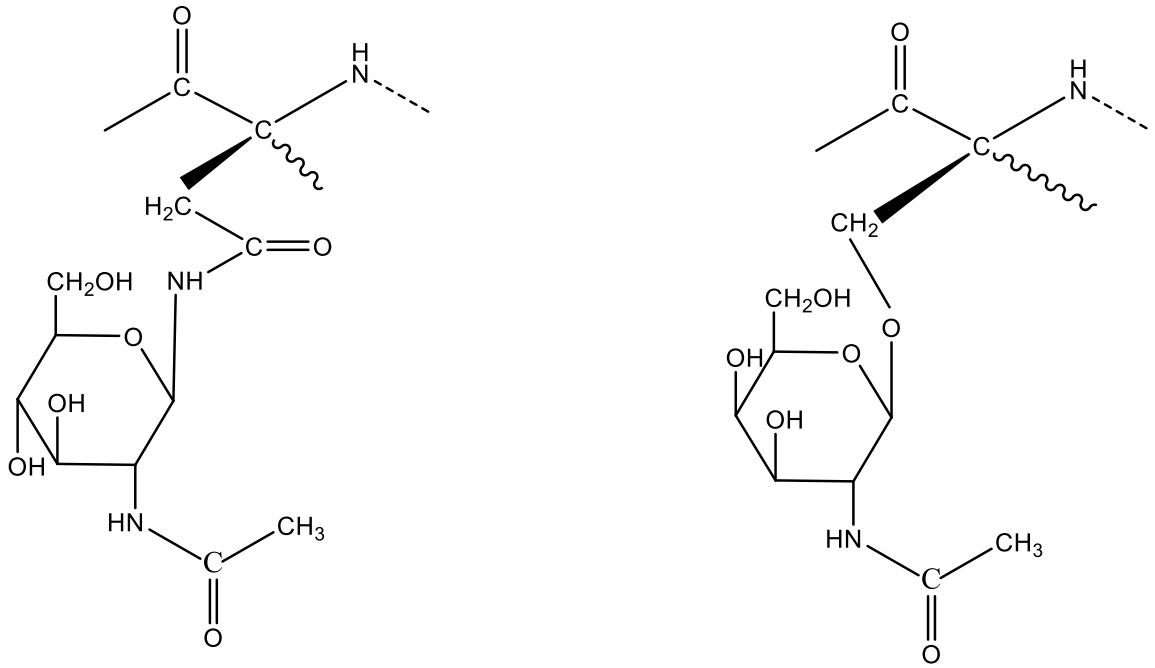

***N*-linked GlcNAc** ***O*-linked GalNAc**

Figure 1.1. Glycosidic bonds between proteins and carbohydrates. A glycosidic bond links a carbohydrate to the side chain of Asp (*N*-linked) or to the side chain of Ser or Thr (*O*-linked) (*figure adapted from ref no. 137).*

A third glycan form of attachment is known as *C*-linked, involving an α-mannopyranosyl residue linked to the indole C2 position of tryptophan (Trp). *C*-glycosylation was first discovered in a protein found in human urine.[7] *S*-linked glycosylation is another type of attachment of oligosaccharides to the sulphur atom of cysteine. This modification seems to be extremely rare in comparison to other glycosylation events and was first seen in human and bacterial peptides.[140] Limited number of *C*-linked glycans have been described and are not as common as *N*-linked or *O*-linked glycans.

1.1.2. Biosynthesis of glycans

The structural and functional characteristics of glycoproteins is derived from their biosynthesis. Glycosylation of most proteins occurs in the ER/Golgi organelles. Glycosyltransferases present in the ER and Golgi are enzymes responsible for the sequential addition of glycans. Endoglycosidases are responsible for the trimming of glycans on glycoproteins. *N*-linked glycan production begins in the ER where a high mannose precursor is synthesized onto a lipid carrier known as dolichol phosphate.[8] For *N*-linked glycosylation, the precursor may subsequently be transferred by an oligosaccharyltransferase (OST) enzyme onto a nascent protein containing an Asn of a consensus motif: Asn-X-Ser/Thr where X can be any amino acid except proline. Now the protein has become post translationally modified. Further trimming takes place in the ER, mostly by the removal of glucose and some of the mannose sugars. Next, the glycoprotein is transferred to the Golgi apparatus which contains the compartments termed *cis*, *medial* and *trans* which together span across roughly six cisternae.[9] As the glycoprotein passes through each cisterna, various sugars may be added or removed. Glycans play an important role in the growth and development of the organism. The alteration of glycans due to enzyme deficiencies can cause different types of pathological diseases.

O-Linked glycopeptides are mainly synthesized in the Golgi apparatus.[10] Monosaccharide units are added in series to a completely synthesized polypeptide chain. In contrast to *N*-glycosylation, *O*-glycosylation does not involve a dolichol phosphate precursor. The process begins with the addition of uridine diphosphate *N*-acetylgalactosamine (UDP-GalNAc) to a Ser or Thr on the polypeptide chain that can be modified by the enzyme GalNAc transferase. The process continues with the addition of galactose, sialic acid, GlcNAc and fucose residues by the action of the respective transferases.[11,12]

In mammalian *N*-glycans, a variety of sugars are typically observed namely glucose (Glc), fucose (Fuc), mannose (Man), GlcNAc, GalNAc, galactose(Gal) and *N*-acetyl neuraminic acid (Neu5Ac). Listed are the most commonly encountered monosaccharide residues that compose glycoprotein glycans in mammals.

Table 1.1. Common monosaccharide residues observed on mammalian proteins

Glycan	Abbreviation	Structure	Symbol	Anomer
α-D-Glucose	Glu	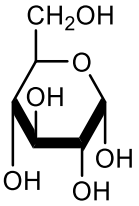		α
β-D-Galactose	Gal	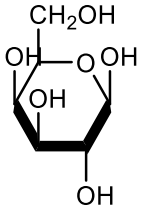		α β
α-D-Mannose	Man	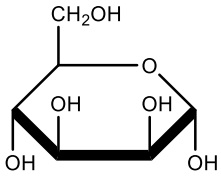		α β
α-D-Fucose	Fuc	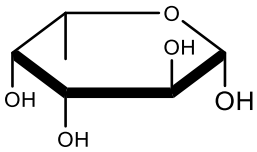		α
β-*N*-acetyl-D-Glucosamine	GlcNAc	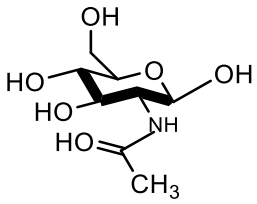		β
α-*N*-acetyl-D-Galactosamine	GalNAc	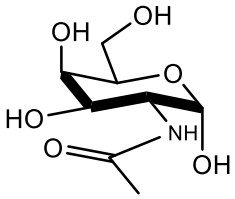		α β
α-5(*N*)-acetyl neuraminic acid (sialic acid)	Neu5Ac	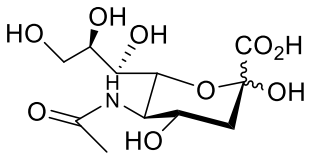		α

All *N*-glycans typically have a pentasaccharide core structure consisting of two GlcNAc residues and three mannose residues to which additional monosaccharides are attached to form a wide variety of *N*-glycans.[13,10] The $(Man)_3(GlcNAc)_2$ ensemble is called trimannosyl core and has been highly conserved during evolution.

N-glycans can be mainly distinguished into three main types based on the monosaccharide residue composition and attachment: they are a) oligomannose (or high mannose type) b) complex-type, and c) hybrid-type (Figure 1.2). High mannose *N*-glycans contain several highly-branched mannose residues on both branches of the glycans. Complex glycans are the most frequent glycans found in mammalians and can be bi-, tri- or tetra-antennary. The structures of the complex type glycans can have a bisecting GlcNAc, a core-fucose or terminal sialylation.[14] Hybrid glycans bear a high-mannose branch as well as a complex branch. In contrast, *O*-glycans are extremely diverse in nature. For *O*-glycans, *N*-acetylgalactosamine (GalNAc) is attached to the hydroxyl groups of Ser or Thr residues within the polypeptide.[15]

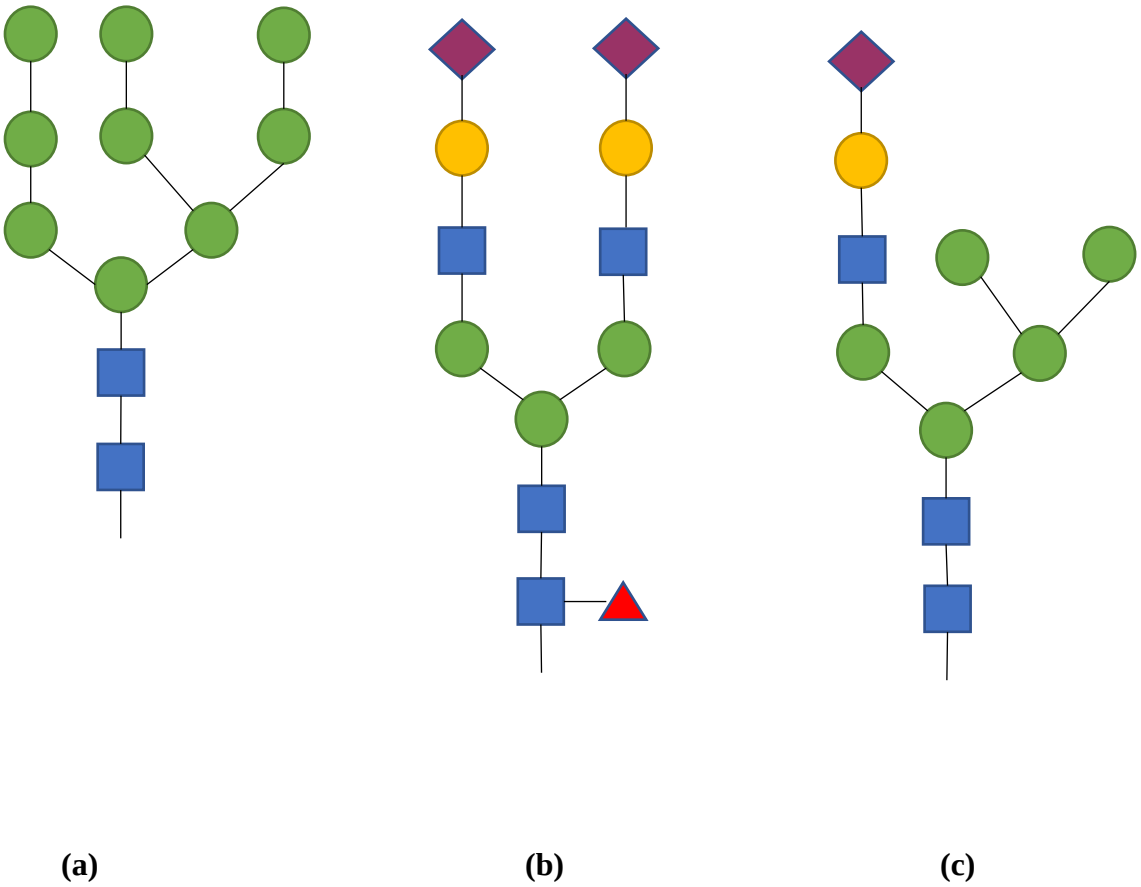

(a) **(b)** **(c)**

Legend

Mannose (Man)

Galactose(Gal)

Fucose (Fuc)

GlcNAc

Sialic acid (*N*-Acetylneuraminic Acid)

Figure 1.2. Three major type of *N*-glycans, (a) high mannose-type, (b) tri-antennary complex-type, and (c) hybrid-type.

In eukaryotes, approximately 50% of proteins are glycosylated. In humans, estimates are even higher, at 70%.[16] Glycans are not fixed structures, but are heterogeneous and exhibit extreme diversity. Due to the complexity of the glycosylation process, glycoproteins produced by living cell systems usually contain macro and micro heterogeneity in terms of glycosylation pattern.

Macro-heterogeneity refers to the variability of glycosylation sites and glycan number, while micro-heterogeneity concerns glycan structural variations at a specific site.

It is a big challenge to obtain specific glycoproteome information in a largescale analysis, including the number of proteins that are glycosylated and where their glycosylation sites are located. To determine such informations, reagents and techniques for the rapid and highly sensitive enrichment and identification of glycoproteins and glycopeptides are required.

1.2. Protein post translational modifications including glycosylation

These modifications occur after the proteins have been translated from the mRNA which in turn is transcribed from the DNA. Post translational modifications (PTMs) could be classified into two common types.

The first type involves the addition of the chemical groups to a side chain residue in the protein, while the second involves the cleavage of the peptide backbone. Based on the covalent additions, PTMs are divided into different types which are phosphorylation, alkylation, acylation, hydroxylation, glycosylation, and oxidation. Glycosylation is the main focus of this work.

It is well documented that protein glycosylation not only increases protein stability *in vitro* but also protects proteins from proteolytic degradation in vivo.[17] Dysregulation of glycoprotein is associated with a wide range of diseases, including cancer, diabetes, as well as congenital, cardiovascular, immunological and infections disorders. Thus, the cellular control of protein glycosylation remains a challenging topic in biology. Protein modifications are essential in biological systems and involved in nearly every cellular event.[18,19] Altered glycosylation is a well-established feature in many disease states. Glycan patterns are known to be associated with

oncogenesis and tumor progression, as well as a host of illnesses like pathogenic multiple sclerosis, rheumatoid arthritis, nephropathy and polycystic linear diseases.[20,21,22]

1.3. Biological roles of glycosylation

Glycosylation plays a variety of biological roles in living system. Glycans play an important role in cell-cell recognition and cell matrix interaction. Studies also show that glycosylation (*O*-linked oligosaccharides on the *zona pellicida* glycoprotein ZP3) plays a role in the binding of the sperm to the egg.[23,24] Studies have also shown that the same glycans on different glycoconjugates which have been expressed in different tissues at various stages of development of the organism have played different roles.[25] A well characterized example is that of mannose-6-phosphate (Man-6-P) containing glycans first found on lysosomal enzymes involved in lysosomal trafficking.[26] Man-6-P is also found on a variety of proteins (including proliferin, thyroglobulin, and the transforming growth factor β (TGF-β) precursor with different biological functions.[27,28]

1.3.1. Aberrations in glycosylation and association with diseases

As glycans are involved in many vital biological processes and functions, acquired changes in glycosylation could result in the formation and development of several diseases, including diabetes, skin diseases rheumatoid arthritis, Alzheimer's disease, cystic fibrosis and cancer.[15,29] Altered *N*-glycosylation has been the cause of a number of genetic disorders of fibrinogen as this protein has a high sialic acid content, also seen in liver disorders.[30] Studies have shown that patients with rheumatoid arthritis have decreased levels of galactose in the *N*-glycans of immunoglobulin (Ig) molecules with some having none (G0 molecules).The sensitivity of the diseases depends on the extent of change in glycosylation.[31,32,33,34]

1.4. Antibody glycosylation

Antibodies, especially Igs, play a central role in the immune system of living organisms. Igs are produced by B lymphocytes to identify and neutralize foreign antigens and pathogens that are exposed to the host.[35] Igs are glycoproteins that are produced by plasma cells in response to the presence of antigens. The two main functions of Igs are antigen binding and effector function stimulation. The binding of the antibody paratope and the epitope of the antigen allow formation of an antigen-antibody complex. It gives the signal to the effector cells of the immune system, indicating to them to destroy the antigen.

IgG is one of the most abundant proteins in human serum. Healthy adult serum contains 76% of IgG in the total immunoglobulin protein composition.[36] It is the major class of the five classes of immunoglobulins in human beings, IgM, IgD, IgG, IgA and IgE. Those closely related glycoproteins, composed of 82-96% protein and 4-18% carbohydrate, differ in heavy chain structure and have different effector functions.[36] Back in 1964, heavy chain subclasses of human IgG were identified.[37,38] Human IgG is not a single type of molecule but rather a class of the immunoglobulins divided in four subclasses (IgG1 to IgG4). These are named according to their decreasing average natural abundances, IgG1 being the most abundant and IgG4, the least. [39,40] In healthy individuals, the relative proportions of each of these subclasses have been found to vary in relatively narrow ranges. There is 60-71% of IgG1, 19-31% of IgG2, 5-8% of IgG3 and 1-4% of IgG4.[36] These ranges vary slightly in other reports.[41-43] In terms of amino acid sequence, human IgG subclasses have more than 90% in common, however each subclass has different properties regarding the binding of antigens, formation of immune complexes, complement activation, half-life, effector cell activation, and transport into the placenta.[40]

The IgG immunoglobulin molecule consists of four polypeptide chains, composed of two identical 50 KDa γ heavy (H) chains and two identical 25 KDa κ or λ light (L) chains, linked together by inter-chain disulfide bonds. Each heavy chain consists of an *N*-terminal variable domain (VH) and three constant domains (CH1, CH2, CH3), with an additional "hinge region" between CH1 and CH2 (Figure 1.3). Similarly, the light chain consists of an *N*-terminal variable domain(VL) and a constant domain (CL). The light chain associates with the VH and CH1 domains to form a Fab arm ("Fab" = fragment antigen binding), and functionally, the V (variable) regions interact to form the antigen binding region. The antigen binding site is formed by the convergence of six hypervariable peptide loops known as complementarity determining regions (CDRs), which determine the protein's affinity and specificity for specific antigens. Two heavy chain-light chain hetetrodimers (HL) combine into a single antibody molecule (H2L2) via disulfide bonds in the hinge region and non-covalent interactions between the CH3 domains. The part of the antibody formed by the lower hinge region and the CH2/CH3 domains is called "Fc" ("fragment, crystallizable").[40]

Fc receptors of IgG are important components of the immune system that bind to the effector region of the IgG molecules and communicate information with in the innate and adaptive immune system. Figure 1.3 shows the general schematic for the IgG molecule.

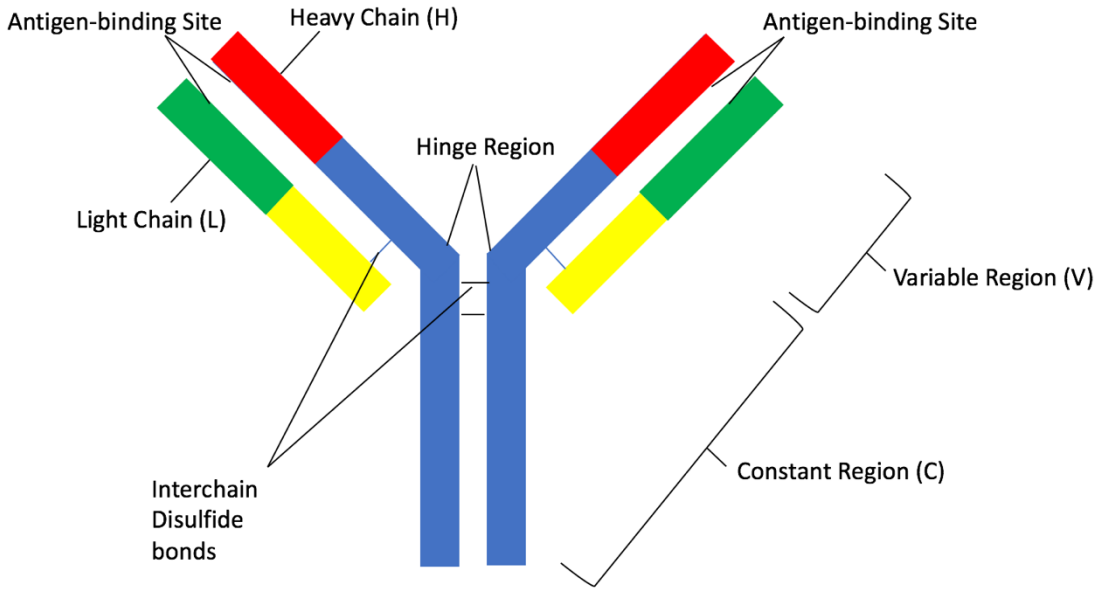

Figure 1.3. General schematics of an IgG molecule (*figure adapted from ref no. 111).*

Being heavily stabilized by cysteine S-S bonds, antibodies subjected to cysteine protease papain digestion are cleaved at the hinge region on the H-H inter chain bonds, resulting in three fragments of approximately identical sizes. Two of the fragments are Fab as they contain the antigen binding sites of the antibody. The third fragment that is produced is Fc region, which supports the effector properties of IgG.

1.5. The contribution of the Fc glycan to Ig

All four human IgG subclasses have a conserved *N*-glycosylation site at Asn-297 of the heavy chains. The Fab domain of the IgGs is also glycosylated in about 10-20% of the cases.[40] Human IgG *N*-glycosylation has been documented extensively, and is has been reported that Fc (fragment crystallizable) receptors bind to the Fc (effector) region of IgG and communicate information within the innate and adaptive immune system.[44]

The IgG Fc fragment is comprised of two domains of the constant heavy chain (Cγ2 and Cγ3). A key component of IgG is located at the conserved *N*-linked glycosylation site, Asn-297 (N297), near the hinge region in the Cγ2 domain.[45,46] The *N*-linked glycans influence the static hindrance between the two heavy chains, maintaining the IgG Fc in an opened conformation.[47] The *N*-glycans in the IgG Fc have a common core structure composed of $(GlcNAc)_2(Man)_3$, where GlcNAc=N-acetylglucosamine and Man = mannose. This core is usually extended by the presence of more GlcNAc residues, Fucose (Fuc), galactose (Gal), and N-acetylneuraminic acid (Neu5Ac). Healthy serum IgGs have been found to contain several glycoforms, with dominant species being biantennary with one Fuc and zero, one or two Gal residues and sometimes a Neu5Ac group.[48]

A single *N*-glycosylation site is present in the Fc portion of all IgG subclasses. Glycans at this site are essential for initiating many IgG effector functions. Therefore, detailed analysis of the glycosylation pattern of antibodies is not only essential, but also challenging due to the heterogeneous structure of this post translational modification.[49]

X-ray crystallography indicates that in a single IgG molecule, the two Asn-297 sites may be differently glycosylated. Each Asn-297 site contains one family up to 32 glycans that can be assigned to three subsets, IgG-G0, -G1, and -G2[50] depending on the number of galactose residues present. Figure 1.4 shows the three most abundant glycoforms of EEQYNSTYR (IgG1) and EEQFNSTFR (IgG2).

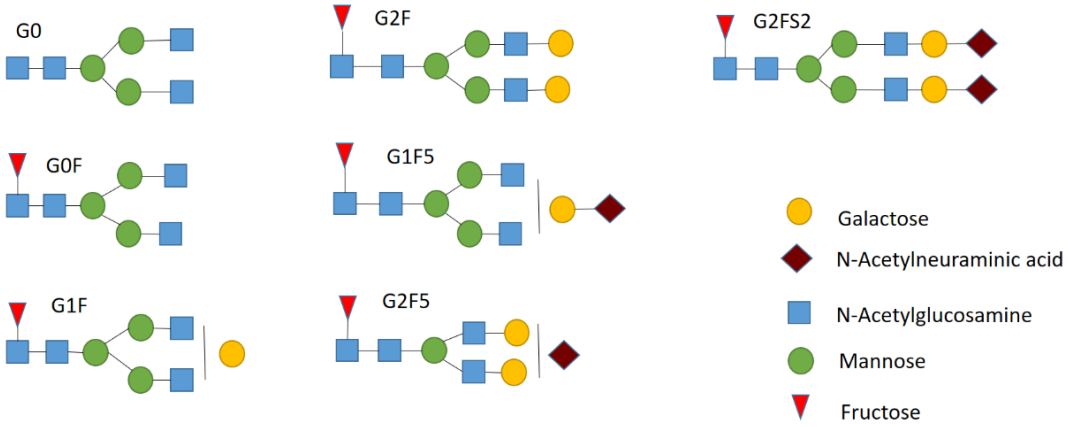

Figure 1.4. The three most abundant glycoforms of EEQYNSTYR (IgG1) and EEQFNSTFR (IgG2). The glycans are attached at the N site at the reducing end of the fucosylated *N*-acetylglucosamine.

1.6. Glycosylation of monoclonal antibodies (mAbs) bioengineered for therapeutic uses

In the past 50 years, the use of mAbs for therapeutic applications against cancer and autoimmune disorders has been widely developed. There are more than thirty-five therapeutic monoclonal antibodies (mAbs) approved for clinical use.[51,52,53] Most contain the human IgG1 Fc portion.

mAbs are considered some of the most successful and widely used-antibody related reagents for clinical and diagnostic applications. Therapeutic mAbs are glycoproteins produced by living cell systems by recombinant DNA technology. The glycan moieties attached to the proteins can directly affect protein stability, bioactivity and immunogenicity. mAb, that have high selectivity and specificity, with a low toxicity.[54] They constitute a large and growing portion of the bio-therapeutics market. A challenge in mAb production for therapeutic use is that their efficacy is highly dependent on the accuracy of their glycosylation pattern.[55] Changes in antibody glycosylation are a major cause to batch variability during production by bioengineering methods. For this reason, it is essential to measure and control antibody glycosylation accurately and

reliably. Over the past few decades, there have been several studies exploring the structural, biological and clinical roles of Ig glycosylation, mainly focusing on Fc-glycosylated IgG molecules. Fc glycans influence the protein's characteristics such as solubility,[56] aggregation,[57] and interaction with receptors.[58]

mAbs are a specific type of therapy made in laboratory. They can be used in immunotherapy. Researchers can design antibodies that specifically target a certain antigen, such as one found at the surface of cancer cells. They can make many copies of that antibody in the lab. Different types of mAbs are used in cancer treatment. The most common mAbs used for treating cancer are naked mAbs where there is no drug or radioactive material attached to them. Some naked mAbs work mainly by attaching to and blocking antigens on cancer cells or other nearby cells that help cancer cells grow or spread. For example, Trastuzumab™ [59] also known as Herceptin[60] is an antibody against the HER2 protein. Breast and stomach cancer cells sometimes have large amounts of this protein on the surface. Herceptin works by attaching itself to the HER2 receptor on the surface of cancer cells, and blocking it from receiving growth signals. By blocking the signals, Herceptin can slow or stop the growth of breast cancer. Herceptin works in a different way relative to standard cancer therapies, such as chemotherapy or hormonal therapies.

In the immune system, soluble protein antigens and membrane protein antigens mostly contain IgG1, although low quantities of the other subclasses are also involved.[61] Different levels of antibodies cause characteristic deficiencies in humans, like the serum of patients being affected with monoclonal gammopathy have shown to contain higher than normal levels of IgG1.[62] On the other hand, low levels of IgG1 have been linked to the recurrence of infections.[41] In either instance, it is important to enable the rapid monitoring of subclass proportion changes.

The four subclasses of human IgG (IgG1-4) show differences in amino acid compositions and hinge region sequences. Hence, IgG1-4 show differences in physiological characters and biological properties. So, it is important to enable the rapid monitoring of subclass proportion changes in IgG from different sources. With the availability of mass spectrometry (MS) and ionization methods adapted to proteins, it is useful and practical to propose the development of a quantitative method for human IgG subclasses.

1.7. Production of mAb

The biological importance of antibodies in different types of diseases such as cancer and rheumatoid arthritis justifies the growing production of recombinant mAbs as potential biotherapeutic agents that can be used as a newer class of drug. For the production of mAb the most common antibody used is IgG1. Moreover, all licensed therapeutic mAbs are IgG1s.[63]

Uses of IgG1 as biopharmaceuticals have become challenging due to their size (~150 KDa), which cause undesirable pharmacokinetics and poor tissue penetration.[64] To solve this problem, several methods have been developed, like antibody fragments with different sizes have been constructed.[65,66,67,68] In another method, the scFv is fused directly to the Fc in order to reduce the size of the antibody.[69,70] Another method is based on the use of heavy chain antibodies (HCAbs) discovered in camelids[71] (camel, llama, alpaca) which are composed of two heavy chains and no light chain. The variable regions of HCAbs are responsible for the antibody's ability to bind antigens. HCAbs are small (80 KDa relative to 150 KDa for IgG1), but they can still be created to have high antigen binding affinity.[72] Camelid single domain antibodies are known to have high thermostability, relatively high proteolytic resistance and high yields in various expression systems. [141,142] All these important characteristics makes HCAbs ideal candidates with small recombinant antibodies and intact human IgG1 Fc domains. In this study, synthetic peptides

and glycopeptides are used to quantitate a humanized camelid HCAbs prepared in cell culture, Eg2-hFc.

1.8. Qualitative and quantitative methods to characterize IgG glycosylation by MS

The characterization of IgG *N*-glycosylation by MS has long been conducted using glycomic approaches where *N*-glycans are detached with an enzyme such as peptide *N*-glycosidase F (PNGase F), labelled and analyzed separately from the polypeptide chain, and there have been several recent studies that have used this approach. [73,74] The other glycosidases routinely used for the removal of *N*-glycans are endo-β-N-acetylglucosaminidase (Endo H)/Endo S[75] and peptide-N-glycosidase A (PNGase A)[76] that cleave glycans at different locations. Endo H primarily targets the release of high mannose glycoforms[77] and of some hybrid forms,[78] whereas Endo S is known to target hybrid forms. Both Endo H/Endo S cleave the glycan leaving the primary GlcNAc attached to the peptide. In contrast, PNGase A is able to cleave glycans which contain an α1,3-fucosylated core,[79] a common trait observed in insects and plants, whereas PNGase F is known to hydrolyze glycans that have an α1,6-fucosylated core observed in mammals. PNGase F is the standard enzyme for the release of most *N*-linked oligosaccharides.[80] Analysis using glycosidases produce glycan profiles, however no specificity is obtained pertaining to glycosylation site. Profiling of released *N*-glycans can be replaced by glycoproteomic approaches, where IgGs are digested with a proteolytic enzyme (most often trypsin), and *N*-glycopeptides are characterized. This allows accurate determination of glycosylation sites and glycan composition.[81,82,83] For quantitative analysis in glycoproteomics, it is possible to use synthetic glycopeptides corresponding to the antibody's proteolytic glycopeptides. The synthesis of such peptides is described in the next section.

1.9. Peptide Synthesis

A good way to access glycopeptides and glycoproteins of defined structure to be used as qualitative/quantitative standards is through chemical and enzymatic synthesis. The synthesis of glycopeptides and glycoproteins for readily available components is therefore an important goal. Peptide synthesis efforts typically rely on solid phase peptide synthesis (SPPS) which is a process that allows efficient assembly of different amino acid residues. Bruce Merrifield was the pioneer of the idea to generate the peptide bonds on an insoluble resin where a single cleavage helps to obtain the desire peptide in solution.[84] The main advantages of this method are (1) simplicity and speed and (2) efficiency of obtaining high yields of final products through the use of excess reactants. The two most widely used *N*-terminal protecting groups for SPSS are the *tert*-butoxy-carbonyl (Boc) group (sensitive to acids such as trifluoracetic acid (TFA).[85,86] and the 9-fluorenyl methyl carbamate (Fmoc) group (sensitive to bases such as piperidine). Figure 1.5 have shown the picture of both Boc and as well as Fmoc group.

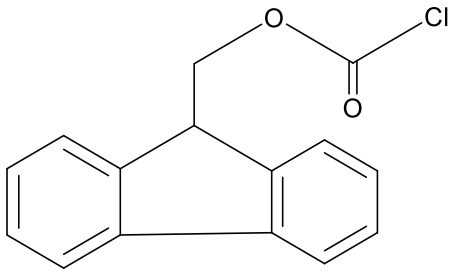

Fmoc Chloride

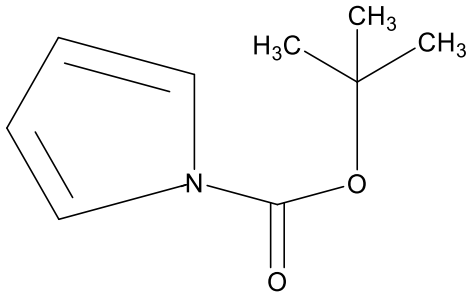

N-Boc-Pyrrole

Figure 1.5. Fmoc Chloride and *N*-Boc-Pyrrole (*figures adapted from ref no. 112 and 113)*

.

Fmoc-based SPPS is usually favoured in the synthesis of glycopeptides because the glycosidic linkages are relatively labile in the presence of strong acid necessary for the removal of Boc protecting groups.

Glycoproteomics studies on human IgG rely the different amino acid sequences of the heavy chain's tryptic *N*-glycopeptides EEQYNSTYR(IgG1), EEQFNSTFR(IgG2), EEQYNSTFR (IgG3) and EEQFNSTYR (IgG4).[83] It is thus possible to prepare a quantitative method based on the availability of synthetic glycopeptides with these four sequences. It is well established that similar size peptides with different amino acid composition and sequences yield different responses in MS detection which makes it important to determine the amount of each different IgG -glycopeptide independently based on a synthetic peptide of same amino acid sequence and composition. Stavenhagen and co-workers[87] have conducted a quantitative and comparative study of this type. Several variations of a tryptic *N*-glycopeptide and non-glycosylated peptide from human protein C (EVFVHPNYSK) were synthesized in order to compare signal strengths and signal intensities with different ionization methods: electrospray ionization (ESI) and matrix-assisted laser desorption/ionization (MALDI) on a range of analyzers: ion trap, quadrupole, time of flight (TOF) and Fourier-transform ion cyclotron resonance (FT-ICR). They observed that glycopeptide signals tended to be lower than non-glycosylated peptides. The bias varied according to the technique and instrument used.[87] These observations emphasize the need for a rigorous calibration method when different peptide backbones are to be investigated and compared on a specific instrument. Many quantitative methods developed for glycopeptides are relative, i.e. they allow the comparison of structures with the same amino acid backbone between two or more samples (duplex to multiplex).[88,89]

There is not a large variety of commercially available glycopeptides that can be used as an internal standard for MS or other techniques. For this purpose, custom synthesis of peptides is required. Specifically, for human IgG subclasses IgG1 and IgG2, the purpose of this work is to determine if it is convenient to use some EEQYNSTYR and EEQFNSTFR glycosylated and non-glycosylated standards for absolute quantitation. These two peptides are differentiated by mass whereas IgG3 (EEQYNSTFR) and IgG4 (EEQFNSTYR) are isobaric. Although IgG3 and IgG4 can be separated on Protein-A or Protein G columns,[83] it would be easy to find or make labelled standards corresponding to other tryptic peptides unique to these two subclasses. Some important work has been reported based on the quantitative analysis of IgG subclasses using this selecting subclass specific tryptic peptides, and the MS technique have been used with liquid-chromatography/ESI-MS/multiple reaction monitoring (LC-MS-MRM) in order to detect the fragments of peptides and glycopeptides.[90,91] In the present work, it was attempted to develop an absolute quantitative method for human IgG1 and IgG2, the two most abundant forms of IgG in healthy individuals.[40] The method is based on the synthesis of EEQYNSTYR and EEQFNSTFR peptides and glycopeptides and their use as internal standards in glycopeptides enriched from human IgG tryptic digest mixtures which can be analyzed by MALDI-TOF-MS without tandem mass spectrometry (MS/MS) or MRM. The topics explored also include the different sensitivities of the two peptides under MALDI conditions, and the determination of IgG1/IgG2 percentages in IgG samples obtained commercially and samples purified from healthy patients and patients affected with different degrees of monoclonal gammopathy of unknown significance (MGUS).[62]

1.10. Detection of aberrations in glycosylation

Glycans have different attributions which make them excellent disease markers. Glycoproteomic studies combine the enrichment techniques of glycoproteins/glycopeptides with

proteomic technologies to identify and quantify glycosylated proteins in a complex sample.[92] MS is a rapid, sensitive and versatile technique which has become one of the most widely used analytical tool in glycomics and glycoproteomics. Quantitative glycosylation analysis typically rely on MS to identify or quantitate selected peptides or glycopeptides, although MS/MS is required for peptide identification. During the first round of MS (MS1), ionized peptides produce precursor ions that represent all ionized peptides in the sample. For different glycoforms of the same peptide, relative quantitation relies on the comparison of signals. This does not hold for glycoforms of two different peptide sequences. Individual ions are then selected to go a second round of MS (MS2), which yields a fragment ion spectrum for each precursor ion.

1.11. Glycosylation analysis by mass spectroscopy

Traditionally, IgG subclass levels have been determined by specific immunoassay methods involving monoclonal antibodies.[36] With the availability of mass spectrometry (MS) and ionization methods adapted to the analysis of proteins. It is useful and practical to propose the development of a quantitative method for human IgG subclasses. Due to its sensitivity and selectivity, MS has become one of the most powerful modern analytical technique for the analysis of glycopeptides. There is a wide range of mass spectrometers that are commonly used in analysis of peptides and glycopeptides, including ion trap mass spectrometers, quadrupole mass spectrometers, and more recently orbitrap ™ mass spectrometers. The first mass spectrometer was constructed by Sir J.J. Thomson in 1912. Since then, many advancements took place and MS has come played an important role in proteomics i.e. identification and characterization of proteins, being especially useful for post translational modifications. As far as specific MS techniques are concerned, for a long-time gas chromatography-MS (GC-MS) and fast atom bombardment MS (FAB-MS) have been important in terms of providing structural information and related biological

problems. Together, these techniques could define the complete primary structure of an oligosaccharide or glycoconjugate.[93] In the present research, all experiments have been performed using MALDI-TOF-MS. MALDI-MS was first introduced in 1988 by Hillenkamp and Karas[94] and has since become a widespread analytical tool for peptide, proteins and most other biomolecules (oligonucleotides, carbohydrates and natural products and lipids).

1.11.1. Principal components of mass spectrometers

All MS instruments comprise the following fundamental elements: an ion source, a mass analyzer and a detector. In the ion source, ions are generated and transmitted to the mass analyzer, where they are separated by mass to charge ratio (*m/z*) and subsequently detected and reported by *m/z* and abundance.

1.11.2. Ionization sources in mass spectrometry

MS identifies the compounds by producing characteristic ions in the gas phase and subsequently effecting their separation based on *m/z* ratios with a high level of specificity and sensitivity. In biological MS, two modes of ionization are common, 'hard' and 'soft' which refer to the ability of the technique to form intact ions and to the level of fragmentation produced. Hard ionization such as electron impact (EI) produces a higher number of small fragments and is mostly adapted to volatile molecules. Proteomic studies mainly focus on larger intact structures and hence soft ionization processes are required. ESI-MS and MALDI-MS are two such processes. Both MALDI and ESI ion sources can be interfaced to different types of mass analysers, some of the more common used in bioanalysis being quadrupoles, ion traps and TOF instruments.

1.11.3. Matrix Assisted Laser Desorption Ionization (MALDI)

In MALDI analysis, the analyte is first co-crystallised with a large molar excess of matrix compound, usually a UV-absorbing weak organic acid. The matrix also serves as a proton donor and receptor, acting to ionize the analyte in both positive and negative ionization modes respectively. The most useful matrices are 2,5-dihydroxy benzoic acid (DHB), α-cyano-4-hydroxycinnamic acid (CHCA) and 3,5-dimethoxy-4-hydroxycinnamic acid (sinapinic acid or sinapic acid; SA).

1.11.4. MALDI laser

MALDI involves pulsing a laser at the target loaded with the analyte co-crystallized with a large excess of matrix which absorbs at the laser wavelength. Most MALDI devices use a pulsed UV laser (N_2: λ= 337 nm). Neodymium-yttrium aluminium garnet (Nd: YAG) lasers (λ = 355 nm) as equipped on the Bruker UltraFleXtreme^{TM} MALDI-TOF/TOF. The pulsed laser causes the sample to desorb from the solid crystal into the gas phase and simultaneously become charged molecules, forming ($M+H^+$; $M+X^+$, where $X=Na^+, K^+$) ions. A voltage is then applied to the target, which propels the plume of ions towards the mass analyser component of the mass spectrometer.

The target plate is positioned in the high vacuum source region of the mass spectrometer. The matrix, being present in a greater concentration than the analyte, absorbs most of this energy in the form of heat making the analytes such as proteins remain intact. A dense gas cloud is formed by sublimation of the matrix and rapid expansion of matrix and analyte into the gas phase. This cloud heads towards the instrument's vacuum and the energy is transferred from matrix to analyte. Figure 1.6 shows a possible process of ionization in MALDI.

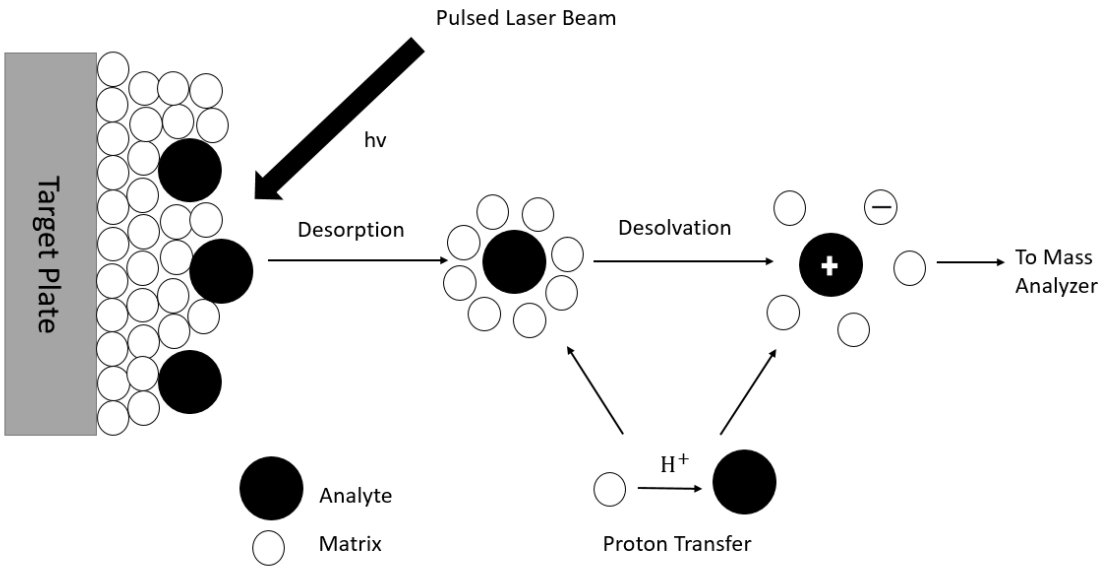

Figure 1.6. Diagram showing ionization in a MALDI source (*figure adapted from ref no. 138).*

Single protonated molecular ions are dominant in MALDI ionization. Non-volatile biological macromolecules, such as glycoprotein hormones, are readily ionized by MALDI and interpretation of spectra is relatively simple due to the presence of singly charged ions. The use of suitable matrix materials to promote efficient ionization is central to the success of MALDI-MS.

1.11.5. Time of flight (TOF) analyzer

One of the simplest mass analyzers used in MS is the TOF, often interfaced with a MALDI ionization source. Modern TOF analysis is extremely rapid and offers high resolution and sensitivity, making the instrument a popular choice for proteomics and glycoproteomics. After production of ions by MALDI, a fixed potential difference (typically 20 to 30 kV) accelerates all the ions into a field free drift tube (the analyzer) where TOF separation occurs.

As all the ions are accelerated with the same potential then they all have same kinetic energy (KE). The TOF analyzer works by measuring the time required for ions generated in the source to fly through the analyzer and strike the detector. The principle is based on an ion of mass m leaving the ionization source with a charge z =1 and accelerating potential V, thus having energy zV equal to the kinetic energy of the ion:

$KE = zV = \frac{mV^2}{2}$ (eq. 1)

The relationship between time, distance (in this case d, the length of the drift tube) and velocity is expressed as

$t = \frac{d}{v}$ (eq. 2)

Substituting (2) into (1) gives

$t^2 = m/z(\frac{d^2}{2V})$ (eq. 3)

The terms in parentheses (related to a fixed distance and accelerating potential) remain constant thus m/z can be determined from t^2. The arrival time at the detector is dependent upon the mass, charge, and KE of the ion.

Ions will separate according to their velocity along the flight tube from the MALDI plate towards the detector. For singly charged ions, those with larger mass will travel with a lower velocity while the smaller ions will reach the detector first because of their greater velocity. Hence, the analyzer is called TOF because the mass is determined from the ions 'time of flight'. It is the simple feature of TOF analyzers that makes it ideal for coupling with pulsed MALDI sources for the analysis of large intact biomolecules such as proteins. Figure 1.7 shows a schematic picture of

a MALDI-TOF-MS instrument. The discussion above applies to the linear mode of this instrument, i.e. detection in a straight line at the "linear detector".

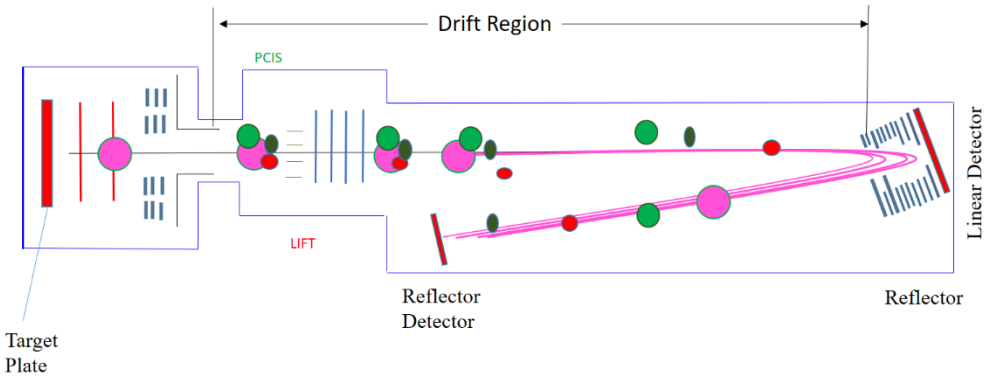

Figure 1.7. Schematics of the Bruker UltraFleXtreme™ MALDI-MS instrument used in this work.

Resolution of TOF analyzers is an important factor in MALDI analysis. Most often in MALDI-MS, resolution is defined by the mass of a peak divided by its width at half height ($\frac{m}{\Delta m}$ or $\frac{t}{\Delta t}$). Upon ionization, KE spreads will cause a lack of velocity focus for the ions, thus causing widening of the peaks and contributing to lower the resolution in the linear detection mode. This phenomenon tends to be accentuated at higher mass.

To overcome the low resolution, an ion mirror was first introduced by Mamyrin in 1973, which is refers to as reflectron™, more commonly called, a reflector.[95] Ions with high KE penetrate deeper into the reflection, taking longer distance and more travelling time than those with lower KE, that spend less time in the reflector. The reflector mode provides enhanced resolution whereas the linear TOF spectrum is limited in resolution leading to lower mass accuracy. The increased resolution, however, often comes at the expense of sensitivity and covers a relatively low mass

range, typically up to only10,000 *m/z*. Figure 1.8 compares examples of low and higher resolution MALDI-TOF-MS spectra obtained for the same sample.[96]

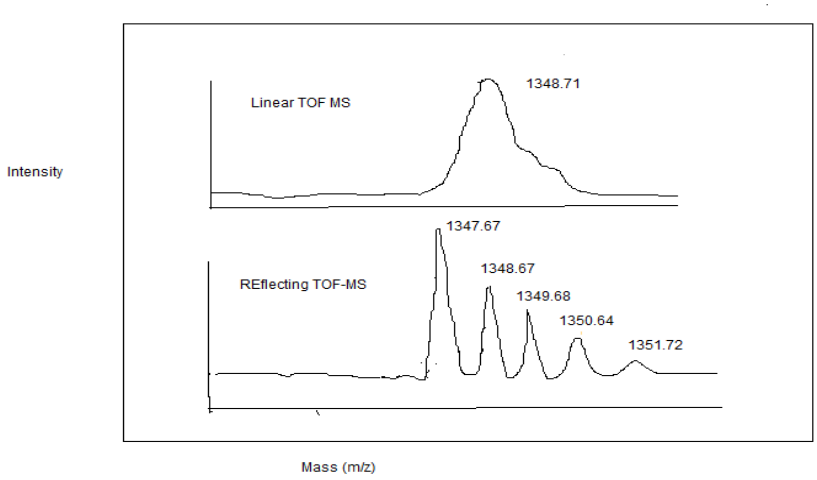

Figure 1.8. Comparing the resolution of linear and reflecting MALDI-ToF-MS spectra of substance P comparing linear and reflecting mode (*figure adapted from ref no. 96).*

The simplicity of the instrumentation and high sensitivity are the two major advantages of MALDI. The detection limit for glycopeptides has been achieved at the level of 500 femtomoles and that for underivatized oligosaccharides at low picomole levels.[97]

Since the late 1970s, tremendous progress has been made in the analysis of peptides and proteins by MS. Nowadays it is routine to analyze peptides, glycopeptides and proteins at the femtomole level, which makes MALDI-MS well suited for protein mapping and structural determination. With the ToF analyzer MALDI can detect all ions in a very short time with high mass accuracy and good resolving power (<5 ppm accuracy and >20,000 resolving power on commercially available TOF analyzers).

1.11.6. Tandem mass spectrometry

Tandem mass spectrometry (MS/MS) is used to produce structural information about a compound by fragmenting specific sample ions inside the mass spectrometer and identifying the resulting fragment ions. For instance, some amino acids exist as isomers (leucine & isoleucine), and some sugars exist as isobaric species so that a single mass spectrum will be not sufficient for identification. MS/MS experiments can help to describe the sequence patterns of peptides and glycopeptides, and to determine the glycosylation site in the latter. In MS/MS precursor molecular ions are separated in MS (the first mass analyzer, TOF1 in this work) according to mass. The role of TOF2 is to analyze the fragments according to their kinetic energy which becomes directly proportional to the mass as the velocity is assumed constant. This technique is performed in MALDI on the Bruker UltraFleXtreme® in the context of this work. The great advantage of the MALDI–TOF-TOF spectrometer used in this work is its low ppm accuracy.

1.11.7. Peptide sequencing by tandem mass spectrometry

The most common usage of MS-MS in bioanalysis is the product or daughter ion scanning experiment which is particularly successful for peptide sequencing. Peptides fragmentation was first described by P. Roepstorff, J. Fohlmann and later by K. Biemann. [98,99]

There are three different types of bonds that can fragment along the amino acid backbone: the NH-CH, CH-CO, and CO-NH bonds. Each bond breakage gives rise to two fragment species, one neutral and another charged when precursors are singly charged. Only the charged fragments are monitored by the mass spectrometer. The charge can stay on either of the two fragments depending on the chemistry and relative proton affinity of the two species. Hence there are six possible fragment ions for each amino acid residue and these are labelled with “a, b and c” (ions

having charge retained on the *N*-terminal fragment) and the x, y and z ions having the charge retained on the *C*-terminal fragment. The most common cleavage sites are at the CO-NH bonds which give rise to the b and/or the y ions. *N*-terminal fragments are known as b ions and are numbered starting from the *N*-terminus. *C*-terminal fragments are known as y-ions and are numbered starting from *N*-terminus. Below Figure 1.9 give an overview of the types of fragmentations encountered, and Figure 1.10 shows the peptide fragment ions formed. [98,99,100]

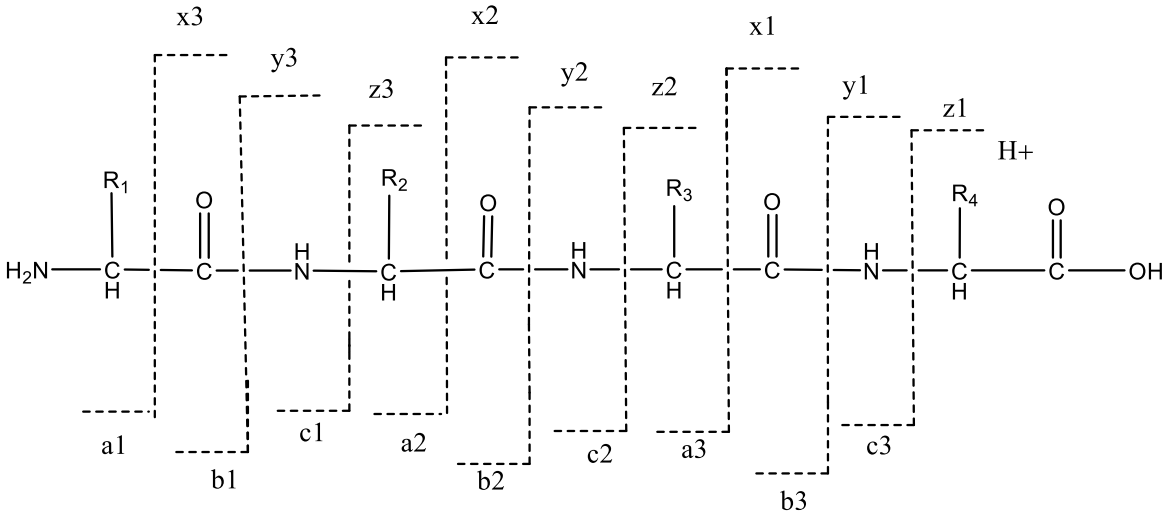

Figure 1.9. Peptide fragmentation nomenclature: b, y and a ions. Fragmentation method by Roepstorff P, Fohlman J., and Biemann K ((*figure adapted from ref no. 98,99,100).*

The mass difference between two adjacent b ions, or y ions indicate the amino acid. The extent of side chain fragmentation detected depends on the type of analyzers used in the mass spectrometer and collision energies. A magnetic sector instrument accommodates high energy collision resulting in many different types of side chain cleavages. Triple quadrupole and quadrupole-TOF mass spectrometers generate low energy fragmentations with fewer types of side chain fragmentations.

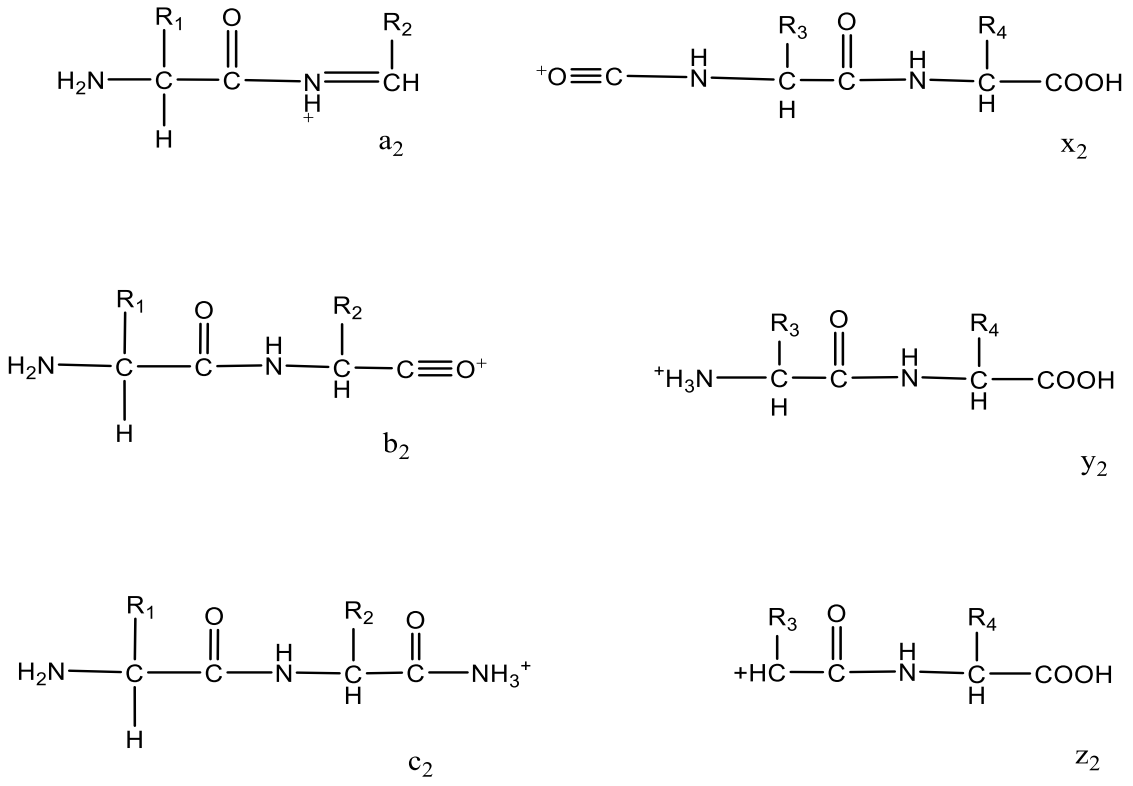

Figure 1.10. Peptide fragment ions (*figure adapted from ref no. 139).*

1.11.8. Glycopeptide fragmentation in MALDI-MS/MS

MALDI-MS/MS spectra are divided into three different areas: the peptide sequencing region, the glycan sequencing region and the area between the glycopeptide and peptide sequencing areas. This also helps in describing the variety of glycoprotein samples including sialylated, [101,102] and asialylated [103] glycoproteins. High mannose glycoforms have been analyzed by MALDI-MS/MS. Characterization of glycopeptides has also been conducted by several research groups using MS/MS of doubly and triply charged precursor ions generated by ESI. [105,106,107,108,109] MALDI generally produces $[M+H]^+$ singly charged peptide and glycopeptide ions. In most cases, MS/MS spectra of $[M+H]^+$ of ions of glycopeptides become useful for determining

sugar composition, peptide sequences and glycosylation sites. The characterization of glycopeptides, sugar content and glycosylation sites were done by MS/MS fragmentation by Krokhin et al.[110] In their experiment, they reduced, alkylated and digested commercially available proteins and glycoproteins with trypsin altogether.[110] Peptides were separated by micro-column reverse-phase HPLC into several fractions, each of which was analyzed by MALDI-MS and MS/MS. In this experiment, MS/MS analysis of $[M+H]^+$ ions generated by MALDI gave the consistent fragmentation patterns[110] with the observation of dominant group of four peaks near the mass of the peptide itself, namely, $[peptide+H-17]^+$, $[peptide + H]^+$, $[peptide+GlcNAc+H]^+$, and $[peptide+CHCHNHAc]^+$. It is possible to calculate the oligosaccharide composition in terms of $[GlcNAc]_v[Man]_w[Gal]_x[NeuNAc]_y$ by subtracting the *m/z* value of $[Peptide+H]^+$ ions from that of $[Glycopeptide+H]^+$ precursors. Below Figure 1.11 shows the fragmentation pattern observed in the MS/MS spectra of precursor ions of glycopeptides generated by MALDI. The presence of sialic acid was clearly identified by the loss of (291u), whereas GlcNAc was identified through loss of 203u. Successive losses of 162u from the precursors indicated high mannose glycan structures, whereas mixed losses of 162u and 203u indicated the presence of complex oligosaccharides. Moreover, for most glycopeptides analyzed, MS/MS spectra at the $[peptide+H-17]^+$ ions resembled that of the peptide without any sugar.

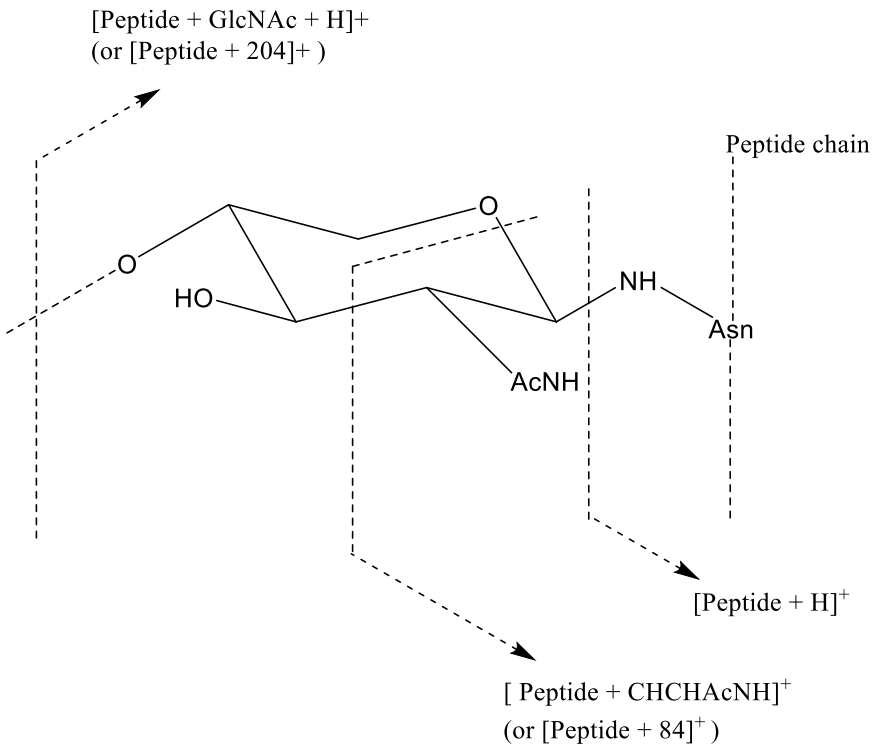

Figure 1.11. Fragmentation pattern observed in the MS/MS spectra of precursor ions of glycopeptides generated by MALDI. The tryptic peptide chain is represented by a vertical dashed line. The first *N*-acetyglucosamine residue of a glycan attached to asparagine (Asn) is shown, with corresponding fragment ions observed (*figure adapted from ref no. 110).*

1.12. Research Goals

Human polyclonal IgG comprises different subtypes, which have so far not been separable for quantification by chromatography or another technique. Most proteomic methods used nowadays enable relative quantitation and not absolute quantitation. The main objective is to develop an absolute quantitation method for IgG1 and IgG2, the two most abundant subclasses of human IgG. The method of subclass differentiation relies on the quantification of tryptic *N*-glycopeptides that are specific to IgG1(EEQYNSTYR) and IgG2 (EEQFNSTFR).

Peptides and glycopeptides have to be synthesized to use as internal standards using solid phase synthesis,[36] with sequences that correspond to those of tryptic glycopeptides of IgG1 and IgG2. The internal standard is necessary to measure the absolute quantity of glycopeptides in the tryptic digestion samples. It is important first to test if the MALDI-ToF-MS $(M+H)^+$ signals of those (glyco)peptide standards vary in a linear fashion with the amount deposited on-target. The next goal is to determine the amount of glycopeptide from a mAb sample (IgG1), where the standard glycopeptide has the exact same molecular structure as the unknown, but is isotopically labelled. One by one, glycopeptides from other mAbs (one IgG1, the other IgG2) with higher glycosylation states than the standard need to be quantified independently to verify the linearity of the relationships between the standards and three different higher glycoforms.

The same experiment needs to be repeated, substituting the mAb for a polyclonal human IgG sample for quantification. The next step is to determine if the $(M+H)^+$ signals of glycopeptides from IgG1 and IgG2 in mixtures vary linearly with respect to each other and with concentration. The last step is to quantify both subclasses in polyclonal antibodies with internal standards corresponding to these subclasses.

Due to time restrictions, analytical parameters such as limit of detection and linearity range were not determined in this work. Concentrations used were representative of those currently analyzed in the laboratory for mAbs and polyclonal Abs, and thus this study is very useful for routine quantitation of many Ab samples received in the laboratory for structural and quantitative analysis.

Also, only glycopeptides with charge-neutral glycans were considered in this study (i.e. sialylated species were not taken into account), as the presence of negatively charged sialic acid results in a regression of signal in the positive ionization mode. Sialylated species must undergo

esterification prior to analysis along with the neutral species, but again this was not performed in this work.

Chapter -2 Materials and Methods

2.1. Synthesis of glycopeptides to be used as internal standards: Solid phase peptide synthesis (SPPS) on silicycle™ (amino silica) resin

At First, the aim of this project was to design a novel stationary phase for glycopeptide enrichment, by developing a resin modified with the glycopeptide sequence of IgG. To make this and to learn about SPPS (solid phase peptide synthesis), the "straight" chain peptide GGGEEQYNSTYR was prepared based on the Fmoc(9-fluorenylmethyloxycarbonyl) strategy,[86] directly onto the silica beads. For sequence verification, the modified beads were subjected to trypsin, an enzyme that cleaves peptides after arginine or lysine residues, to liberate the peptide in solution. The synthesis proceeded in a linear fashion from the *C*-terminus to the *N*-terminus of the peptide.

The three glycine residues were added to give more room to the enzyme during cleavage. Enzymes are rather large in comparison with the relatively short propyl group, and direct synthesis of peptide on the beads without a spacer did not allow the digestion. With GGGEEQYNSTYR, on-bead digestion was completed using a modified version of the Promega protocol for Trypsin gold ™. [114]

(1) Materials and reagents

The silica-propyl-NH_2-beads, with average particle size of 40-63 µm, and a 1.66 mmol/g loading capacity, were obtained from Silicycle Inc. (Quebec City, QC, Canada). These beads contain propyl alkyl chain linkers functionalized with a free amine group. Figure 2.1 shows a representation of the aminopropyl silica resin.

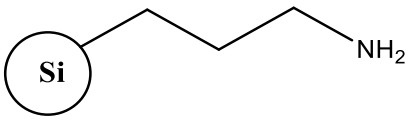

Figure 2.1. Commercially available amino propyl silica resin (Silicycle, Quebec City, Canada)

Fmoc amino acids were obtained from Bachem (Bubendorf, Switzerland). Organic solvents and reagents, including *N*,*N*-dimethylformamide (DMF), dichloromethane (DCM), *N*, *N*-diisopropylethylamine (DIPEA), piperidine, p-chloranil, Trifluoro acetic acid and 2,4 dihydroxybenzoic acid (DHB), were purchased from Sigma Chemicals Co. (St. Louis, MO,USA). [O-(Benzotriazol-1-yl)-*N, N,N', N'*-tetramethyluronium tetra fluoroborate (TBTU) was purchased from AK Scientific Inc. (Union City, CA, USA). Trypsin gold ™ mass spectrometry grade, was purchased from Promega (Madison, WI, USA). Starta ™ x 33 µm polymeric reverse phase C18 SPE cartridge (60 mg/3 mL) were obtained from Phenomenex (Torrance, CA 90501-1430) USA. Methanol, acetonitrile solvents were HPLC grade and obtained from Fischer Scientific. Milli-Q water was used for all experiments. Solvent evaporations were completed using a Savant SC110 Speed Vac (Savant Instrument Inc, Holbrook, NY), equipped with a Welch Vacuum pump (Mt. Prospect, IL)

(ii) Solid phase peptide synthesis

Synthesis of the IgG glycopeptide sequence GGGEEQYNSTYR was performed using Fmoc procedure on aminopropyl silica beads as the resin. Silica beads of 350 mg silica were first placed inside the reaction vessel (peptide synthesis vessel), and washed with DMF. Fmoc amino acids (3 equiv.) were activated with TBTU (2 equiv.) and DIPEA (8 equiv.) in DMF for at least 5 minutes in a separate vial. The solution was then transferred to the reaction vessel containing the silica resin for coupling (2-2.5 hours). The Fmoc group was removed under basic conditions using

two volumes of 4:1 DMF/piperidine, keeping reacting for a minimum of 15 minutes each. To get the elongation of protein sequence, the process was continued by repeating activation, coupling and deprotection process for each amino acid. Between each step, the beads were washed with 3 volumes of each solvent DMF, DCM and DMF. At the end of the sequence, side chain groups of the amino acids were deprotected using a mixture of 95:2.5:2.5 of TFA/H_2O/TIPS for 2 hour 45 minutes. The beads were finally washed using 3 volumes each methanol, DCM, and methanol.

The peptide synthesis was monitored using a chloranil test.[115] P-chloranil of 2% was prepared in DMF (w/v). A small sample of resin beads was stained with a few drops of the chloranil solution. The chloranil test can detect free amines after coupling and deprotection reactions. Primary amines stain the beads red, while secondary amines stain turn blue.[115]

(iii) Trypsin digestion

The required-on bead digestion was completed using a mass spectrometry grade Trypsin Gold ™. Sample beads of 200 mg were initially prewashed with 2 x 500 µl of 50:50 acetonitrile: water, and 2 x 500 µl acetonitrile. This was followed by a wash of 2 x 500 µl of 50 mM ammonium bicarbonate solution. Trypsin Gold was dissolved in 50mM ammonium bicarbonate solution and added to the beads in a peptide: beads ratio, by weight, of 1:20. Tryptic digestion was allowed to take place at 37°C for approximately 18-20 hours. Termination of trypsin activity was achieved by freezing the sample at -20°C.

(iv) Desalting and clean up

Samples were desalted prior to MS analysis with a C18 SPE column. To the samples were taken in a centrifuge tube and 50 µL of 50 mM ammonium bicarbonate was added to it and the samples were subjected to centrifugation. Then the supernatant was taken out for the clean up. The

C18 SPE cartridges conditioned with 5x (1 ml acetonitrile + 0.1% TFA) and then with 5x (1 ml of water + 0.1 % of TFA). The sample was loaded onto the column, and then rinsed with 3x (1 ml of water). All peptide samples were collectively eluted with ACN: H_2O + 0.1% TFA. The elution solvents consisted of acetonitrile / water fractions of 10:90, 15:85, 20:80, 25:75 and 30:70) at 2x200 µl volumes each. Each eluted sample was collected and concentrated by centrifugal evaporation by Speedvac ^{TM}. Samples were resuspended in 4µL of TA30 (30:70 ACN: H_2O + 0.1 % TFA).

(v) MS analysis

A Bruker UltraFleXtreme^{TM} MALDI-TOF-MS (Bruker, Bremen, Germany) was used for all MALDI detection experiments in the reflector positive mode. 2,4 dihydroxybenzoic acid (DHB) [20 mg in 1 ml TA30 (30:70 ACN: water + 0.1% TFA)] was used as the matrix. DHB (0.5 µl) was first spotted onto the MALDI target and allowed to dry. The tested samples were applied directly onto the matrix (1µl). A standard peptide mixture was used to calibrate the instrument before each analysis.

A standard calibration mixture composed of eight well-characterized peptides with masses ranging from 700 to 5000Da was used. (American peptide company, Vista, CA]: Bradykinin [1-7] 757.3992; angiotensin II 1046.542; angiotensin I 1296.685; Substance P 1347.72540; bombesin 1619.822; ACTH clip (1-17) 2093.086; ACTH Clip [18-39] 2465.198; ACTH [1-39] 4539.267, where ACTH = adrenocorticotropic hormone and numbers are calculated *m/z* values of $[M+H]^+$ ions. For the calibrant the solutions were prepared at the concentration of 1 mg/ml in milliQ water. Then solutions were mixed with saturated DHB matrix in TA30 (30:70 ACN:0.1% TFA in water) in 1:1 ratio and spotted directly onto the MALDI target (0.5µl). All experiments presented in the report were conducted in positive ionization reflector mode. Each sample was prepared by spotting

0.5µl of matrix solution (DHB) matrix in TA30 solvent, followed by 0.5 µl of sample and then allowing the mixture to dry on the target.

2.2. Solid phase peptide synthesis (SPPS) of peptides and glycopeptides on Wang resin

2.2.1 Synthesis of EEQYNSTYR and EEQFNSTFR peptide sequence

These peptides, which represent the backbone of tryptic *N*-glycopeptides of the Fc portion of human IgG, were prepared using a SPPS protocol based on Fmoc protection on Wang resin [116,117,118] The synthesis proceeded in a linear fashion from the *C*- to the *N*-terminus. Wang resin [116] is the most widely used solid phase support for acid substrates. The linker attached to the polystyrene core is a 4-hydroxybenzyl alcohol moiety. It is attached to the resin through a phenyl ether bond and the substrate is attached to the linker by a benzylic ester or ether bond. This linkage has good stability to different reaction conditions, but they can be readily cleaved by moderate treatment with an acid, generally TFA. But if the exact reaction conditions are not maintained, impurities can be formed where the linker is attached to the resin through the benzylic position leaving a reactive phenolic site. Figure 2.2 shows the structure of Wang resin.

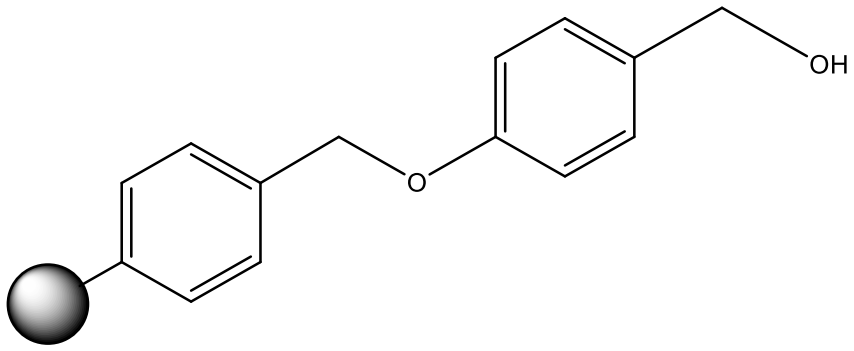

Figure 2.2. Generic structure of Wang resin (*Figure adapted from reference no 116*).

(1) Materials and reagents

The Wang resin used already had 9-fluromethyloxycarbonyl(Fmoc),2,2,4,6,7-pentamethyl dihydro benzfuran-5-sulfonyl (Pbf) protected arginine and was obtained from Bachem (Torrance, CA). The resin had an average particle size of 100-200 mesh, pale yellow in colour and a 0.6 – 1.0 mmol/g loading capacity. Other Fmoc protected amino acids Fmoc-Glu(OtBu)-OH, Fmoc-Thr(tBu)-OH, Fmoc-Gln(Trt)-OH, Fmoc-Asn(Trt)-OH, Fmoc-Tyr(tBu)-OH, Fmoc-Ser(tBu)-OH all are also purchased from Bachem (Bubendorf, Switzerland) where Fmoc = 9-fluoromethyl oxycarbonyl, Trt=Trityl, tBu=tertbutyl, OtBu=O-tertiary butyl group. Asparagine attached with peracetylated *N*-acetyl glucosamine (GlcNAc) used in this synthesis of the glycopeptide, or by its chemical name (Fmoc-L-Asn((Ac)$_3$-β-D-GlcNAc)-OH [N-α-(fluorenylmethoxycarbonyl)-N-Y-(2-Acetamido-3,4,6-tri-O-acrtyl-2-deoxy-β-glucopyranosyl)-L-asparagine] was obtained from Carbosynth (San Diego, USA). Isotopically labelled Fmoc-Tyr(t-Bu)-OH containing 9 X ^{13}C and 1 X ^{15}N was obtained from Cambridge Isotopes Laboratories, Inc (Andover, MA USA). Trypsin Gold^{TM}, mass spectrometry grade, was purchased from Promega (Madison, WI, USA). Solid phase extraction [SPE] Starta ^{TM} x 33 µm polymeric reverse phase C18, 60mg/3 ml cartridge are acquired from Phenomenex (Torrance, CA). Polyclonal human IgG purchased from Sigma, and the Herceptin mAb, modified with enzyme endoglycosidase-F (Her2F, MW 150 KDa), was obtained by cell culture[119] from J. Rini's laboratory at the University of Toronto. A fully glycosylated hybrid human-camelid mAb sample (Eg2fHc MW 150 kDa) was obtained from M. Butler's laboratory (University of Manitoba)[120,121], *O*-(Benzotriazol-1-yl)-*N,N,N',N'*-tetramethyluronium tetra fluoroborate (TBTU) was purchased from AK Scientific Inc. (Union City, CA). Methanol and acetonitrile were HPLC grade and obtained from Fisher Scientific (Nepean, ON). Distilled de-ionized water was obtained using a Milli-Q^{TM} filtration system supplied by a reverse-osmosis for all experiments.

(ii) Solid phase peptide synthesis (SPPS)

Functionalization of the resin

Initially, Wang resin (with protected arginine attached) of 150 mg were swelled in DMF for 10-15 min, then transferred into a peptide synthesis reaction vessel and washed with DMF. Each Fmoc protected amino acid (3 equivalents) was added to a coupling reagent TBTU (2 equivalents) and methyl morpholine (8 equivalents) in DMF for at least 5 min in a separate vial. The solution was then transferred to the reaction vessel containing the Wang resin for coupling (2-2.5 h). The solvent was drained off and the resin was washed with DMF (3 x 2 ml), DCM (3 x 2 ml) and DMF (3 x 2 ml).

Fmoc protecting groups were removed as before with two volumes of 4:1 DMF /pipeidine and the resins were washed with 3 volumes of each solvent DMF, DCM and DMF. After each bond formation chloranil test has been done.

Cleavage

Once the sequence was complete, after all amino acids were sequentially added to the beads, the side chain groups of the amino acids were deprotected using a mixture of 95:5 of TFA/H_2O for 2 hour 45 minutes. The resin was finally washed using 3 volumes each methanol, DCM, and again methanol. After detaching from the resin bead the peptide solution was neutralised to pH 7 by ammonium hydroxide (28.0-30.0 % solution, Sigma Aldrich) and the solvent was evaporated by rotavap^{TM} at 40°C for evaporation and kept for overnight drying and then stored at -20°C. Figure 2.3 shows the schematic representation of Solid phase peptide synthesis.

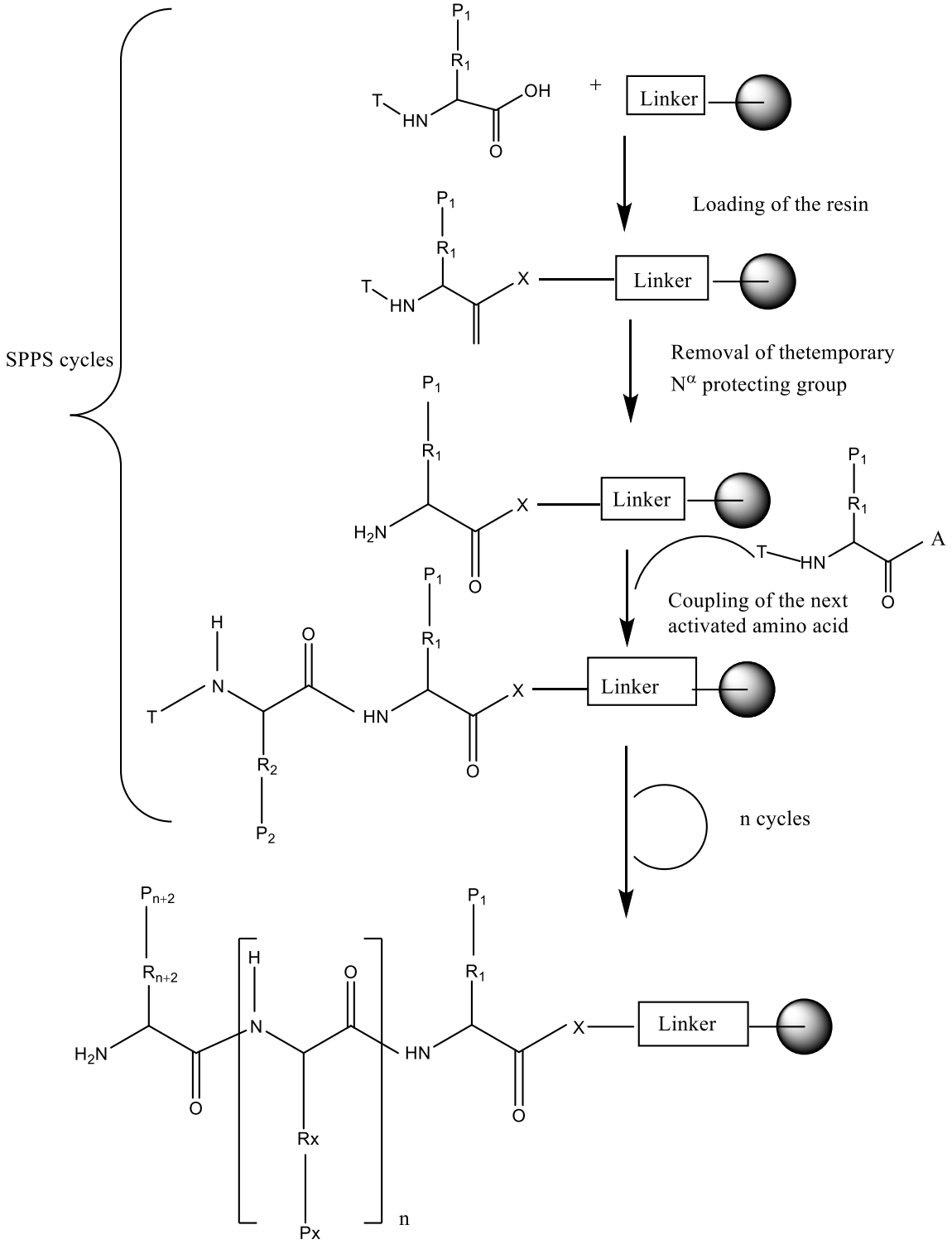

Figure 2.3. Schematic representation of solid phase peptide synthesis (*figure adapted from reference no 122*).

Clean up the peptide using a C18 cartridge (Starta^{TM}, Phenomenex, Torrance, CA)

The C18 SPE cartridge was conditioned with 5 x (1 ml of ACN+0.1 % TFA) and then with 5 x (1 ml water + 0.1 % of TFA). Each sample was applied to the column and washed with 3x (1 ml of milli Q water. Desalting and clean up of the samples were done as mentioned in section 2.1.

2.2.2. Synthesis of glycopeptide EEQYN(GlcNAc)STYR and EEQFN(GlcNAc)STFR

(1) Materials and reagents

Synthesis of IgG glycopeptide sequences EEQYN(GlcNAc)STYR and EEQFN(GlcNAc)STFR was also performed using the Fmoc procedure on Wang resin. The reagents were same as used in the previous peptide sequence. Only instead as Fmoc asparagine amino acid Fmoc-L-Asn(β-D-GlcNAc(Ac)$_3$)OH[2-acetamido-3,4,6-tri-O-acetyl-2-deoxy-b-glucopyranosyl-Fmoc-aspargine] was purchased from Carbosynth Inc (An doer, MA, USA). Moreover, K_2CO_3 and 30% ammonium hydroxide solution was purchased from Sigma Aldrich (St. Louis MO, USA) and acetic acid from Fischer Scientific (Nepean, Ontario). Figure 2.4 shows the structure of GlcNAc asparagine.

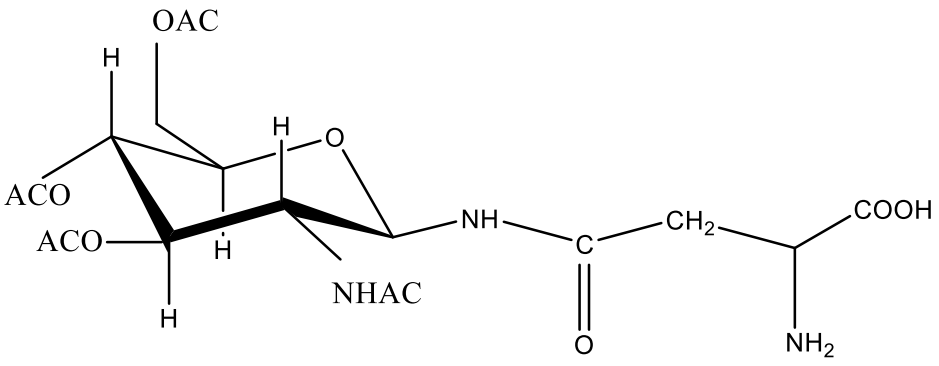

Figure 2.4. Structure of Fmoc-L-Asn(GlcNAc(Ac)$_3$-β-OH

(ii) Solid phase peptide synthesis

Synthesis of the IgG glycopeptide sequence EEQYN(GlcNAc)STYR was performed using Fmoc procedure on Wang resin. The synthesis proceeded in a linear fashion from the *C*-terminus to the *N*-terminus of the peptide. In using the Fmoc strategy, the glycopeptide runs the risk of deglycosylation only during the final deprotection strep of side chain groups with TFA. To bypass this, the hydroxyl groups on the glycan could also be protected with acetyl groups, serving as electron withdrawers to stabilize glycosidic linkages under acidic conditions.

The cycle of coupling, washing, deprotection and washing should be repeated as before till the desired sequence of glycopeptide was obtained. After the final cleavage from resin the glycopeptide was neutralized by ammonium hydroxide was dried in rotavap under vacuum.

For the removal of acetyl groups, the glycopeptide dry powder was dissolved in methanol. Then potassium carbonate solution (30%) was added at room temp. The solution was allowed to stir vigorously overnight until it turned yellow. Then the solution was neutralized to pH 7 using acetic acid. Lastly the solvent was evaporated completely in a rotavap and lastly keep it in drying station for complete drying. The same C18 cartridge clean up as described earlier was followed.

2.2.3. Synthesis of Isotopically labelled glycopeptide EEQYN(GlcNAc)ST*YR

(1) Materials and reagents

The reagents were same as used in the previous peptide sequence. Only L-Tyrosine-N-Fmoc, O-Tert-Butyl Ether ($^{13}C_9$, 99%; ^{15}N 99%) was purchased from Cambridge Isotope Laboratories Inc (Andover MA, USA) which was used as instead of normal Fmoc tyrosine. Figure 2.5 shows the structure of Isotopically labelled tyrosine. In order to get obtain absolute quantitative

information from the target samples, isotopically labeled glycopeptides were used as internal standards.

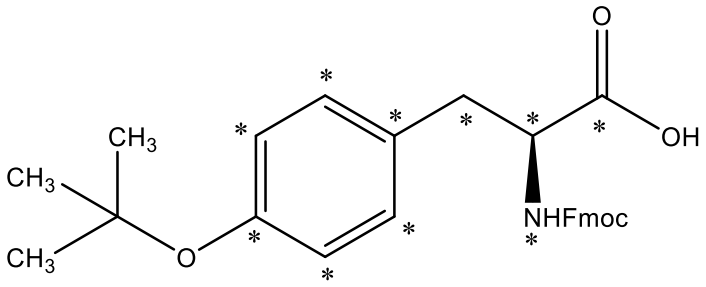

Figure 2.5. Structure of labelled Fmoc-*Tyr(t-Bu)-OH, where each * denotes a ^{13}C.

(ii) Solid Phase Peptide synthesis

Synthesis of the IgG glycopeptide sequence EEQYN(GlcNAc)ST*YR was performed using Fmoc procedure on Wang resin. The synthesis was carried out at the similar fashion as mentioned in section 2.2.2.

2.2.4. Preparation of samples for MALDI-MS analysis

Quantitative analysis.

A series of standard addition experiments were performed as listed in Table 2.1. For all experiments, four or five spots of saturated DHB (20 mg/mL in TA30) (0.5 µL) were deposited onto a 384-stainless steel polished MALDI target, and on top of each 0.5 µL of the sample solution (in TA30) was added. Then, increasing volumes of the standard solutions (in 0.1% TFA in water) were added to the spots as specified in Table 2.1. Samples were allowed to dry allowed to dry, either at room temperature, or at 37°C in the incubator for MALDI-TOF-MS analysis. The standard addition experiments were divided in three different categories:

Absolute quantitation of IgG1 in mAbs and polyclonal human IgG (Expts. i-x in Table 2.1).

Absolute quantitation of IgG2 in mAbs and polyclonal human IgG (Expts. xi-xiv in Table 2.1).

Simultaneous quantitation of IgG1 and IgG2 in polyclonal human IgG (Expt. xv in Table 2.1).

Table 2.1. Summary of standard addition experiments for the quantitative analysis of glycopeptides and peptides specific to antibodies

Expt. no.	Standard (concentration)	Analyte (conc. or est. amount digested)	Est'd total glycopeptide concentration*	Volumes used for standard additions (µL)	Glycopeptide concentration measured◊
i	EEQYN(GlcNAc)STY*R (22 mM)	EEQYN(GlcNAc)STYR (23 mM)	23 mM	0.15, 0.25, 0.50, 0.75, 1.00	23 mM
ii	EEQYN(GlcNAc)STYR (1.32 µM)	EEQYN(GlcNAc)STY*R (1.31 µM)	1.32 µM	0.25, 0.50, 0.75, 1.00, 1.25	1.32 µM
iii	EEQYN(GlcNAc)STY*R (3.32 mM)	Her2FS glycopeptides (~22 µg)	5.9 mM	0.15, 0.50, 0.75, 1.00	7.8 mM
iv	EEQYN(GlcNAc)STY*R (0.38 µM)	Her2FS glycopeptides (~2.5 ng)	0.67 µM	0.50, 0.75, 1.00, 1.25	0.31 µM
v	EEQYN(GlcNAc)STYR (5.75 mM)	Eg2hFc glycopeptides (~400 µg)	20 mM	0.15, 0.25, 0.75, 1.00	12 mM
vi	EEQYN(GlcNAc)STYR (0.079 mM)	hIgG IgG1 glycopeptides (~100 µg)	2.66 mM	0.25, 0.50, 0.75, 1.00, 1.25	0.58 mM (+0.17 mM)
vii	EEQYNSTYR (8.41 mM)	Eg2hFc glycopeptides (~400 µg)	20 mM	0.25, 0.50, 1.00, 1.25	127 mM
viii	EEQYNSTYR (1.05 mM)	hIgG IgG1 glycopeptides (~100 µg)	2.66 mM	0.5, 1.0, 2.0, 2.5	1.6 mM (+3.6 mM)
ix	EEQYN(GlcNAc)STYR (841 µM)	EEQYNSTYR (875 µM)	N/A	0.25, 0.5, 0.75, 1.0, 1.25	N/A
x	EEQYN(GlcNAc)STYR (100 mM)	EEQYNSTYR (101 mM)	N/A	0.25, 0.5, 0.75, 1.0, 1.25	N/A
xi	EEQFN(GlcNAc)STFR (0.053 mM)	IgG2 glycopeptide Sample 1	unknown	0.5, 0.75, 1.0, 1.25	0.11 mM
xii	EEQFN(GlcNAc)STFR (0.101 mM)	hIgG IgG2 glycopeptides (~100 µg)	2.66 mM	0.25, 0.5, 0.75, 1.0, 1.25	0.17 mM (+0.58 mM)
xiii	EEQFNSTFR (1.01 mM)	IgG2 glycopeptide Sample 2	unknown	0.25, 0.5, 0.75, 1.0, 1.25	0.55 mM
xiv	EEQFNSTFR (1.07 mM)	hIgG IgG2 glycopeptides (~100 µg)	2.66 mM	0.25, 0.5, 0.75, 1.0, 1.25	3.6 mM (+1.6 mM)
xv	EEQYN(GlcNAc)STYR (0.984 µM) EEQFN(GlcNAc)STFR (0.0632 µM)	hIgG IgG1 and IgG2 glycopeptides (~100 µg)	14 µM	0.25, 0.5, 0.75, 1.25	1.5 µM

**Concentration estimated from sample provider before analysis from amount of Ab digested, if known. Numbers in brackets refer to the other subclass concentration for polyclonal human IgG.

Mass spectrometric analysis

An UltraFleXtreme ^{TM} MALDI-TOF-MS instrument (Bruker Inc., Billerica, MA) was used for all most MS experiment. The samples were analyzed in a positive reflector mode. The instrument was equipped with LID-LIFT^{TM} technology for tandem MS experiments. DHB (20 mg/mL in TA30, 0.5 µL) was first spotted onto the MALDI and allowed to dry. The samples in TA30 were applied directly onto the matrix (0.5 µL or otherwise specified).

2.3. Absolute quantitation of IgG1 Abs

2.3.1. Linearity and absolute quantitation of monoclonal antibody(mAb) N glycosylated with only one core GlcNAc samples (Experiment no. i & ii)

Preparation of EEQYN(GlcNAc)STYR (m/z 1392) standard

For the Experiment i: Concentration of standard was 23 mM

For the Experiment ii: Concentration of standard was 1.32 µM

For all standards, initial dilution was done in 0.1% TFA in water. Other serial dilutions were done in TA30 (30:70 ACN: water + 0.1 % TFA)

*Preparation of EEQYN(GlcNAc)STY*R standard*

For the Experiment i: Concentration of standard was 22 mM

For the Experiment ii: Concentration of standard was 1.31 µM

For all standards, initial dilution was done in 0.1% TFA in water. Other serial dilutions were done in TA30 (30:70 ACN: water + 0.1 % TFA)

Spiking of the samples. In the experiment i and ii, saturated solution of DHB matrix in TA30 is spotted at 0.5 µl on MALDI plate, on the top of that the volume of spotted Isotopically spotted labelled standard (*m/z* 1402) was increased from 0.25,0.50,0.75,1.0,1.25µl while keeping

constant the nonlabelled glycopeptide (*m/z* 1392) at 0.5µl. All the spots were dried on the MALDI target was checked in reflector positive mode.

2.3.2. Measurement of the amount /concentration of unknown monoclonal antibody (mAb) by glycopeptide EEQYN(GlcNAc)STYR (Experiments no. iii and iv)

Preparation of mAb samples

Herceptin mAb, modified with enzyme endoglycosidase-F (Her2FS, MW 150 kDa), was obtained by cell culture and received from Dr. James Rini's Lab at the University of Toronto. These mAbs has been treated with the enzyme endoglycosidase F, so that only GlcNAc remained on asparagine. Her2FS concentration given: 0.2 µg/ µl. So approximately 22 µg sample was taken and evaporated in the speedvac and reconstituted in 44µl of the saturated solution of 50 mM ammonium bicarbonate. Then the sample was digested by Trypsin Gold ™ in 20:1 ratio. The Tryptic digestion was allowed to take place at 37°C for 18-20 hour. The digestion was stopped by freezing the sample mixture at -20°C for 30 min. After that the sample was cleaned up using a C18 reverse phase column (Starta™, Phenomenex, Torrance, CA) by following descriptive procedure. The sample solution was dried in the Savant ™ speed vac concentration. The sample fraction was reconstituted with 4 µl of TA30 which was ready for sample spiking.

The C18 SPE cartridge was conditioned with 5 x (1 ml of ACN+0.1 % TFA) and then with 5 x (1 ml water + 0.1 % of TFA). Each sample was applied to the column and washed with 3x (1 ml of milli Q water. The following elution was then performed: 0.1% TFA in 10:90 ACN: Water, 0.1% TFA in 15:85 ACN: Water, 0.1% TFA in 20:80 ACN: Water. All the eluted fractions were collected, dried and concentrated by centrifugal Speedvac™ evaporation. The sample were suspended in 4 µl of 30:70 ACN: water + 0.1% TFA in (TA30) in preparation for MALDI-T0F-MS analysis. Fractions containing the product of interest were combined.

Preparation of Isotopically labelled glycopeptide sample 1402 ($[M+H]^+$

For the Experiment iii: Concentration of standard was 3.32 mM

For the Experiment iv: Concentration of standard was 0.38 µM

All Isotopically labelled glycopeptide standard was prepared in the solution TA30 (30:70 ACN: 0.1% TFA in water).

Spiking of Isotopically labelled glycopeptide (1402) with mAb Her2FS (unknown)

The volume ratio of solutions of unknown mAb sample (1392) $[M+H]^+$ over known standard m/z 1402 $[M+H]^+$ (3.32 mM) was increased stepwise from 0 to 2.In each experiment 0.5 µl DHB matrix solution in TA30 was spotted onto the MALDI target. Then 0.5 µl of the standard solution (1402) was spotted on the top of the matrix. At last the volume of the unknown solutions was added in 0.15,0.5,0.75,1.0µl to match the ratios 0.3,1.0,1.5 and 2. All the spots were dried on the MALDI target was checked in reflector positive mode.

2.3.3. Absolute quantitation of IgG1 glycoforms from fully glycosylated mAb by glycopeptide (EEQYN(GlcNAc)STYR (m/z 1392) (Experiment no. v)

In the next set of experiments, Synthetic EEQYN(GlcNAc)STYR was used against an enriched fraction of mAb tryptic *N*-glycopeptides. The purpose was to evaluate the response factor between *m/z* 1392 ions and $[M+H]^+$ ions of glycoforms G0F, G1F and G2F.

Preparation of fully glycosylated mAb samples (Eg2hFc)

Sample concentration (fully glycosylated Eg2hFc 400). Considered molecular weight for mAb is 80 KDa. For the analysis 780 µl sample was taken and dried in a Savant SC110 speedvac, equipped with a Welch Duoseal vacuum pump. Then the solution was reconstituted in 400µl of 50 mM ammonium bicarbonate solution (pH 7.8). The sample was digested by Trypsin Gold^{TM} in a 20:1 w/w antibody to trypsin ratio for the digestion. The tryptic digestion was allowed to take place at 37°C for 18-20 hour. The digestion was stopped by freezing the sample mixture at -20° C for

30 min. After that the sample was cleaned up using a C18 reverse phase column (Starta^{TM,} Phenomenex, Torrance, CA) by following the above descriptive procedure. The sample solution was dried in the Savant ^{TM} speedvac concentration. The sample fraction was reconstituted with 4 µl of TA30 which was ready for spiking.

Preparation of glycopeptide standard EEQYN(GlcNAc)STYR (m/z 1392)

The concentration of standard glycopeptide was $5.75x10^{-9}$ moles/µl or 5.75 mM. First dilution was done in 0.1% TFA in water where as the serial dilution was done in TA30.

Standard solutions were prepared so that the spotting of equal volumes of standard and unknown would yield MALDI signals that are approximately equal to the standard and the G1F glycoform. In this experiment, 0.5 µl of DHB matrix was spotted on the MALDI target and the 0.5 µl mAb sample was spotted on the top of it. The volume of the known standard 1392 was added at the volume of 0.15, 0.25, 0.75 and 1.0 µl to match the ratios of 1392 *vs* Eg2 sample at 0.3, 0.5 1.5 and 2.0. All the samples were dried properly on the MALDI target was checked in reflector positive mode.

2.3.4. Measurement of the amount /concentration of Polyclonal Human IgG by glycopeptide EEQYN(GlcNAc)STYR (Experiment no. vi)

The same experiment was repeated with an unknown glycopeptide mixture from a tryptic digest of commercial polyclonal human IgG from Sigma (100 µg) with the known Glycopeptide EEQYN(GlcNAc)STYR standard.

Human polyclonal IgG sample from was purchased from Sigma Aldrich. The sample was digested with Trypsin enzyme. After that the sample was cleaned up using a C18 reverse phase column (Starta^{TM}, Phenomenex, Torrance, CA) by the above procedure.

The concentration of standard solution for glycopeptide EEQYN(GlcNAc)STYR was taken: 0.079 mM in TA30 (30:70 ACN:0.1% TFA in water).

For the spiking, at first 0.5 µl of matrix DHB in TA30 is spiked on the MALDI target. Then keeping constant the human IgG solution (0.5µL), the volume ratio of standard glycopeptide EEQYN(GlcNAc)STYR (*m/z* 1392) was increased from 0 to 2 (spotted volumes were 0.25, 0.50, 0.75, 1.0 and 1.25 µl to match the 1392/ Human IgG glycopeptide ratios of 0.5,1.0,1.5,2.0 and 2.5. The MALDI samples were analyzed by MALDI in reflector positive mode with proper calibration.

2.3.5. Measurement of the amount /concentration of unknown monoclonal antibody mAb by peptide EEQYNSTYR $[M+H]^+$ *m/z* 1189 (Experiment no. vii)

The synthetic peptide EEQYNSTYR (*m/z* 1189 for $[M+H]^+$ ions) was also used as a potential internal standard for the quantitation of mAb glycoform (Eg2-hfc). Considered molecular weight for mAb is 80 KDa. For the analysis of 637 µl sample was taken and dried in a Savant SC110 speed vacuum pump. Then the solution was reconstituted by 400µl of 50 mM ammonium bicarbonate solution. For digestion Trypsin Gold ™ was added to the sample at 20:1 ratio. The tryptic digestion was allowed to take place at 37°C for 18-20 hour. The digestion was stopped by freezing the sample mixture at -20°C for 30 min. The sample was cleaned up using a C18 reverse phase column (Starta™, Phenomenex, Torrance, CA). The samples were eluted with two fractions of 500 µl portions of 0.1% TFA in 5:95 ACN: Water, then 2 X 500 µl portions of, 0.1% TFA in 10:90 ACN: water, 2 x 500 µl portions of 0.1% TFA in 15:85 ACN: water and 2x 500 µl of 0.1% TFA in 30:70 ACN: water. All the eluted fractions were dried using the Savant ™ speedvac concentrator (SC110). Each fraction of the dried sample was reconstituted with 6µl of TA30 and the samples are ready for spiking.

Concentration of standard peptide solution (EEQYNSTYR: *m/z* = 1189) was 8.41mM

At first 0.5 µl matrix DHB was spotted on the MALDI target. Then 0.5 µl of mAb sample was spotted on the top of it on each spot. The known standard 1189 was spiked at 0.25, 0.5, 1.0

and 1.25 µl to get the ratio of 1189 over mAb will be 0.5, 1.0,2.0 and 2.5. All the spotted solutions on the target were dried and checked in MALDI in reflector positive mode.

2.3.6. Measurement of the amount /concentration of Polyclonal Human IgG by peptide EEQYNSTYR (*m/z* 1189) (Experiment no. viii)

The synthetic peptide (*m/z* 1189) can be used in the same fashion to quantitate the commercial polyclonal human IgG from Sigma Aldrich. The sample was digested with the enzyme Trypsin Gold for 18-20 hours at 37°C. After that reaction was stopped by freezing. After that the sample was cleaned up using a C18 reverse phase column (Starta^{TM} , Phenomenex, by using 2 x 500 µl of 10:90 ratio of ACN:0.1% TFA in water, 2 x 500 µl of 15:85 ratio of ACN:0.1% TFA in water and lastly 2 x 500 µl of 30:70 ratio of ACN:0.1% TFA in water. Each fraction was dried in the Savant ^{TM} speed vac concentration. The sample fraction was reconstituted with 10 µl of TA30 (30:70 ACN:0.1% TFA in water) which was ready for spiking.

Concentration of standard peptide EEQYNSTYR (*m/z* 1189): 875µM

For spiking 0.5 µl of matrix solution of DHB in TA30 was spotted on the MALDI target. On the top of that 0.5 µl of human IgG solutions were spotted in each spot. The volume of standard peptide solution was added at 0.5, 0.75, 1.0 and 1.25 µl to match the ratio of 1.0, 1.5, 2.0 and 2.5. The samples were dried and checked by MALDI at reflector positive mode.

2.4. Comparison of the area of equimolar mixture of EEQYNSTYR (*m/z* 1189) *vs* EEQYN(GlcNAc)STYR (*m/z* 1392) (Experiments no. ix and x)

Standard solution of peptide and glycopeptides were spiked at different concentrations to measure the relative areas of both compounds.

In the first set of experiment the concentration of 1189 and 1392 were 875 and 841 µM respectively and for the second set the concentrations were 101 and 100 mM accordingly. The

standard solutions were prepared at two different concentrations range to have a good comparison. All the standard solutions were prepared in TA30 (30:70 ACN:0.1% TFA in water).

First 0.5 µl of DHB matrix in TA30 was spotted on the target. On the top of that peptide standard (*m/z* 1189) was spotted 0.5 µl (keeping constant) varying glycopeptide (*m/z* 1392) to keep the ratio of 1189 over 1392 at 0.5, 1.0, 1.5 and 2.0 for first set of experiments and 0.5, 1.0 1.5, 2.0 and 2.5 for the second set of experiments.

2.5. Absolute quantitation of IgG2 Abs

2.5.1. Measurement of the amount glycoforms in a fraction containing only IgG2 *N*-glycopeptides by glycopeptide EEQFN(GlcNAc)STFR (*m/z* 1360) (Experiment no. xi)

The glycosylated synthetic peptide was used EEQFN(GlcNAc)STFR as an internal standard for the quantitation of IgG2 in samples containing only this subclass of human IgG. For this experiment samples from human IgG came from healthy patients tested during a MGUS study.[62] The given sample concentration was 0.98 mg/mL and the volume used was 51µl as the sample were already in ammonium bicarbonate 100 mM, only 4 µl of trypsin (Promega) was added in 1:25 ratio and left the human IgG samples going to an overnight tryptic digestion at 37°C Then the sample was dried on a speed vacuum.

The concentration of standard glycopeptide EEQFN(GlcNAc)STFR (*m/z* 1360): 0.053 mM

For the spotting experiment, at first 0.5 µl matrix DHB was spotted on the MALDI target. Then 0.5 µl of human IgG2 sample was spotted on the top of it on each spot. The known glycosylated standard 1360 was spiked at 0.5, 0.75, 1.0 and 1.25 µl to get the ratio of 1189 over mAb will be 1.0, 1.5, 2.0 and 2.5. All the spotted solutions on the target were dried and checked in MALDI in reflector positive mode.

2.5.2. Measurement of the amount /concentration of glycopeptide from polyclonal human IgG by glycopeptide EEQFN(GlcNAc)STFR (*m/z* 1360) (Experiment no. xii)

The human polyclonal IgG sample was prepared as the same procedure as Experiment no. vi. The concentration of standard glycopeptide EEQFN(GlcNAc)STFR (*m/z* 1360): 0.101 mM.

For the spotting purpose, at first 0.5 µl matrix DHB was spotted on the MALDI target. Then 0.5 µl of human polyclonal IgG sample was spotted on the top of it. The known glycosylated standard 1360 was spiked at 0.25, 0.5, 0.75, 1.0 and 1.25 µl to get the ratio of 1189 over mAb will be 0.5, 1.0, 1.5, 2.0 and 2.5. All the spotted solutions on the target were dried and checked in MALDI in reflector positive mode.

2.5.3. Measurement of the amount glycoforms in a fraction containing only IgG2 *N*-glycopeptides by peptide EEQFNSTFR (*m/z* 1157) (Experiment no. xiii)

The sample was prepared following the same procedure as Experiment no. xi.

The concentration of standard peptide EEQFNSTFR (*m/z* 1157): 1.01 mM

For spotting, 0.5 µl matrix DHB was spotted on the MALDI target. Then on top of that 0.5 µl of human IgG sample was spotted. The known glycosylated standard 1157 was spiked at 0.5, 0.75 and 1.25 µl to get the ratio of 1189 over mAb will be 1.0, 1.5 and 2.5. All the spotted solutions on the target were dried and checked in MALDI in reflector positive mode.

3.5.4. Measurement of the amount of tryptic glycopeptide fractions from polyclonal human IgG by internal peptide standard EEQFNSTFR (Experiment no. xiv)

The sample was prepared following the same procedure as Experiment no. viii

The concentration of standard peptide EEQFNSTFR (*m/z* 1157): 1.07 mM

For analysis, 0.5 µl matrix DHB was spotted on the MALDI target. Then on top of that 0.5 µl of human IgG sample was spotted. The known peptide standard 1157 was spiked at 0.25, 0.5, 0.75 1.0 and 1.25 µl to get the ratio of 1189 over mAb will be 0.5, 1.0, 1.5, 2.0 and 2.5. All the spotted solutions were dried and checked in MALDI in reflector positive mode.

2.6. Comparison of IgG1 and IgG2 signals when respective (glyco)peptides are mixed on-target.

i) Relative ionization efficiencies of IgG1 and IgG2 glycopeptides

For the first experiment, both synthetically prepared glycopeptides EEQYN(GlcNAc)STYR (*m/z* 1392) and EEQFN(GlcNAc)STFR (*m/z* 1360) are spiked together on the MALDI target along with DHB matrix. The known glycosylated standard (For IgG2 EEQYF(GlcNAc)STFR (*m/z* 1360) was spiked at the other synthetic glycopeptide at the volume of 0.25, 0.5, 0.75 1.0 and 1.25 µl to get the ratio of 1360 over 1392 will be 0.5, 1.0, 1.5, 2.0 and 2.5. All the spotted solutions were dried and checked in MALDI in reflector positive mode.

Next the tryptic glycopeptides fractions from Eg2 (for IgG1) and human IgG2 from polyclonal human IgG (for IgG2) were spiked together. On the 0.5 µL of DHB, Eg2 (sample was spotted at 0.5 µL, on the top of that human IgG2 sample was spiked at the volume of 0.25, 0.5, 0.75 1.0 and 1.25 µl to get the ratio of Eg2 over IgG will be 0.5, 1.0, 1.5, 2.0 and 2.5. All the spotted solutions were dried and checked in MALDI in reflector positive mode.

In the third experiment, both synthetically prepared glycopeptides (*m/z* 1392 and 1360) will spike to the tryptic glycopeptides from mAb sample as well as human IgG sample. To a constant amount of analyte, both standards were added in identical increasing amounts. In each experiment, 0.5 µL of the analyte solution (human IgG) was spotted onto the target, and the

volumes of both standard glycopeptide solutions (1360 and 1392) were added to match the ratios of 0.5, 1.0, 1.5 and 2.0.

ii) Different solubilities of the peptides having an impct on ionization

In this experiment an equimolar mixture of EEQYNSTYR and EEQFNSTFR was prepared in water and spotted on MALDI target.

Concentration of peptide EEQYNSTYR : 1.2 µM in water

Concentration of peptide EEQFNSTFR : 1.16 µM in water

First 5µL DHB was spotted on the MALDI target, then mixture of the both peptides were spotted on it. The mixture was dried and analyzed by MALDI. Then a drop of water was added onto dry pipetted water withdrawn from the sample after 90 s was also spotted on the target and analyzed by MALDI.

For the next experiment, equimolar solution of the synthetic peptides prepared in 0.1% TFA in water and in an aqueous acetonitrile solution (TA30) and compared the intensity of both peaks. This experiment was done to observe the effect of introduction of acetonitrile as a solvent.

Chapter-3 Results and Discussions

Intact human IgG1 and IgG2 which are the most abundant subclasses of human IgG have very similar molecular weights but also a few different amino acids in the conserved gamma sequences of the heavy chains. It is difficult to measure the abundance of subclass components of intact polyclonal IgG by direct ESI-MS or MALDI-MS, especially if the variable portions are unknown. In order to quantify these two subclasses in a variety of IgG samples, the use of internal standards EEQYNSTYR (peptide), EEQYN(GlcNAc)STYR (glycopeptide) and EEQYN(GlcNAc)STY*R has been attempted for IgG1, and EEQFNSTFR (peptide) and EEQFN(GlcNAc)STFR for IgG2. These correspond to tryptic peptides from the *N*-glycosylated portion of the Fc of IgG1 and IgG2. Assuming that 100% of the Fc's are glycosylated on asparagine-297, the quantitation of these segments will directly reflect subclasses concentrations.

3.1. Attempt to prepare novel stationary phase

In another context, the original aim of this M.Sc. project was to design a novel stationary phase for chromatography, by developing a silica resin modified with EEQYNSTYR. As this stationary phase did not meet expectations of better peptide separation relative to C18, it was decided to use this method to synthesize and release peptides for internal standard use. Thus, the first successful attempt at preparing non-glycosylated EEQYNSTYR consisted of using an aminopropyl silica as the solid support and building the sequence EEQYNSTYRGGG, such that the R-G bond could be hydrolysed by trypsin and the triglycine segment (GGG) acted as a spacer was added to the synthetic peptide EEQYNSTYR because tryptic cleavage was not functioning as a result of arginine being too close to the silica beads. Glycine was chosen, as its hydrogen side chain group is the simplest, and least likely to interfere with the action of the enzyme.

Initial efforts were thus concentrated on learning the well-established method of solid phase peptide synthesis (SPPS) based on the (9-fluorenylmethyloxycarbonyl (Fmoc) strategy [86] directly onto the silica beads. For sequence verification, the modified beads were subjected to trypsin to liberate the peptide in solution with subsequent clean up by C18 SPE. The sample elution fraction yielded the peptide with 64% purity. Purity was obtained as the % peak areas in the mass spectrum. Reversed phase C18 clean up did not allow of these impurities from the main components. The peak of the desired peptide EEQYNSTYR is shown at *m/z* 1189 ($[M+H]^+$ Figure 3.1). The sequence was further verified with MS/MS, with most peaks identified as characteristic fragments of the peptide. (Figure 3.2)

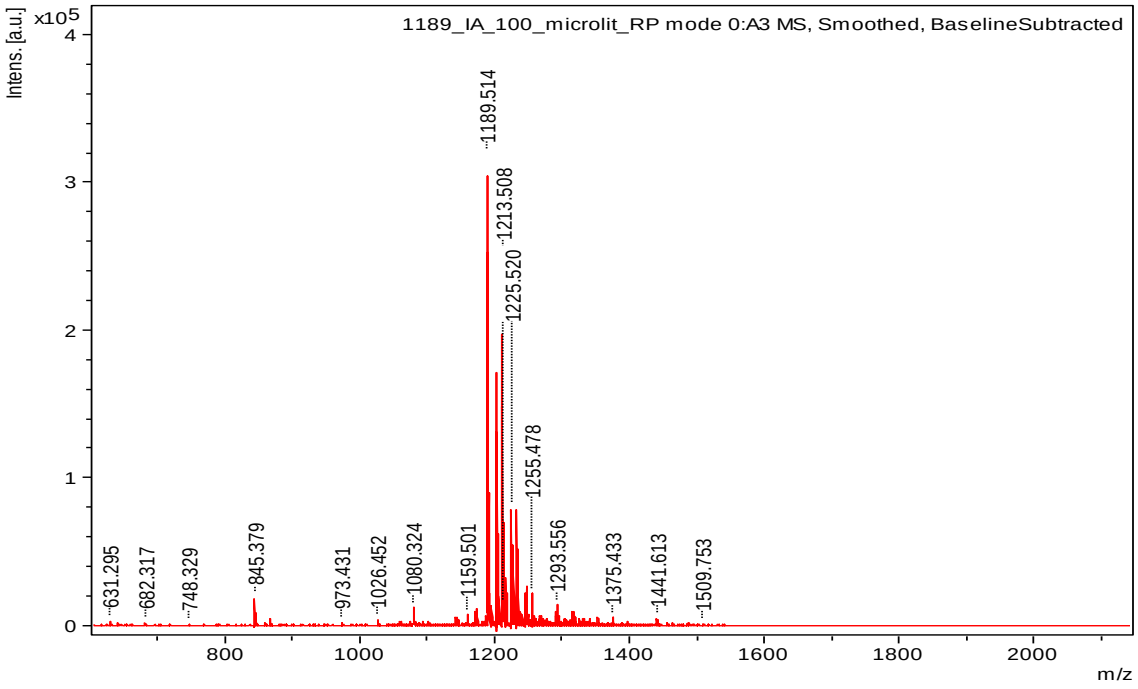

Figure 3.1. MALDI-ToF-MS of EEQYNSTYR peptide synthesized on silicycle (amino silica) resin. A peak at *m/z* 1189 corresponding to the $[M+H]^+$ ions of the peptide EEQYNSTYR is observed.

To verify the amino acid sequence of the peptide, MS/MS was conducted. Figure 3.2 shows the fragment ions of the EEQYNSTYR and the Figure 3.3 shows the y ion and b ions cleavage sites of the corresponding peptides.

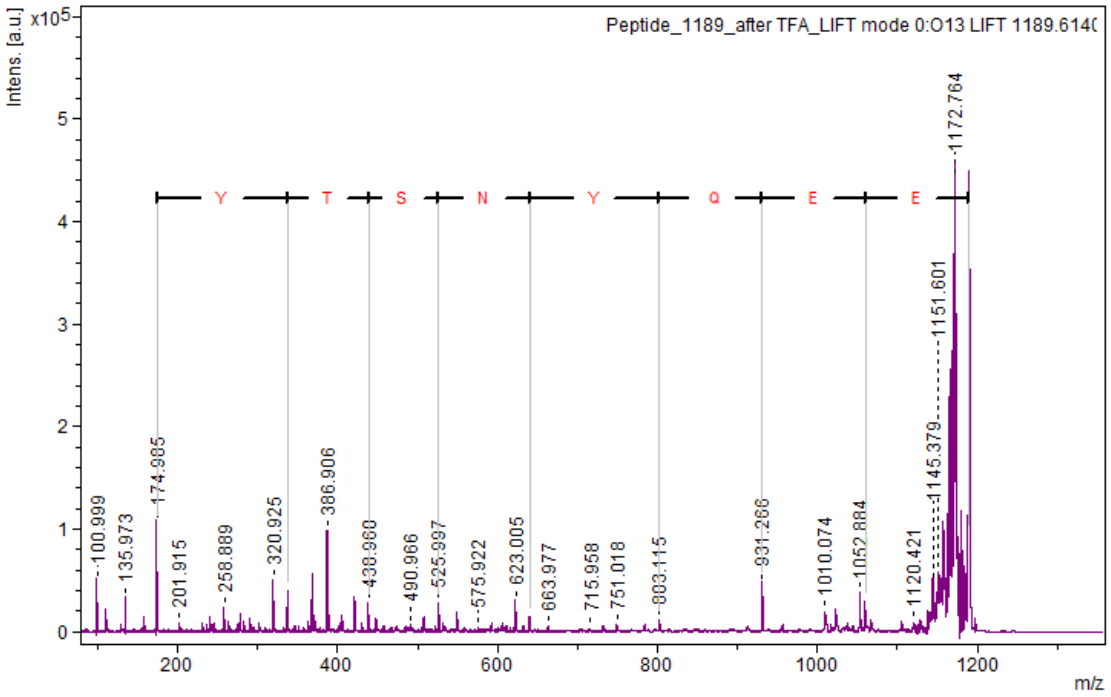

Figure 3.2. MALDI-ToF MS/MS spectrum of EEQYNSTYR at *m/z* 1189 corresponding to the $[M+H]^+$ ions of peptide.

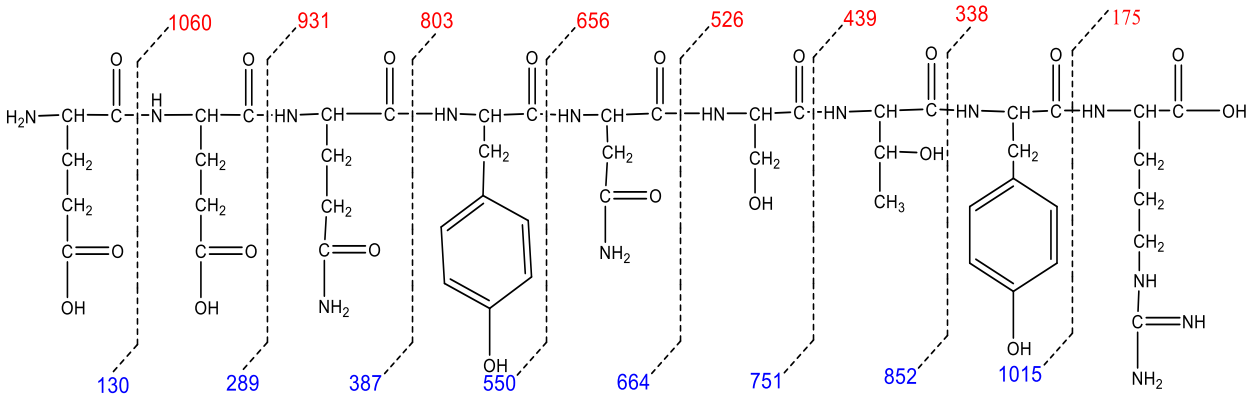

Figure 3.3. MS/MS mode: **Red indicates "y" ions,** where as **blue indicates "b" ions**

This synthetic experiment was successful; however, it was difficult as aminosilica particles tended to adhere to the wall of the glass apparatus used for SPPS. A decision was then made to use the Wang resin method[116] for the synthesis of peptide and glycopeptide standards, where neither GGG spacer nor tryptic digestion are needed to yield the desired sequence.

3.2. Synthesis of IgG1-related (glyco)peptides

The desired peptide [EEQYNSTYR (*m/z* 1189)] of interest was then synthesized on Wang resin. In SPPS, the starting *C*-terminal amino acid is linked to an inert solid support (Wang resin). Peptide bond formation is achieved by the activation of the free carboxyl group of the incoming amino acid. Then the synthesized peptide is cleaved from the resin, and cleaned up. Figure 3.4 gives the MALDI mass spectrum of the peptide (*m/z* 1189) after clean up on SPE C18 cartridge.

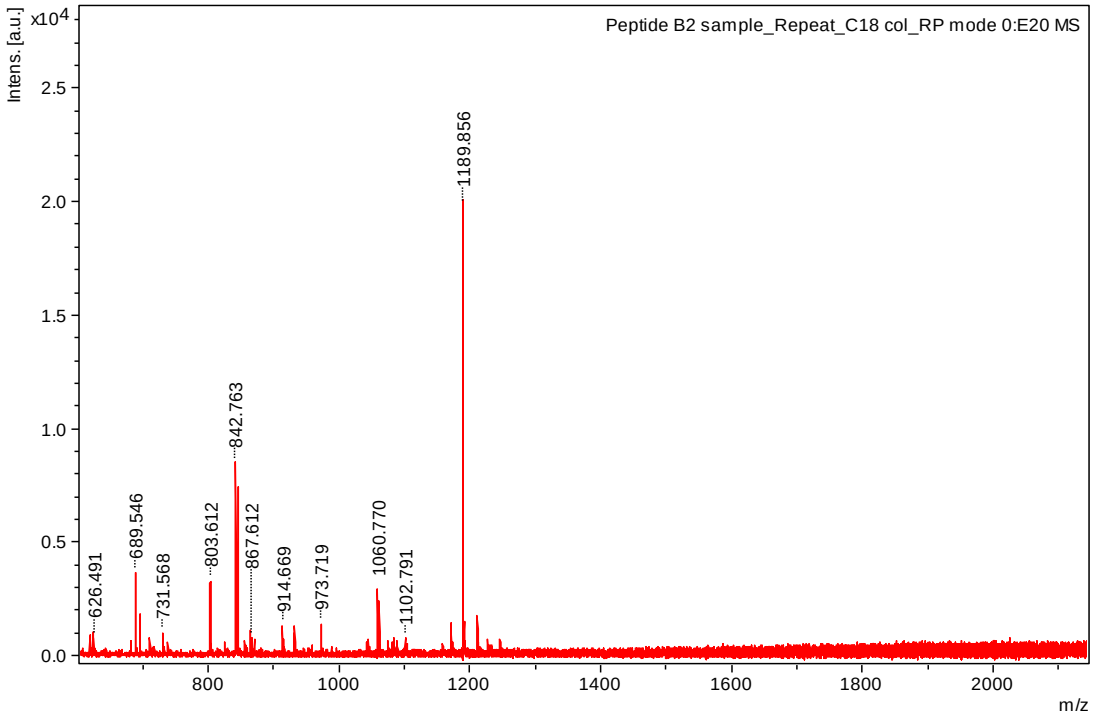

Figure 3.4. MALDI-ToF-MS of EEQYNSTYR peptide synthesized on Wang resin. A peak at *m/z* 1189 corresponding to the $[M+H]^+$ ions of the peptide EEQYNSTYR is observed.

Purity of the peptide was estimated at 57.60%. Figure 3.5 shows the MS/MS spectrum of *m/z* 1189 ions to confirm the amino acid sequence and Figure 3.3 shows the **y** ions and **b** ions cleavage sites of the corresponding peptide.

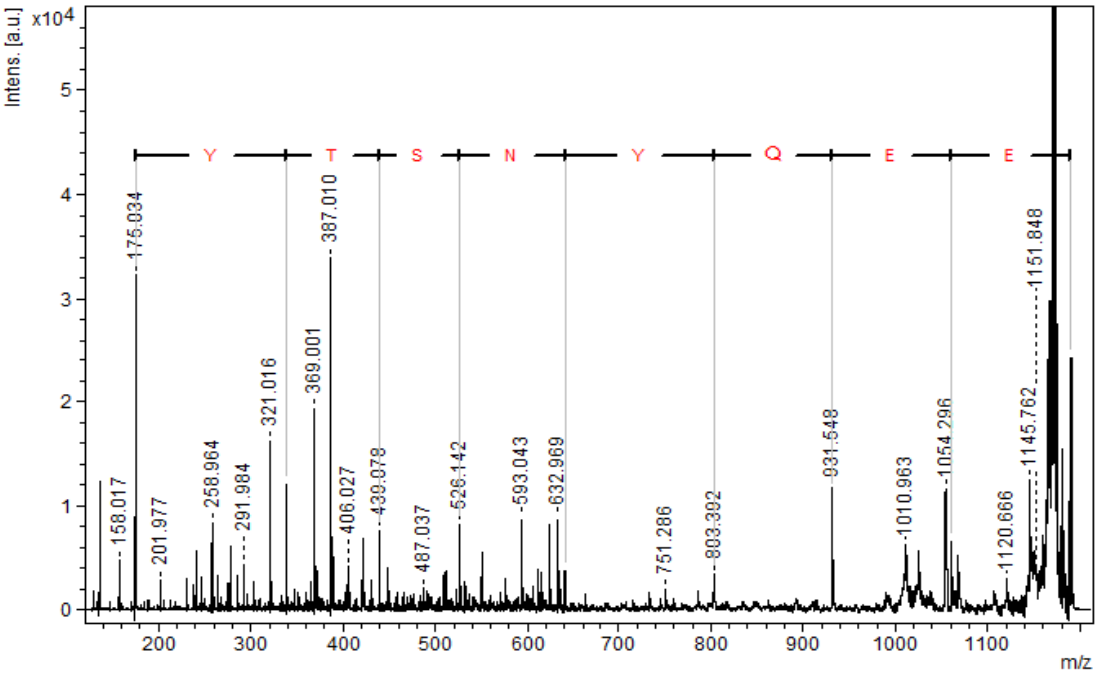

Figure 3.5. MALDI-ToF MS/MS spectrum of non-glycosylated EEQYNSTYR at *m/z* 1189 corresponding to the $[M+H]^+$ ions of peptide.

The glycopeptide EEQYN(GlcNAc)STYR was then synthesized on Wang resin. Glycosylated protected asparagine was introduced (with peracetylated GlcNAc) to try and minimize the extent of potential side reactions. This protected Asn(GlcNAc) was thus used as the building block instead of protected asparagine. The synthesis was completed and *O*-deacetylation of GlcNAc was necessary.

It was attempted to dry the acetylated glycopeptide by nitrogen gas drying to avoid any contamination. But still lots of peaks were observed in the mass spectrum. Figure 3.6 shows that deacetylation of the glycopeptide led to many products. The predicted $[M+H]^+$ peak was observed at *m/z* 1518, however several other peaks separated by 14 *m/z* units indicated the possibility of overmethylation, while no intended methylation reagent was used during this reaction. This was due to the use of methanol under acidic conditions, most probably leading to methylation of the

sugar hydroxyl group. But later on it was realized that methylation of the glycopeptides occurred while detaching from the resin using TFA, followed by elution with methanol.

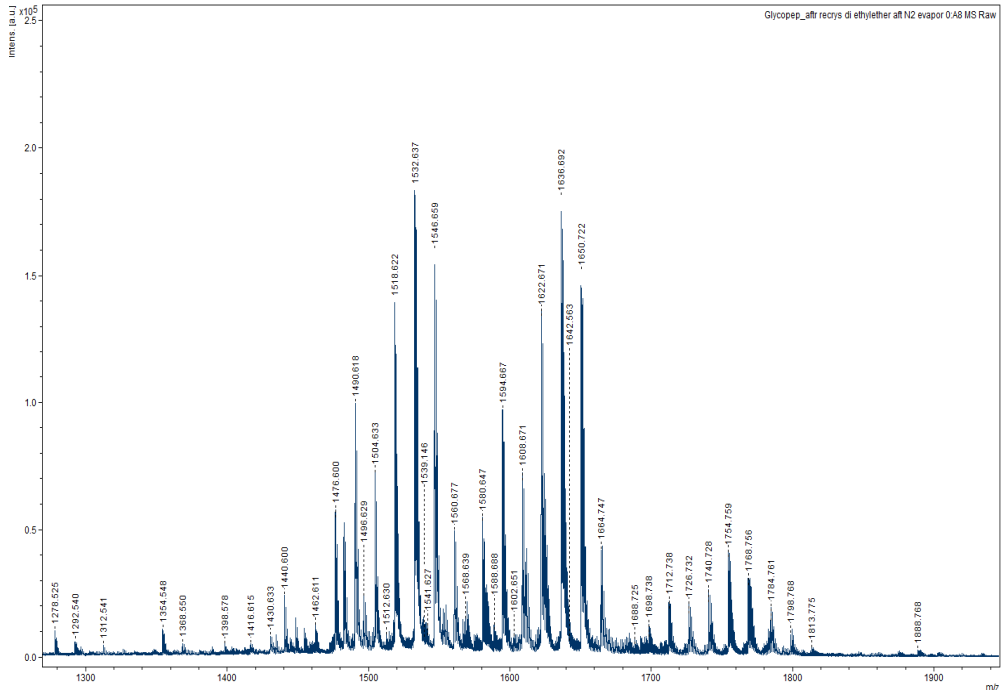

Figure 3.6. MALDI-ToF-MS spectrum of acetylated glycopeptide products around the predicted peak (*m/z* 1518) after nitrogen gas drying.

Then other portion of deacetylated glycopeptide was dried by rotary evaporation and freeze drying also. Both methods succeeded, and Figure 3.7 shows the MS spectrum of the acetylated glycopeptide (*m/z* 1518) after rotary evaporation drying.

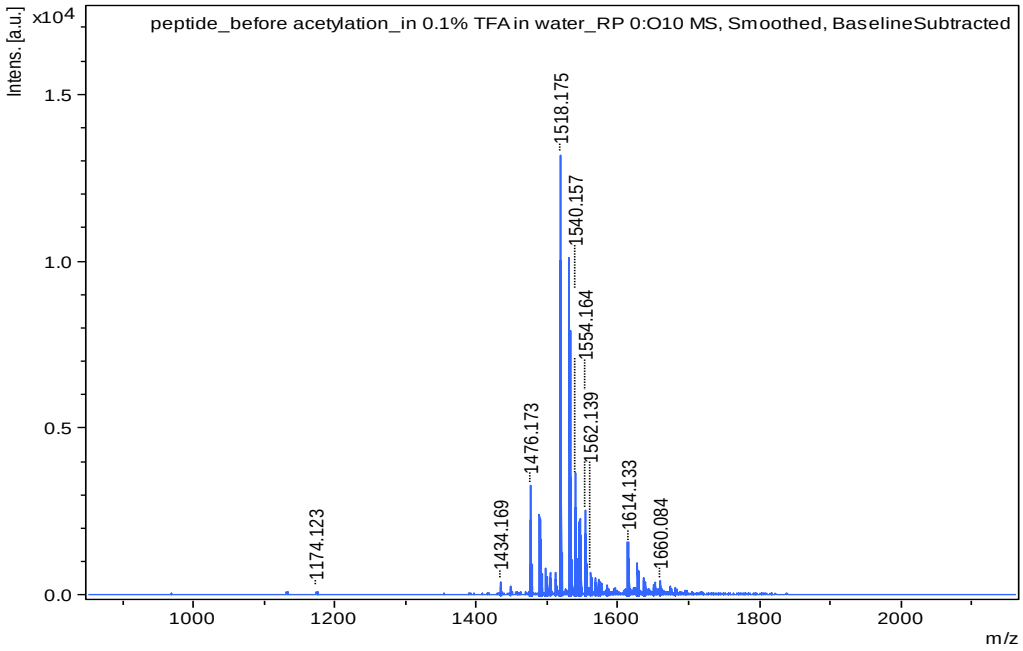

Figure 3.7. MALDI-ToF-MS spectrum of acetylated glycopeptide EEQY(GlcNAc)NSTYR with peak at *m/z* 1518 $[M+H]^+$ after SPE C18 cartridge clean up.

MS/MS fragmentation was used to verify that the proper amino acid sequence and glycosylation site were obtained. Figure 3.8 shows the fragmentation pattern of the acetylated glycopeptide.

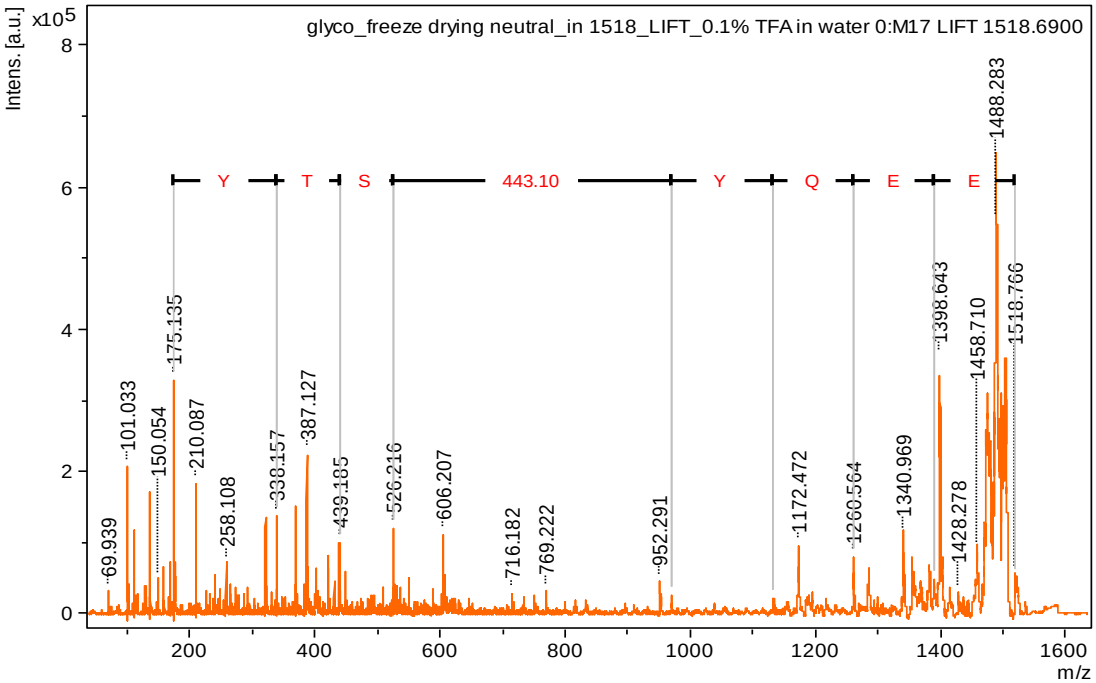

Figure 3.8. MALDI-MS/MS spectrum of acetylated glycopeptide EEQYN(GlcNAc)STYR synthesizing on Wang resin. Sequencing is based on y ions. The gap of 443 *m/z* corresponds to peracetylated Asn-GlcNAc. See Figure 3.9 for fragment ion peak assignments.

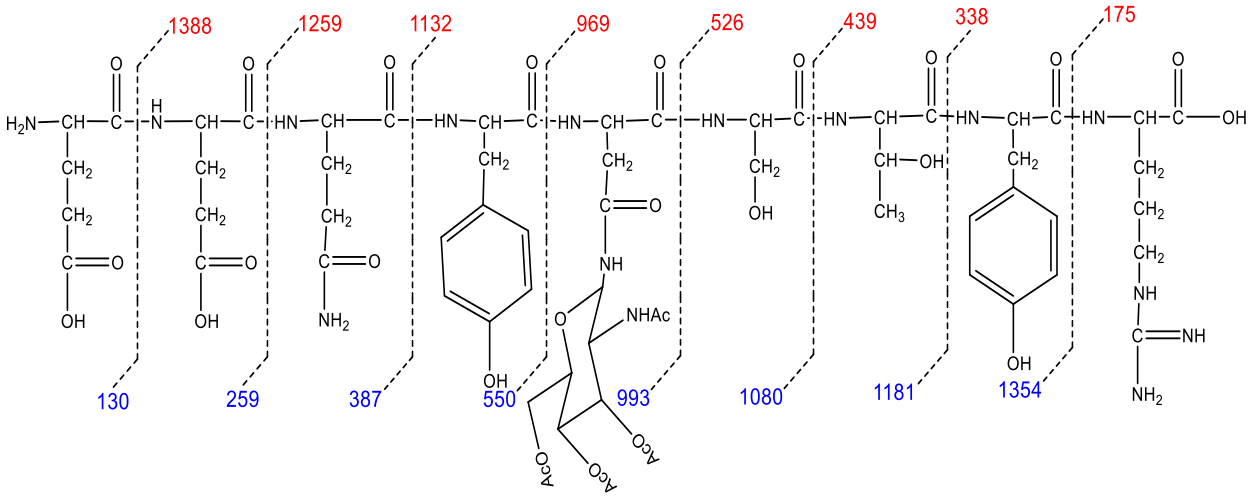

Figure 3.9. MS/MS mode: **Red indicates "y" ions,** where as **blue indicates "b" ions**

Deacetylation was then necessary to obtain the desired glycopeptide EEQY(GlcNAc)STYR, with predicted $[M+H]^+$ ions at *m/z* 1392. Methanolic potassium carbonate was used for this purpose. The first products observed (Figure 3.10) indicated overmethylation (as explained page 65). However, results in Figure 3.6 led to believe that methylation took place prior to the deacetylation. Indeed, during the Wang resin SPPS process, methylation of the glycopeptide occurred while detaching from the resin using TFA, followed by elution with methanol.

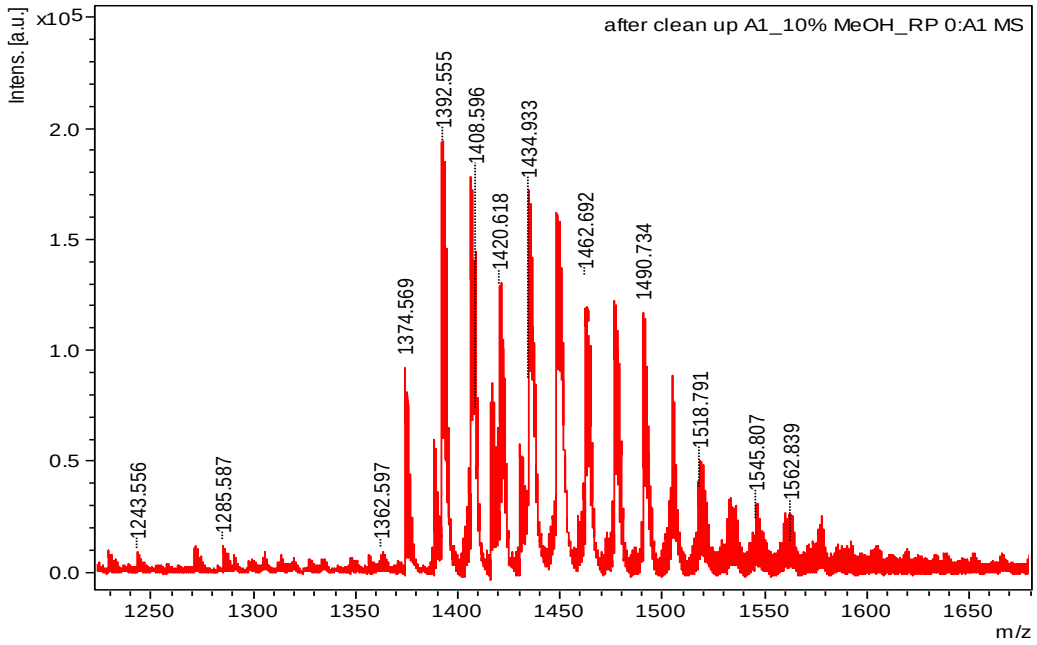

Figure 3.10 MALDI-ToF-MS spectrum of deacetylated glycopeptide EEQYN(GlcNAc)STYR (*m/z* 1392), showing overmethylation.

To avoid methylation due to acidic condition, a quick neutralization of the synthetic peptide mixture with ammonium hydroxide solution immediately after detachment, followed by freeze drying, helped to minimize methylation. Figure 3.11 shows the peak of the glycopeptide at *m/z* 1392 $[M+H]^+$ after neutralizing by ammonium hydroxide and deacetylation. The peak at *m/z* 1374 is due to in-source loss of water from 1392. The peak at *m/z* 1406 results from methylation. The peak at *m/z* 1434 denoted a residual acetyl group attached to the glycopeptide. The peak at 1518 shows that some peracetylated compounds is still left. The purity of EEQYN(GlcNAc)STYR is therefore estimated to 61.42%.

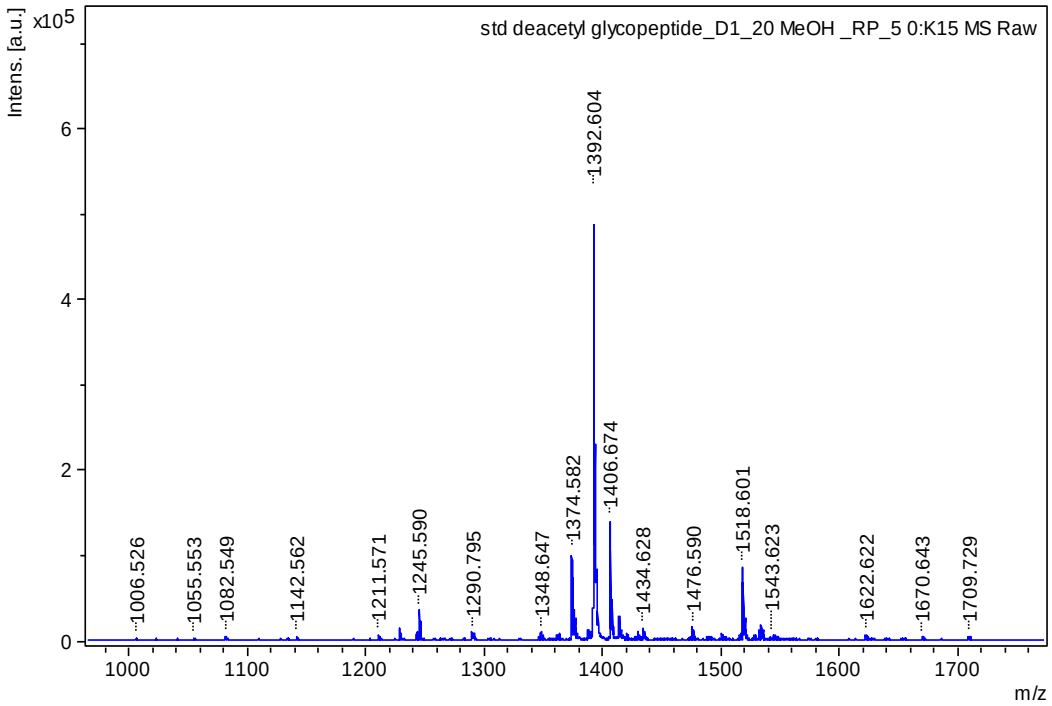

Figure 3.11. MALDI-ToF-MS spectrum of deacetylated glycopeptide EEQYN(GlcNAc)STYR after cleanup by SPE C18 cartridge, showing main $[M+H]^+$ peak at *m/z* 1392.

To verify the sequence, MS/MS was done on *m/z* 1392 ions. Figure 3.12 shows the amino acid sequence in the glycopeptide.

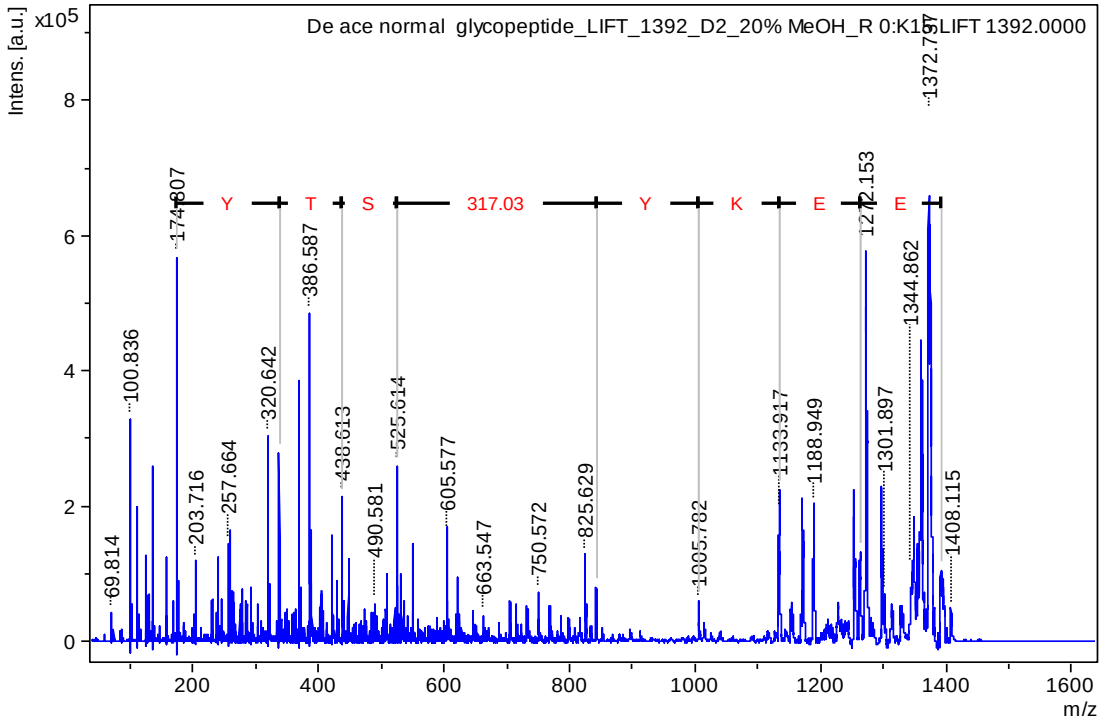

Figure 3.12. MALDI-MS/MS spectrum of $[M+H]^+$ ions of glycopeptide EEQYN(GlcNAc)STYR at *m/z* 1392. Sequencing is based on y ions. The 317 gap corresponds to Asn(GlcNAc).

Then, an isotopically labelled glycopeptide was synthesized by the same method (to be used for absolute quantitation), in which normal tyrosine was replaced by isotopically labelled tyrosine. Figure 3.13 shows MALDI-ToF-MS spectrum of the acetylated isotopically labelled glycopeptide. The main peak is $[M+H]^+$ of the expected product at *m/z* 1528. The mass was increased by 10 units relative to the non-labelled acetylated glycopeptide (1518). The peak at 1542 results from methylation, and that at 1486, from underacetylation.

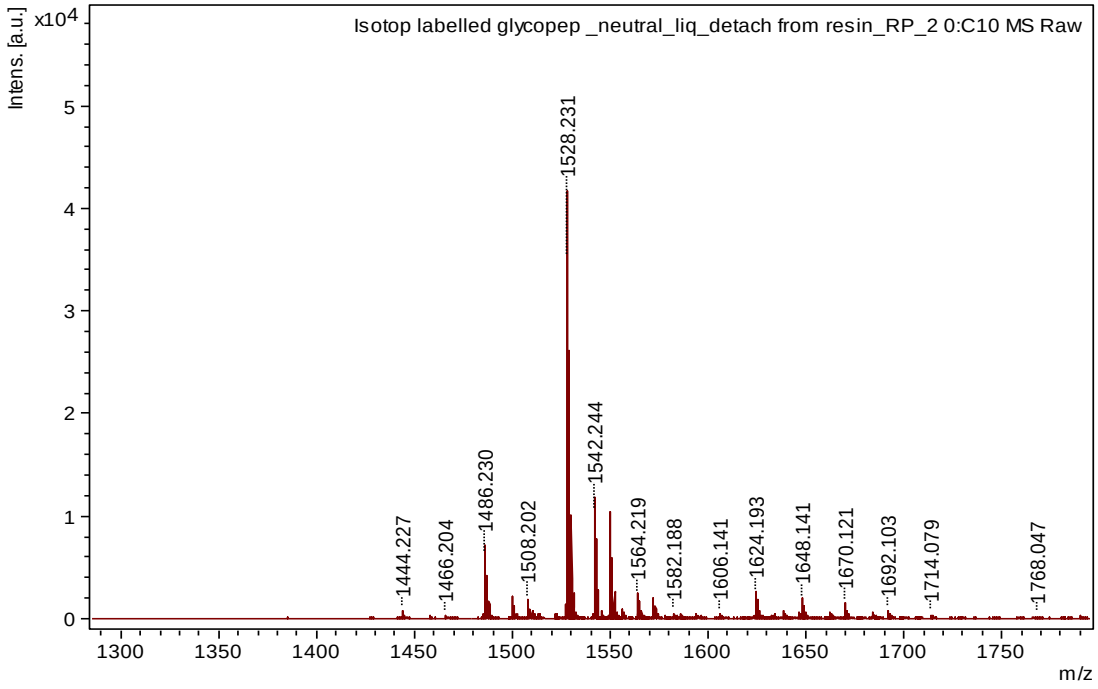

Figure 3.13. MALDI-ToF-MS spectrum of the isotopically labelled acetylated glycopeptide EEQYN(GlcNAc)STY*R (*m/z* 1528, $[M+H]^+$).

The amino acid sequence of the acetylated isotopically labelled glycopeptide was characterised by MS/MS. Figure 3.14 shows the fragmentation pattern of the acetylated glycopeptide. The gap due to the modified Y residue is 173 *m/z* instead of 163.

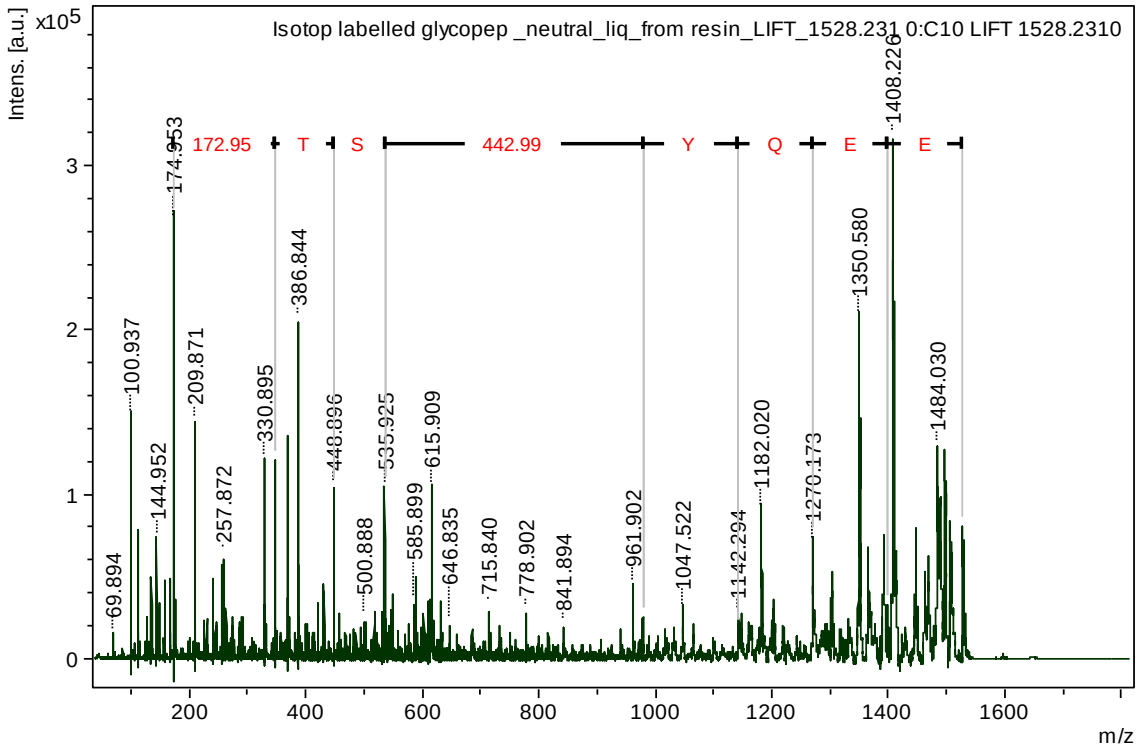

Figure 3.14. MALDI-MS/MS spectrum of the $[M+H]^+$ ions (*m/z* 1528) of isotopically labelled glycopeptide EEQYN(GlcNAc)STY*R. Sequencing was based on y ions. The 443 gap corresponds to peracetylated Asn(GlcNAc). The 173 gap is due to labelled tyrosine.

Deacetylation of the glycopeptide was done by potassium carbonate in methanol. Figure 3.15 shows the MS spectrum of the deacetylated isotopically labelled glycopeptide. The main product produced a $[M+H]^+$ peak at *m/z* 1402, while in-source loss of water gave rise to a peak at 1384, and methylation, a peak at 1416. The peak at *m/z* 1444 denoted a residual acetyl

group attached to the glycopeptide. These products were not separable by C18 SPE and purity was determined to be 68.40%.

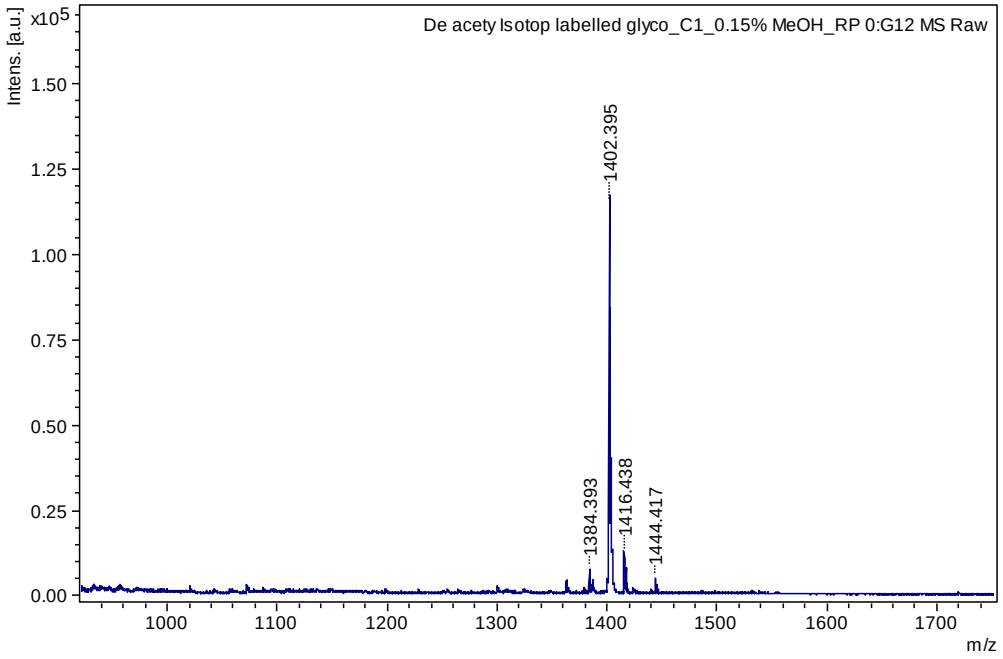

Figure 3.15. MALDI-ToF-MS spectrum of the deacetylated isotopically labelled glycopeptide EEQYN(GlcNAc)STY*R (*m/z* 1402, $[M+H]^+$).

Figure 3.16 shows the MS/MS spectrum of deacetylated isotopically labelled glycopeptide (EEQYN(GlcNAc)STY*R with *m/z* 1402, $[M+H]^+$ ions.

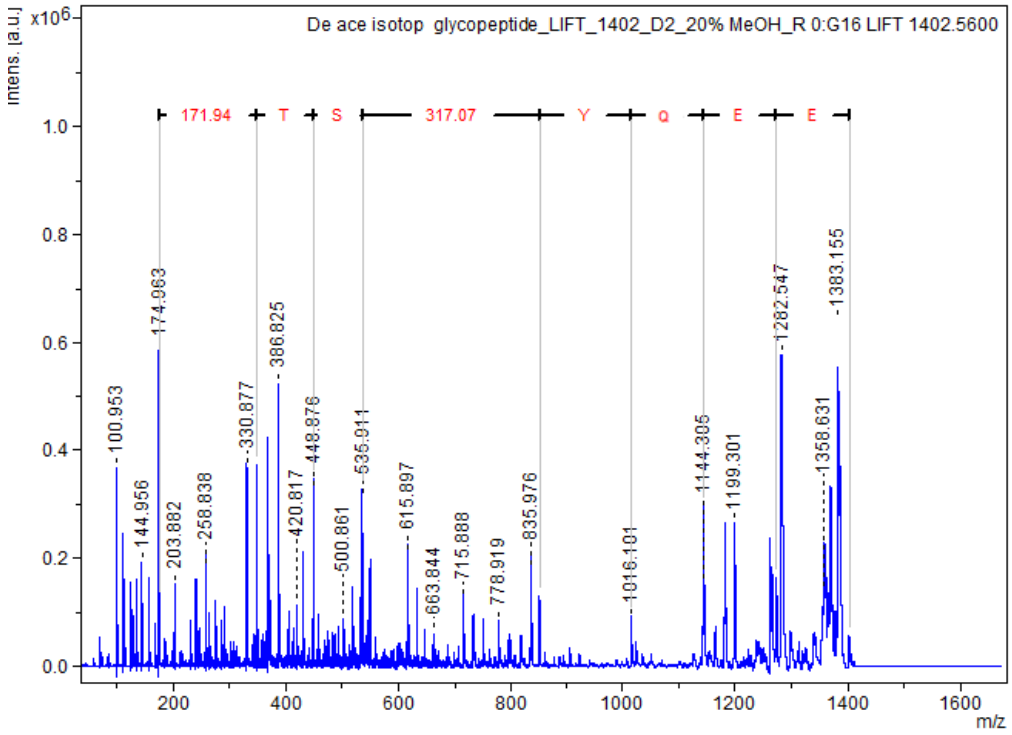

Figure 3.16. MS/MS of isotopically labelled EEQYN(GlcNAc)STYR glycopeptide, after deacetylation. Precursor ions are *m/z* 1402, $[M+H]^+$. Sequencing is based on y ions. The 317 gap represents Asn(GlcNAc).

Figure 3.17 shows the y and b ions of Isotopically modified glycopeptide (*m/z* 1402) $[M+H]^+$.

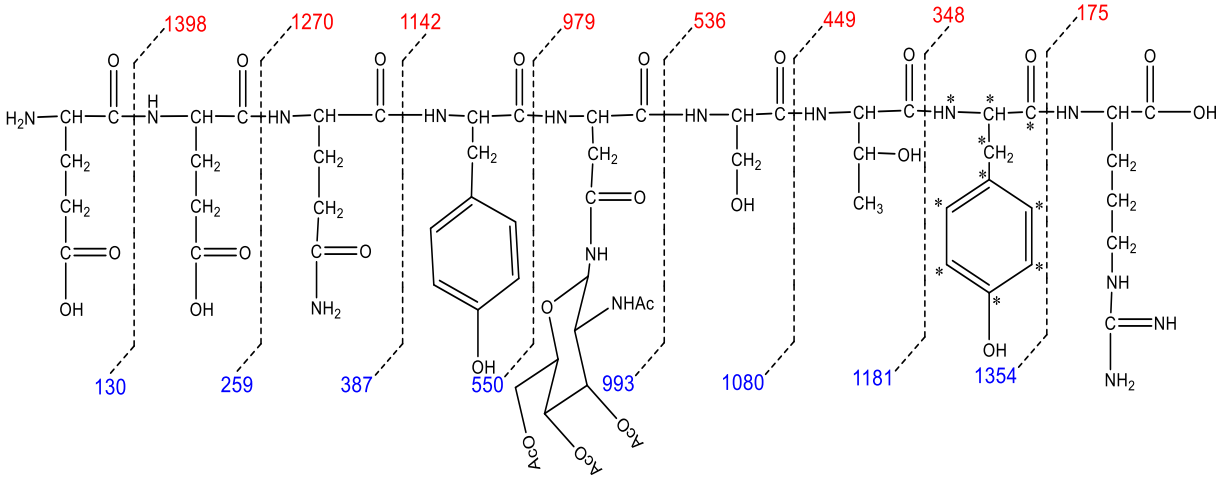

Figure 3.17. Fragmentation pattern of EEQYN(GlcNAc)STY*R $[M+H]^+$ ions (*m/z* 1402), providing the masses for b and y ions as observed by MS/MS. Red indicates "y" ions, blue indicates "b" ions.

Overall for IgG1 the internal standard (glyco)peptides synthesized were EEQYNSTYR, EEQYN(GlcNAc)STYR, and EEQYN(GlcNAc)STY*R (*=isotopically labelled). The first and second compounds were applied to the quantitation of IgG1 mAb and human IgG glycopeptides forms G0F, G1F and G2F. EEQYN(GlcNAc)STY*R was used for the analysis of EEQYN(GlcNAc)STYR in monoclonal antibody (mAb) Herceptin samples that had been treated with endoglycosidase F[123], Her2SF.

3.3. Synthesis of IgG2-related (glyco)peptides

Internal standard peptide EEQFNSTFR (*m/z* 1157 $[M+H]^+$) and glycopeptide EEQFN(GlcNAc)STYR (*m/z* 1360 $[M+H]^+$) were also synthesized to do the absolute quantitation of IgG2. They were spiked in digested samples of human IgG containing only IgG2 and in glycopeptides samples from polyclonal human IgG.

Figure 3.18 shows the MALDI-ToF-MS spectrum of the peptide EEQFNSTFR. The purity was estimated at 70.37%.

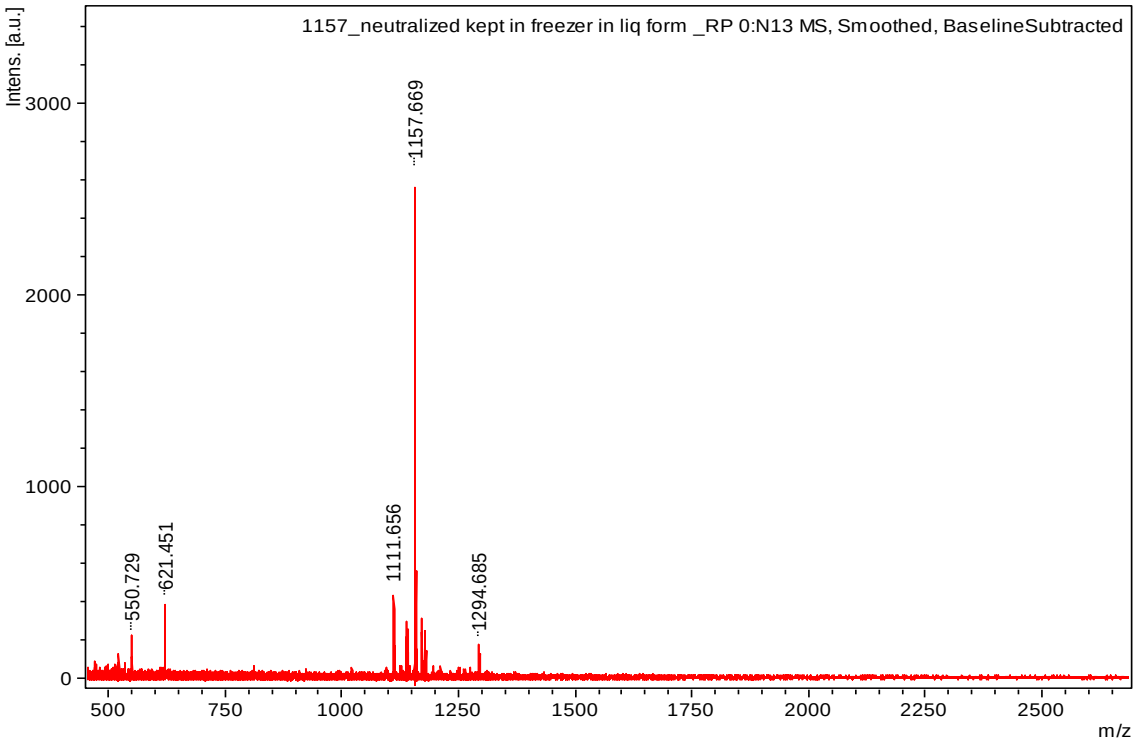

Figure 3.18. MALDI-ToF-MS spectrum of the peptide EEQFNSTFR. $[M+H]^+$ ions appeared at *m/z* 1157.

To verify the sequence, MS/MS was conducted on the peptide $[M+H]^+$ ions. Figure 3.19 shows the determination of the amino acid sequence of the peptide.

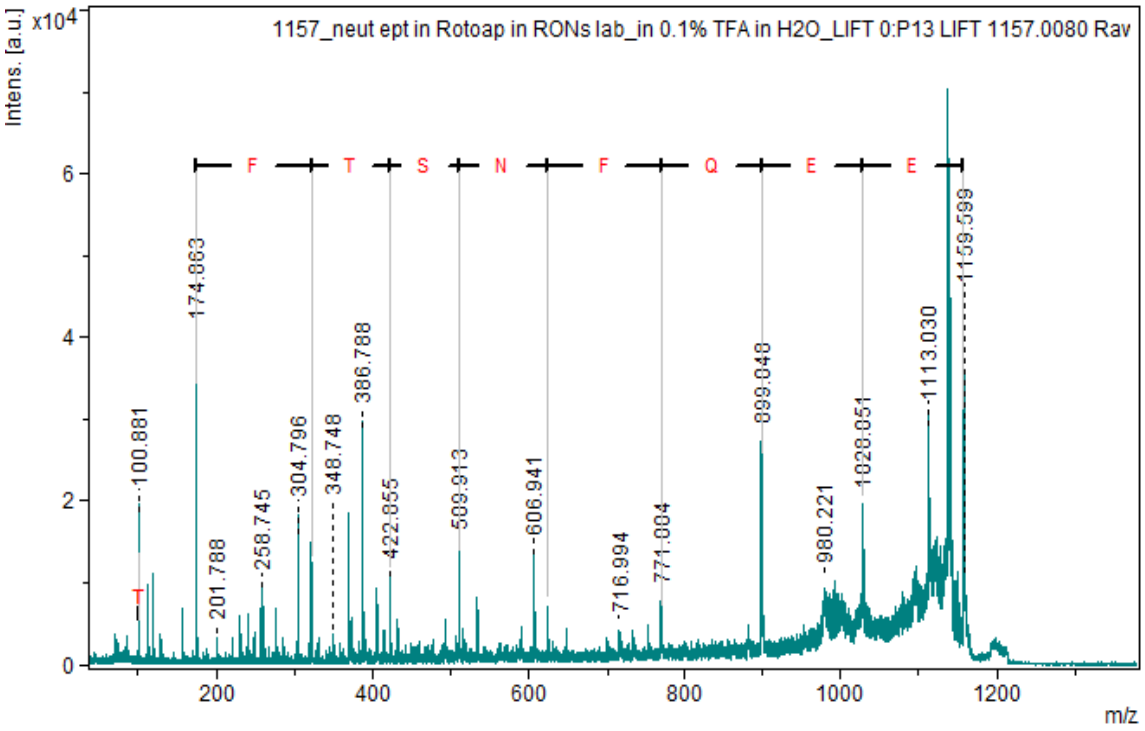

Figure 3.19. MALDI-MS/MS spectrum of peptide EEQFNSTFR at *m/z* 1157 $[M+H]^+$.

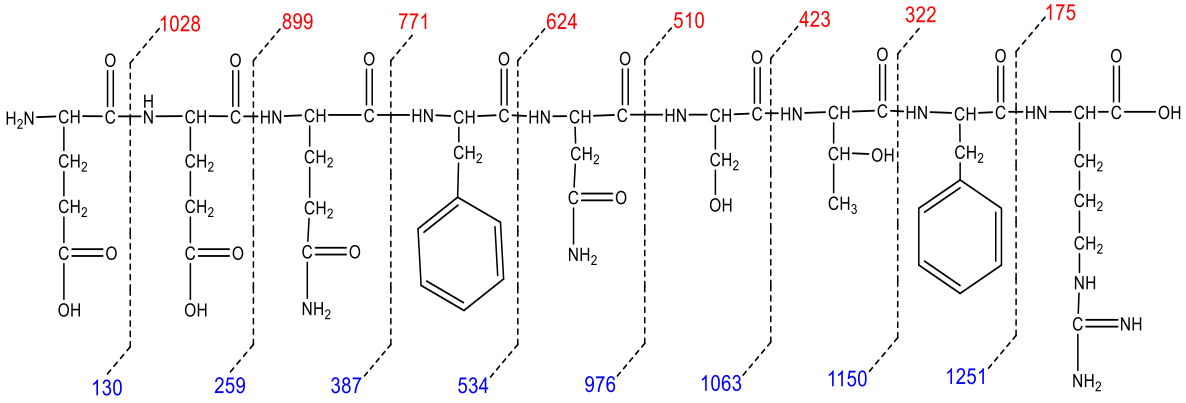

Figure 3.20. Fragmentation pattern of EEQFNSTFR, providing the masses for b and y ions of *m/z* 1157 ions as observed by MS/MS. Red indicates "y" ions, blue indicates "b" ions.

In the next step, the glycopeptide EEQFN(GlcNAc)STFR was synthesized. Glycosylated asparagine was used (with preacetylated GlcNAc) for the synthesis. After the synthesis

deacetylation was done. Figure 3.21 shows the MALDI-ToF-MS spectrum of the glycopeptide while still peracetylated. The main ions are $[M+H]^+$ at *m/z* 1486, and the main side product indicated methylation at *m/z* 1500. Ions at *m/z* 1444 are the result of under acetylation, and *m/z* 1582 ions indicate an unidentified side product.

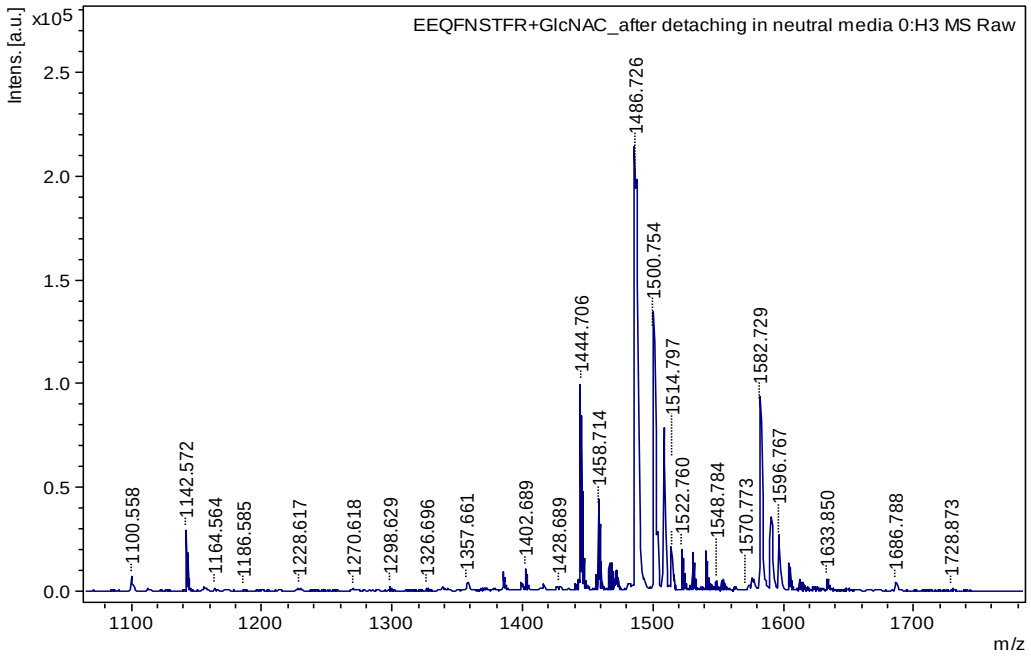

Figure 3.21. MALDI-ToF-MS spectrum of peracetylated glycopeptide EEQF(GlcNAc)NSTFR showing $[M+H]^+$ ions at *m/z* 1486.

To verify the amino acid sequence, MS/MS was done on the glycopeptide $[M+H]^+$ ions. Figure 3.22 shows the fragmentation of the acetylated glycopeptide.

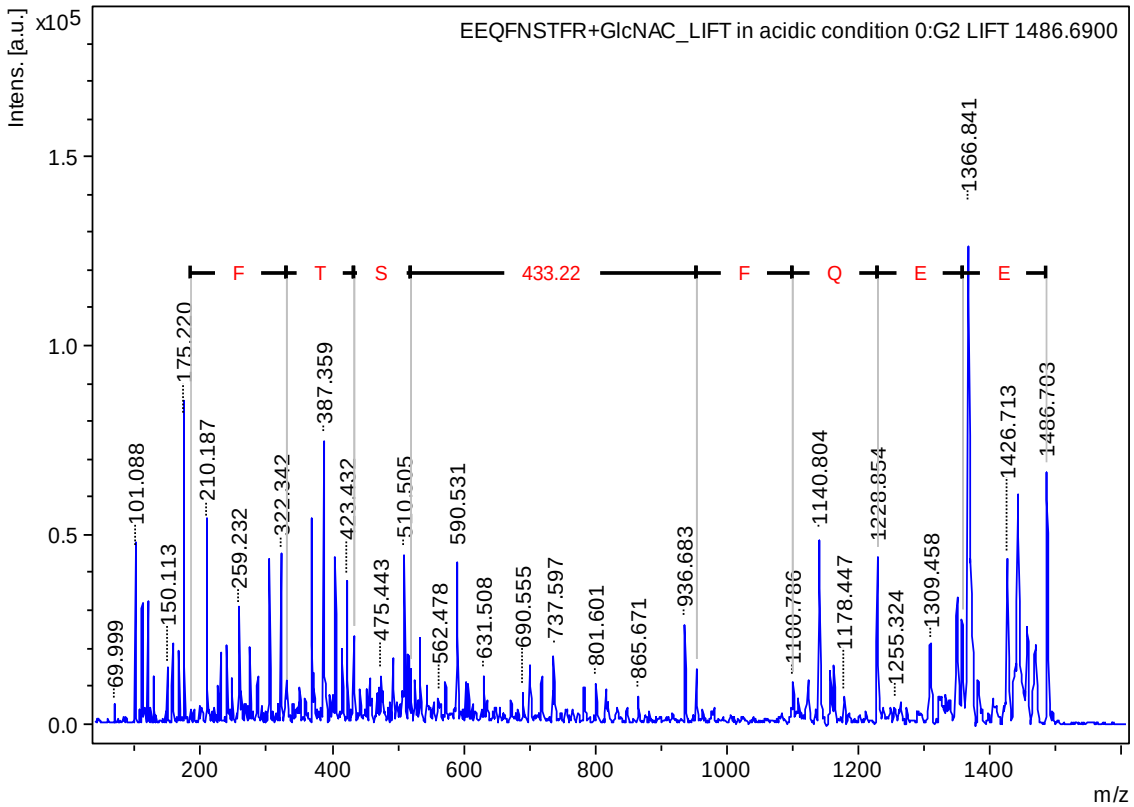

Figure 3.22. MALDI-MS/MS spectrum of *m/z* 1486 ions of peracetylated glycopeptide EEQFN(GlcNAc)STFR. The 433 gap represents peracetylated Asn(GlcNAc).

Next, deacetylation was done on the desired glycopeptide molecular ions. Figure 3.23 shows the MALDI-MS spectrum of the deacetylated glycopeptide. Predominant $[M+H]^+$ ions are at *m/z* 1360, however side products also appear, i.e. the methylated product at *m/z* 1374. Ions at m/z 1456 correspond to those at *m/z* 1582 in Figure 3.21. having lost 3 acetyl groups. This suggests that the side product at *m/z* 1456 is also a peptide bearing GlcNAc. Ions at *m/z* 1456 represent the remainder of the main peracetylated product. Side products coeluted with EEQFN(GlcNAc)STFR on the C18 SPE cartridge, and purity was calculated as 40.2% from the peak areas.

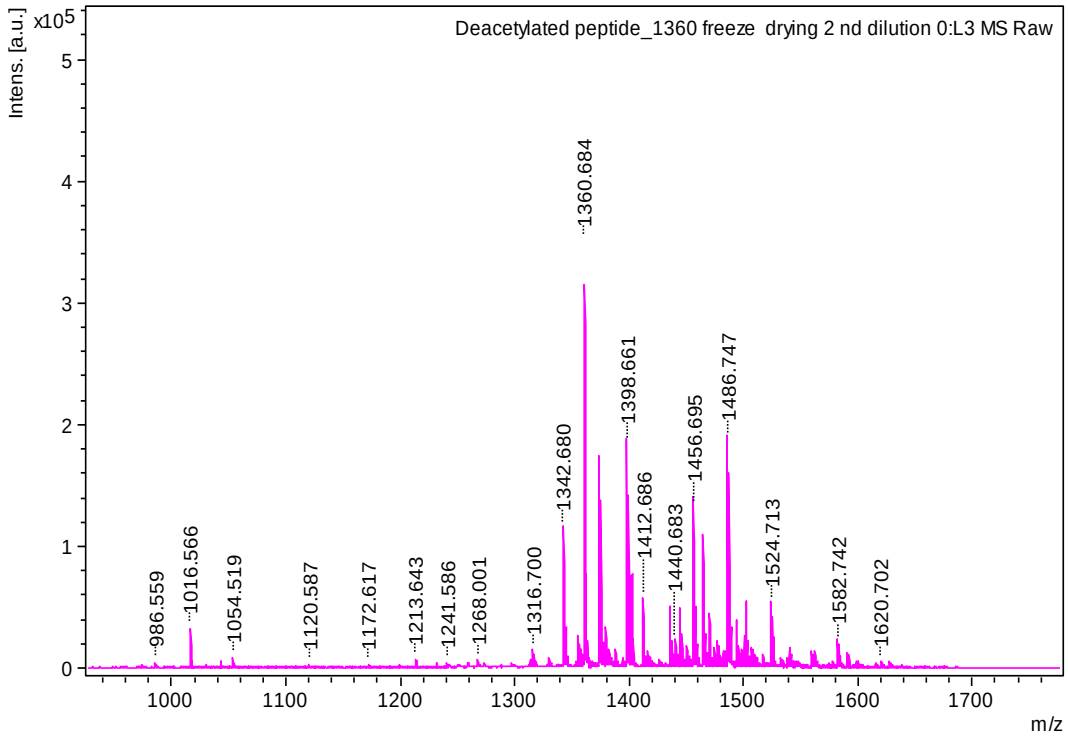

Figure 3.23. MALDI-ToF-MS spectrum of deacetylated glycopeptide EEQFN(GlcNAc)STFR showing $[M+H]^+$ ions at *m/z* 1360 after clean up by SPE C18 cartridge.

The $[M+H]^+$ ions of EEQFN(GlcNAc)STFR were subjected to MS/MS analysis as shown in Figure 3.24. The spectrum confirmed the sequence and glycosylation site.

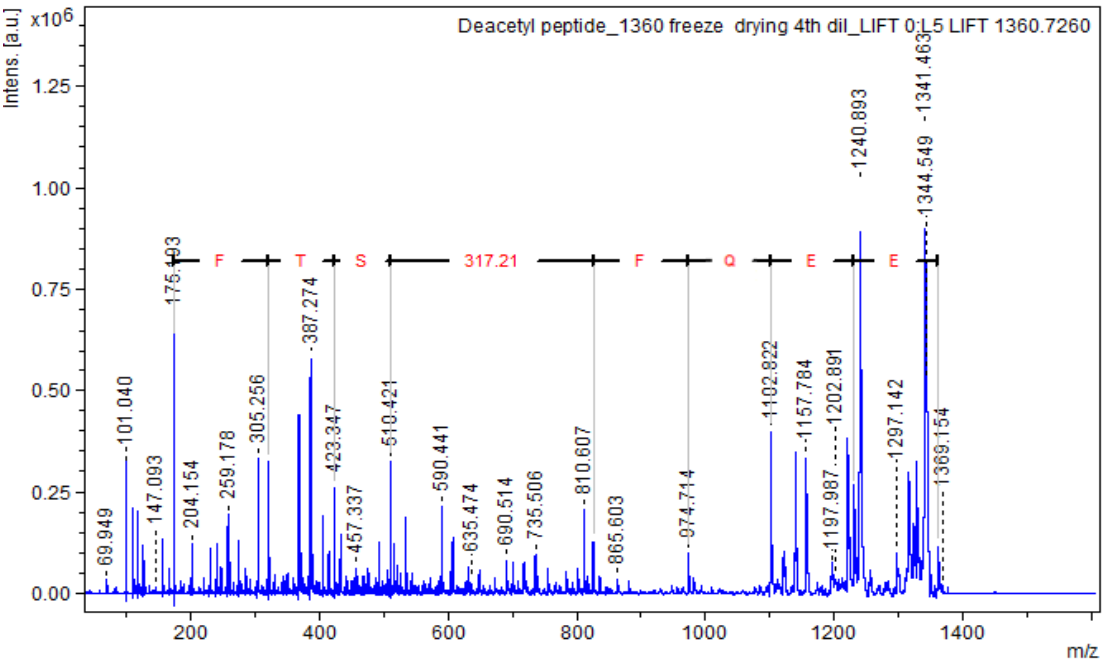

Figure 3.24. MS/MS of EEQFN(GlcNAc)STFR $[M+H]^+$ ions, after deacetylation.

Although all synthesized (glycol)peptides contained impurities, these do not interfere in mass with the compounds to be quantified in the next sections. Calculated standard concentrations took into account the reported purities.

3.4. Absolute quantification of IgG1 Abs

In this section of the discussion, it will be demonstrated that for monoclonal antibody (mAb) samples it is possible to use synthetic EEQYN(GlcNAc)STYR and EEQYN(GlcNAc)STY*R as internal standards for the quantitation of IgG1, the former being more reliable than the latter. The method used in this work consisted of spiking four or five identical unknown samples with increasing volumes of standard solution, measuring peak areas, and plotting signal ratio *vs.* volume ratio.

The first experiment consisted of ensuring that synthetic EEQYN(GlcNAc)STYR ($[M+H]^+$ ions at *m/z* 1392) and EEQYN(GlcNAc)STY*R (*m/z* 1402) deposited in mM-range equal concentrations yielded equivalent signals in MALDI-MS. Increasing amounts of the labelled standard were added to a fixed amount of the non-labelled glycopeptide (Expt. i in Table 3). Figure 3.25 shows the MALDI-MS spectra of synthetic glycopeptide EEQYN(GlcNAc)STYR (*m/z* 1392) and isotopically labelled glycopeptide EEQYN(GlcNAc)STY*R (*m/z* 1402) spiked together. See details in figure caption. Plotted results are presented in Figure 3.26a. The slope is close to 1, showing that basically both compounds yield equivalent signals for $[M+H]^+$ ions. In Experiment ii, standard additions were over a lower µM concentration range (see Table 2.1). A slope close to 1 was also obtained (Figure 3.26b). It was important to perform these experiments over different concentration ranges to assess the reliability of the MALDI-MS response. Often the concentrations of samples received from users are under-or overestimated and it is important that a method be adaptable to these situations where a wide range of concentrations is possible.

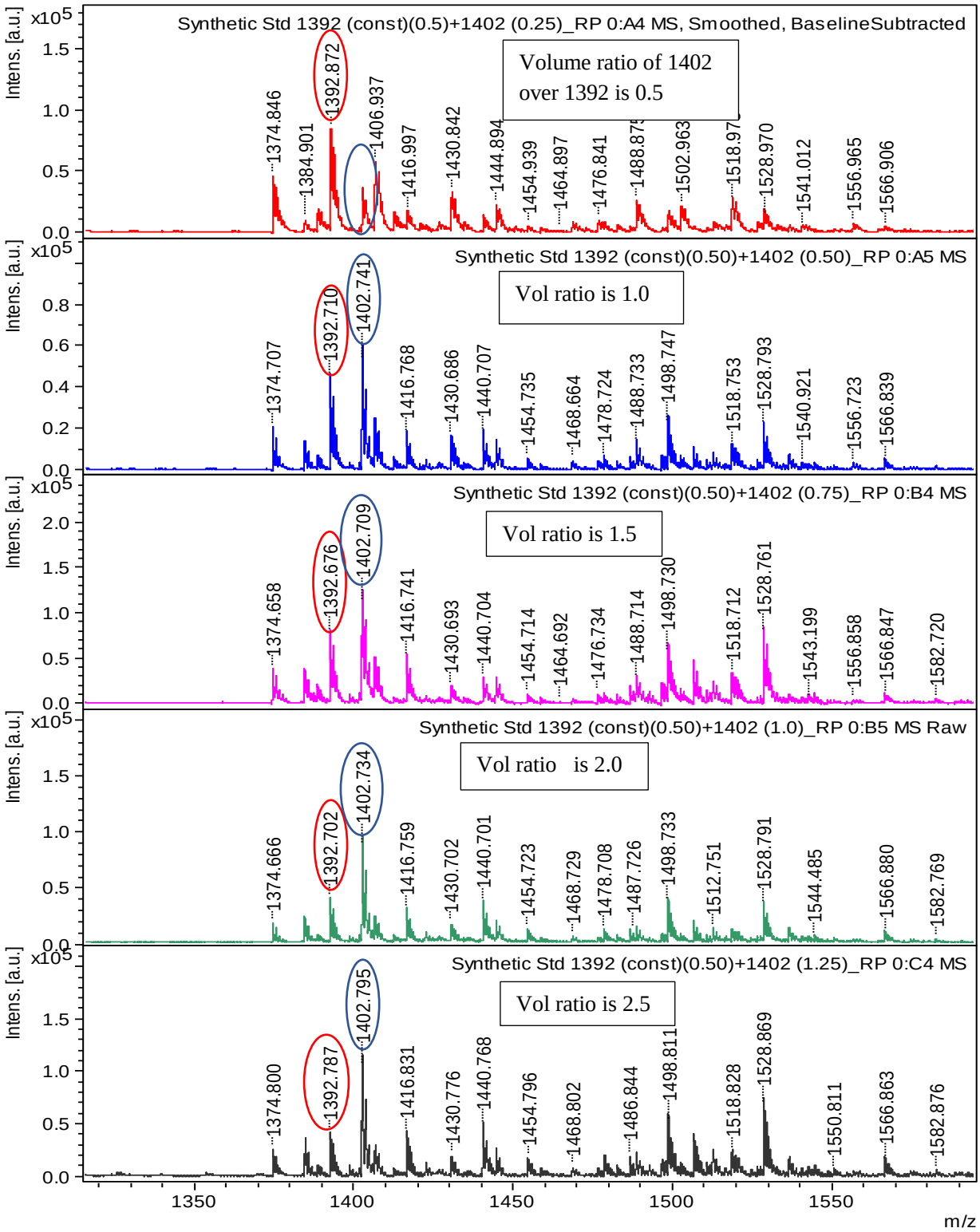

Figure 3.25. MALDI -ToF-MS analysis of standard synthetic glycopeptide EEQYN(GlcNAc)STYR and isotopically labelled glycopeptide EEQY(GlcNAc)NSTY*R.(Expt. ii with lower concentrations (1402: 1.31µM, 1392 : 1.32µM)

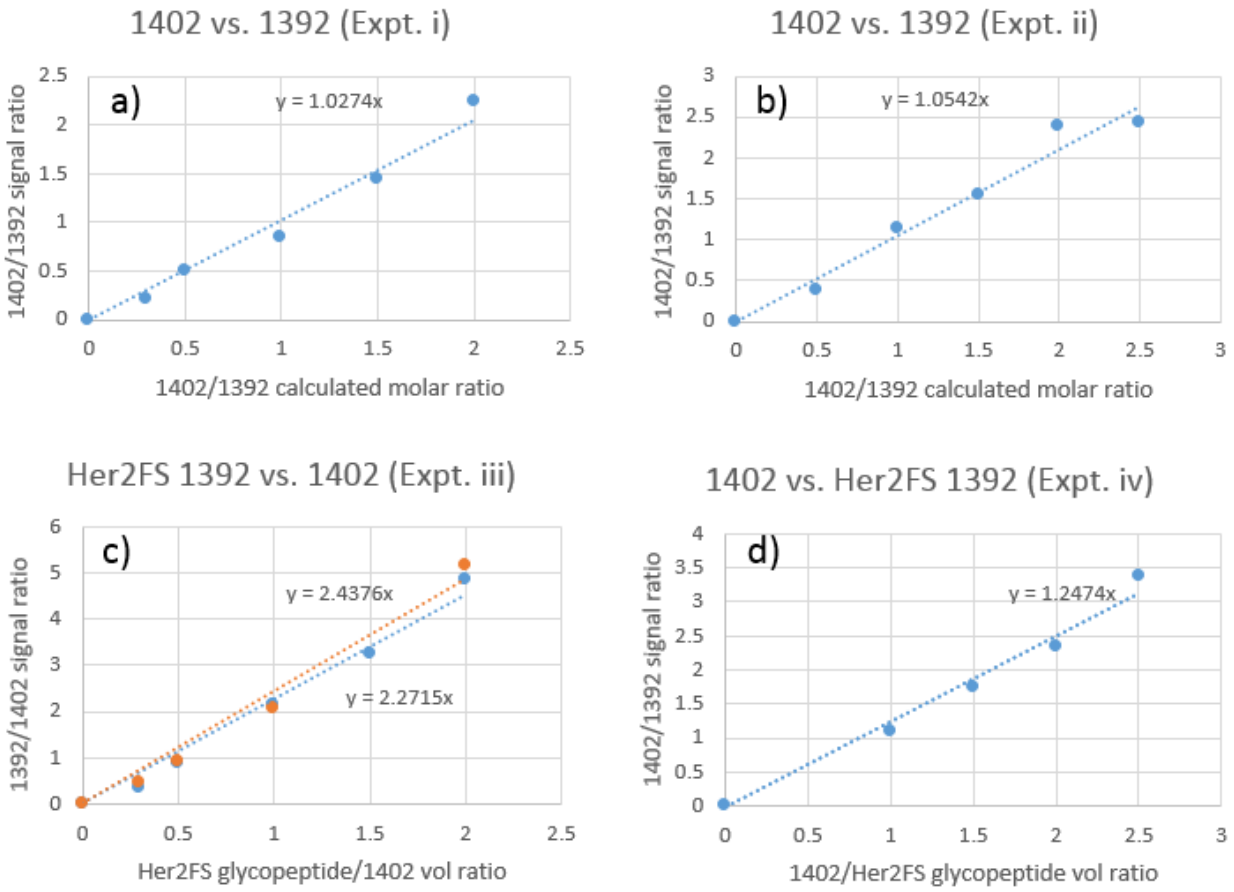

Figure 3.26 a) Additions of incremental volumes of EEQYN(GlcNAc)STY*R (1402, 22 mM) to a fixed amount of EEQYN(GlcNAc)STYR (1392, 0.5 µL of 23 mM solution) on the MALDI target and measurements of relative areas of $[M+H]^+$ peaks; **b)** same as Exp. i with lower concentrations (1402: 1.31µM, 1392 : 1.32µM); **c)** additions of increasing volumes of a solution of EEQYN(GlcNAc)STYR from Her2SF mAb onto constant volumes (0.5 µl) of 1402 at 3.32 mM; For a,b and c, concentration of analyte = concentration of unknown / slope. **d)** additions of increasing volumes of 1402 standard at 0.38 µM to constant volumes (0.5µL) of EEQYN(GlcNAc)STYR from Her2SF mAb. For d concentration of analyte = slope x concentration of unknown.

The next step was to measure the amount/concentration of a monoclonal antibody (mAb) *N*-glycosylated with only one core GlcNAc, Her2SF. Its tryptic *N*-glycopeptide was thus EEQYN(GlcNAc)STYR,producing $[M+H]^+$ ions at *m/z* 1392. Synthetic EEQYN(GlcNAc)STY*R was used as an internal standard with $[M+H]^+$ ions at *m/z* 1402. In Figure 3.26c , in a duplicate experiment (iii) the volume ratio of unknown concentration solution of mass 1392 peptide was increased stepwise from 0 to 2 over that of a 3.32 mM solution of 1402. In each experiment, 0.5

µl of the standard solution (*m/z* 1402) was spotted onto the MALDI target, and the volumes of unknown solution (*m/z* 1392) were added to match the ratios of 0.3, 1, 1.5 and 2. Figure 3.27 shows the MALDI-MS spectra of unknown standard solution spiking to an unknown mAb solution.

As from Figure 3.26(a-b) it can be assumed that the signal ratio is equivalent to the molar ratio, the average slope of the graph represents the concentration factor between the two solutions, standard and unknown. If concentration were equal, the slope would be 1. Therefore the unknown solution spiked onto the target has a concentration of 3.32 mM times the average slope (2.35) = 7.8 mM. In Figure 3.26d, the same experiment was repeated (Expt. iv) at much lower concentration values, with the 1402 standard solution at 0.38 µM. Solutions were made so that the spotting of equal volume of standard and unknown solution would yield MALDI signals that were within the same range. The unknown solution needed to be diluted accordingly, and this time the volume of the sample solution kept constant while increasing the volumes of added standard. The unknown's concentration was determined to be 0.31 µM**.** Figure 3.27 a) and b) shows the MALDI-MS spectra of known standard solution(*m/z* 1402) spiking to an unknown mAb sample.

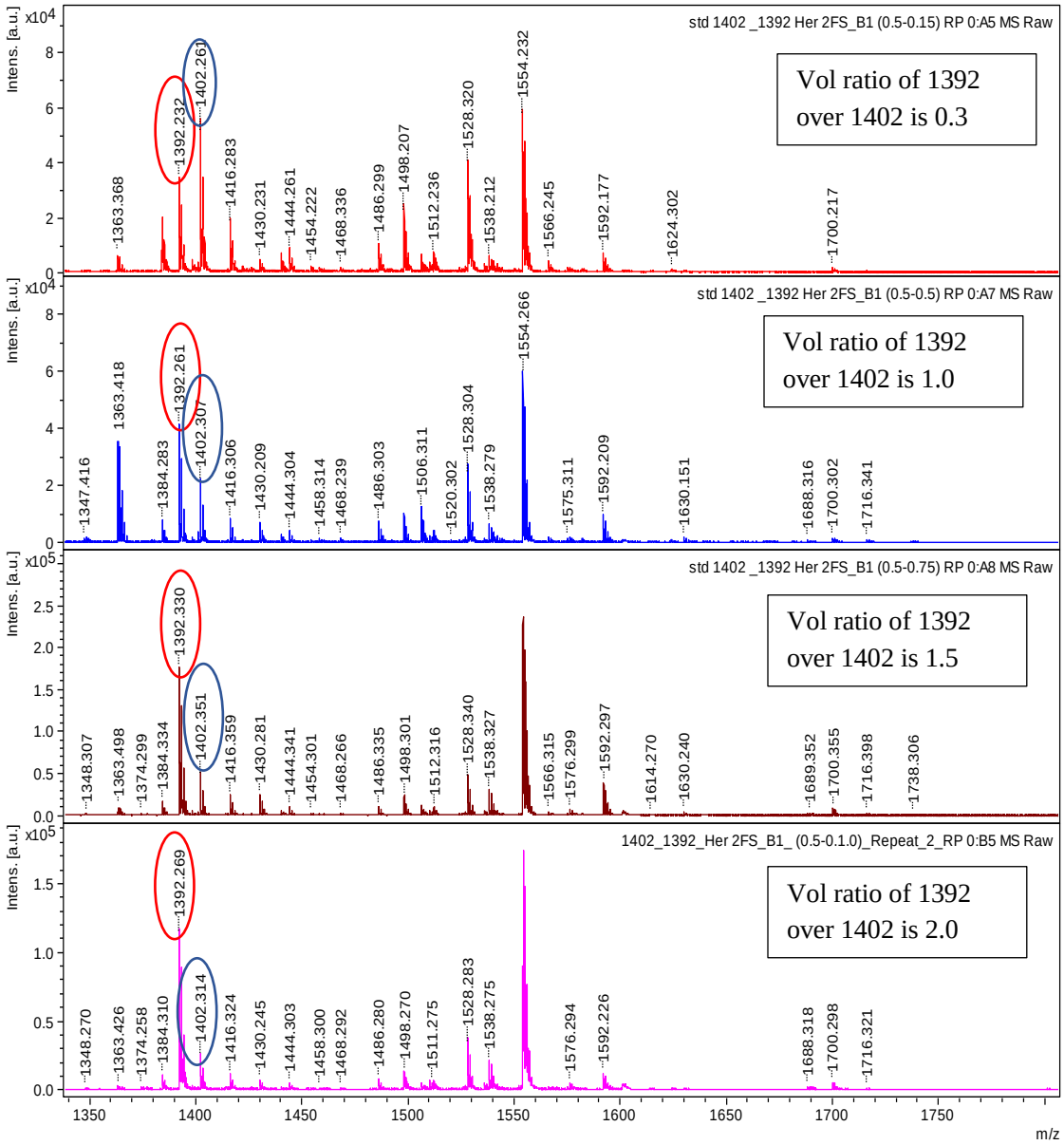

Figure 3.27 a). Typical MALDI-ToF-MS analysis of varying volume ratios of solutions EEQYN(GlcNAc)STYR from mAb Her2FS digest with Endo-F, analyzed with isotopically labelled glycopeptide EEQYN(GlcNAc)STY*R (*m/z* 1402) (Experiment iii)

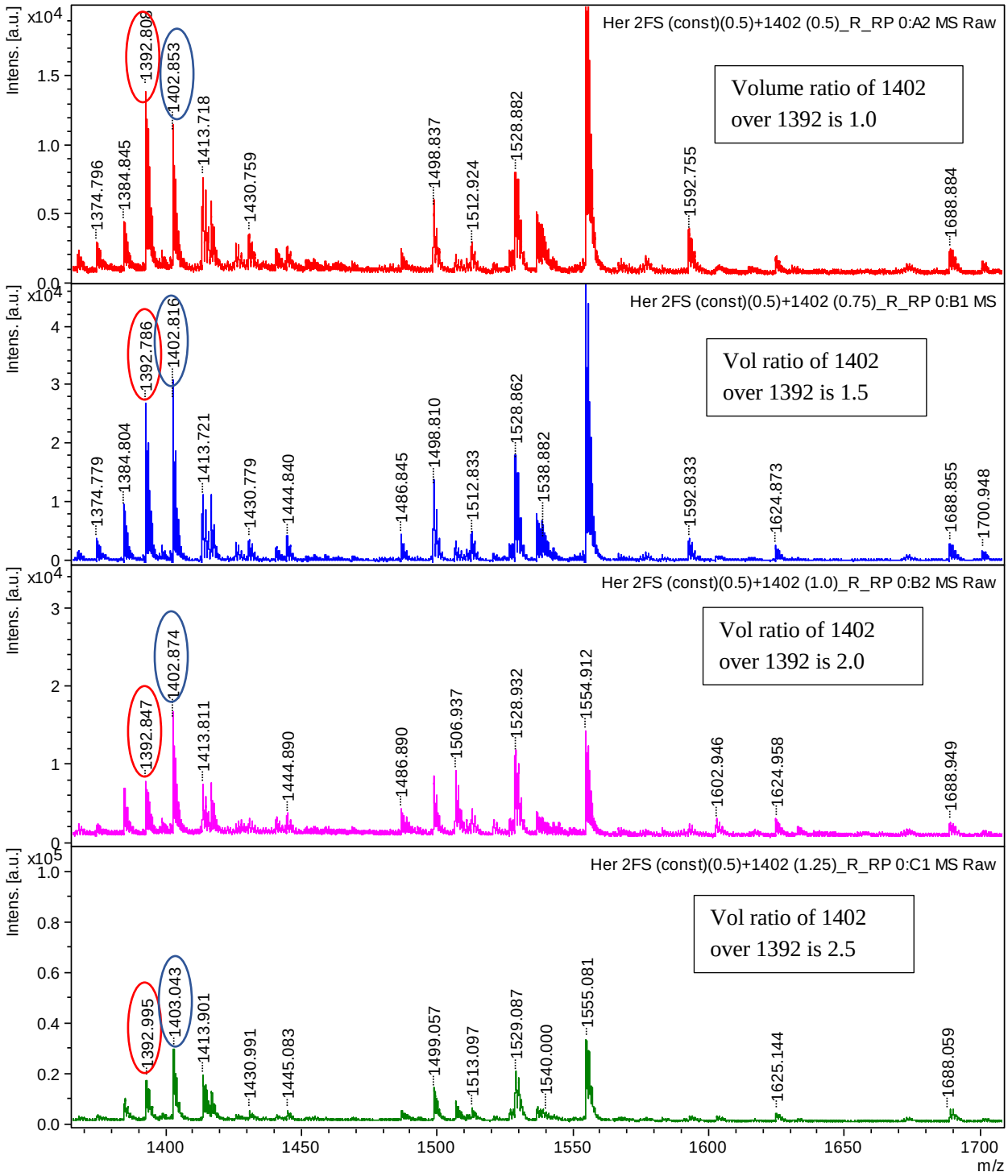

Figure 3.27 b). Typical MALDI-ToF-MS analysis of varying volume ratios of solutions EEQYN(GlcNAc)STYR from mAb Her2FS digest with Endo-F, analyzed with isotopically labelled glycopeptide EEQYN(GlcNAc)STY*R (*m/z* 1402) (Experiment iv)

Another method to calculate the unknown's concentration was to plot a standard additions graph, where the fixed volume compound's signal was normalised to 100 arbitrary units in all spectra and other peak areas were recalculated accordingly. This normalization is necessary, as in MALDI the absolute signals vary from one run to the next due to factors such as laser power, number of laser shots fired, shape and size of crystals. The graphs obtained corresponding to datasets of Figure 3.26c-d are shown in Figure 3.28. The x-intercepts were obtained from equations featured on the graphs and allowed to calculate the molar amount of unknown in the 0.5 µl deposited on-target. Concentrations found were equivalent to those determined above using the "slopes" method. Table 3.1 shows an example dataset treated using this method. In this example, the unknown solution of 1392 was added to a fixed amount of standard 1402 (Expt. iii Trial 1). The unknown concentration was calculated as 7.4 mM, while 7.5 mM was found using the slopes method with the same dataset.

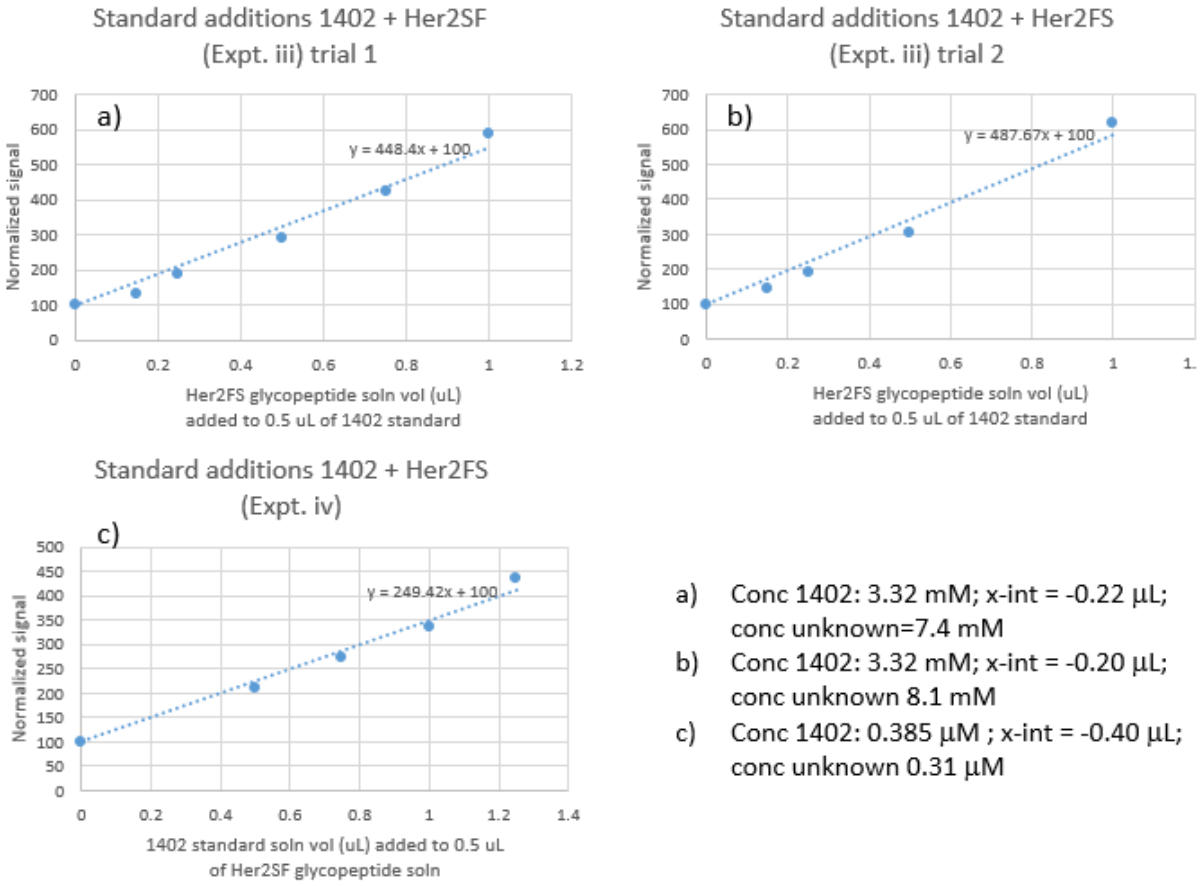

Figure 3.28. Use of the standard additions method to determine concentrations from Experiments iii and iv (see Table 2.1). The analyte (constant volume) was a glycopeptide (*m/z* 1392) from Her2FS. The standard (incremental volumes) was EEQYN(GlcNAc)STY*R (*m/z* 1402).

Table 3.1. Calculations of Her2FS glycopeptide concentration using the standard addition method: Expt. iii, trial 1. By plotting column 6 *vs.* column 1, the graph of Figure 3.28a was obtained. The x-intercept (0.223 µl) represents the volume of unknown solution containing the same amount of analyte at 0.5 µL of 3.32 mM standard. Thus, the concentration of unknown = 0.5 x 3.32/0.223 = 7.44 mM.

Vol. 1392 (µL)	Peak area 1402	Peak area 1392	Peak area 1402, normalized	Peak area 1392, recalc. 100*1392/1402	Sum of normalized 1402 and 1392
0	0	0	100	0	100
0.15	105976	34042	100	32.122	132.122
0.25	55611	48225	100	86.718	186.718
0.50	44545	84991	100	190.798	290.798
0.75	50106	162300	100	323.913	423.913
1	11397	55390	100	486.005	586.005

In a next set of experiments (Expt. v), the synthetic glycopeptide EEQYN(GlcNAc)STYR (1392) was used against a glycopeptide fraction of Eg2-hFc mAb [121,124] tryptic digest. The purpose was to evaluate the linearity and consistency of the response factors between 1392 and higher glycoforms G0F, G1F and G2F of EEQYNSTYR (Figure 3.29). Synthetic EEQYN(GlcNAc)STYR was prepared at 5.75 mM. Solutions were prepared so that spotting of equal volumes of standard and unknown would yield MALDI signals that are approximately equal between the standard and the G0F glycoforms. Figure 3.29 shows the MALDI-MS spectra of tryptic glycopeptide fractions from mAb samples, analyzed by glycopeptide internal standard 1392.

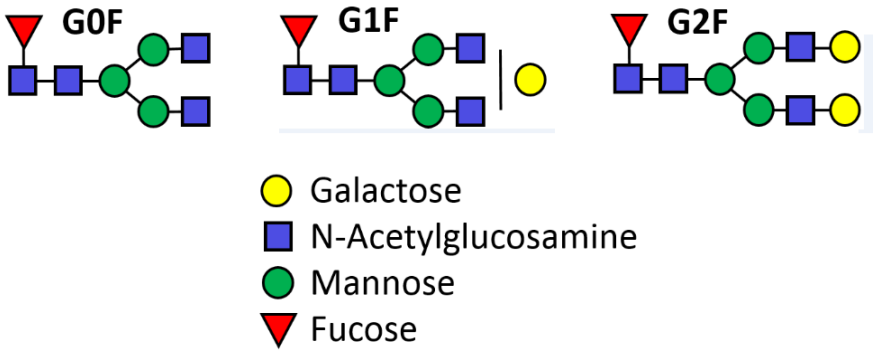

Figure 3.29. The three most abundant glycoforms of EEQYNSTYR (IgG1) and EEQFNSTYR (IgG2). The glycans are attached at the N site at the reducing end of fucosylated *N*-acetyl glucosamine.

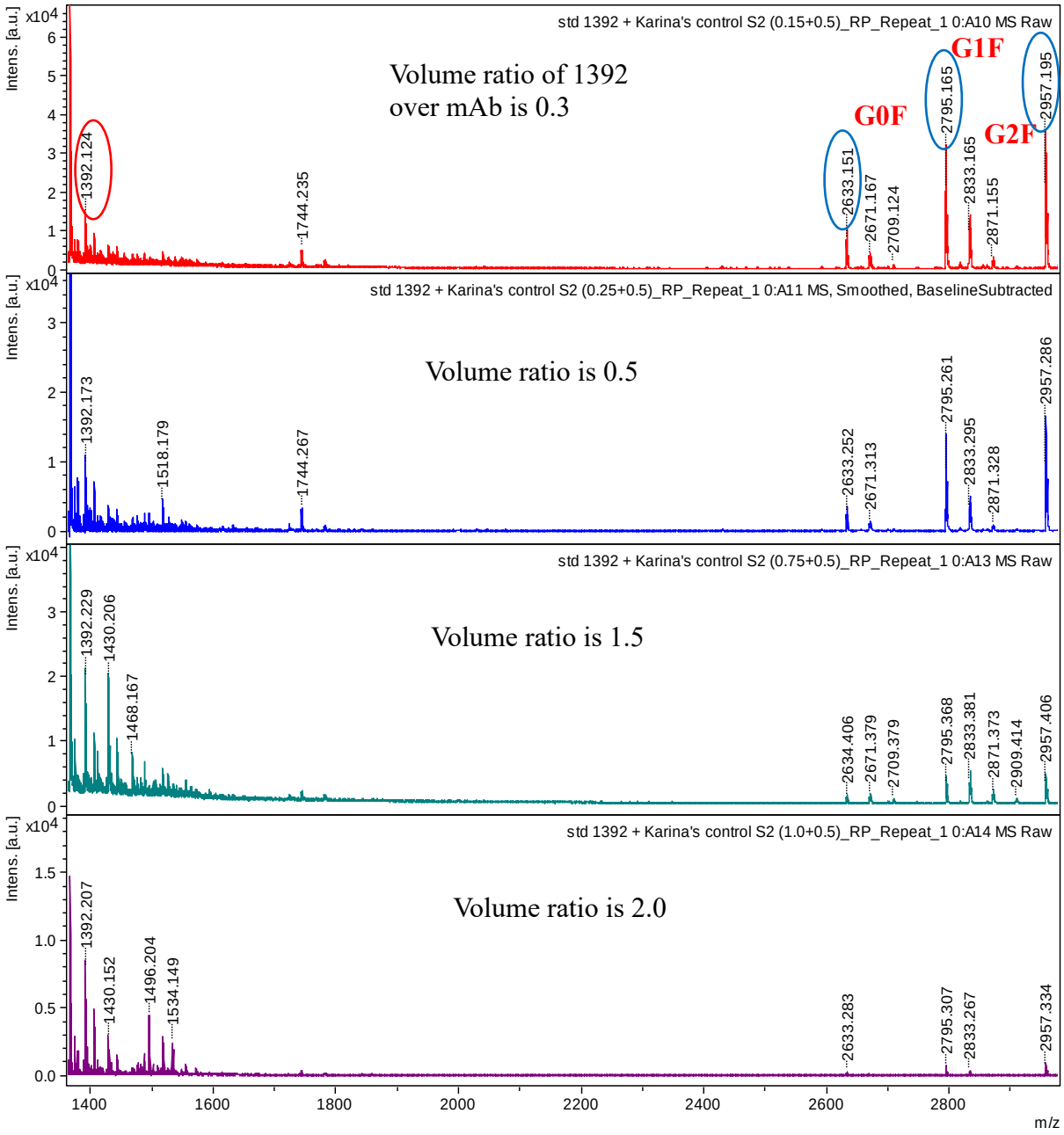

Figure 3.30. MALDI-MS spectra of glycopeptides from fully glycosylated mAb: Spiking with glycopeptide EEQYN(GlcNAc)STYR (*m/z* 1392) standard for quantification.

Plotted results are shown in Figure 3.31a using the slopes method. Before attempting to determine concentrations, a parameter of interest to discuss is the relationship between response ratios and mixed solution volume ratios. The relative abundances of G0F, G1F and G2F $[M+H]^+$ increase in this order in Figure 3.30 (sample spectrum) and the slopes in Figure 3.31a go decreasing

from top to bottom. From MALDI spectra of the glycoforms (e.g. Figure 3.30) average G0F, G1F and G2F peak area ratios are 11.62, 40.38 and 48.01%, while $(slope)^{-1}$ ratios are 11.57, 40.16 and 48.27%. This good agreement values indicates that MALDI-MS responses of the three glycoforms are even relative to EEQYN(GlcNAc)STYR. Table 3.2 shows how glycoform proportions were obtained using the $slope^{-1}$ and peak area ratios. Concentrations of G0F, G1F and G2F glycoforms of EEQYNSTYR are obtained by dividing 5.75 mM by the slopes in Figure 3.31 and are listed in Table 3.2, column 2. Calculations using the standard additions method (See Figure 3.33 for the graphs) yielded the same values.

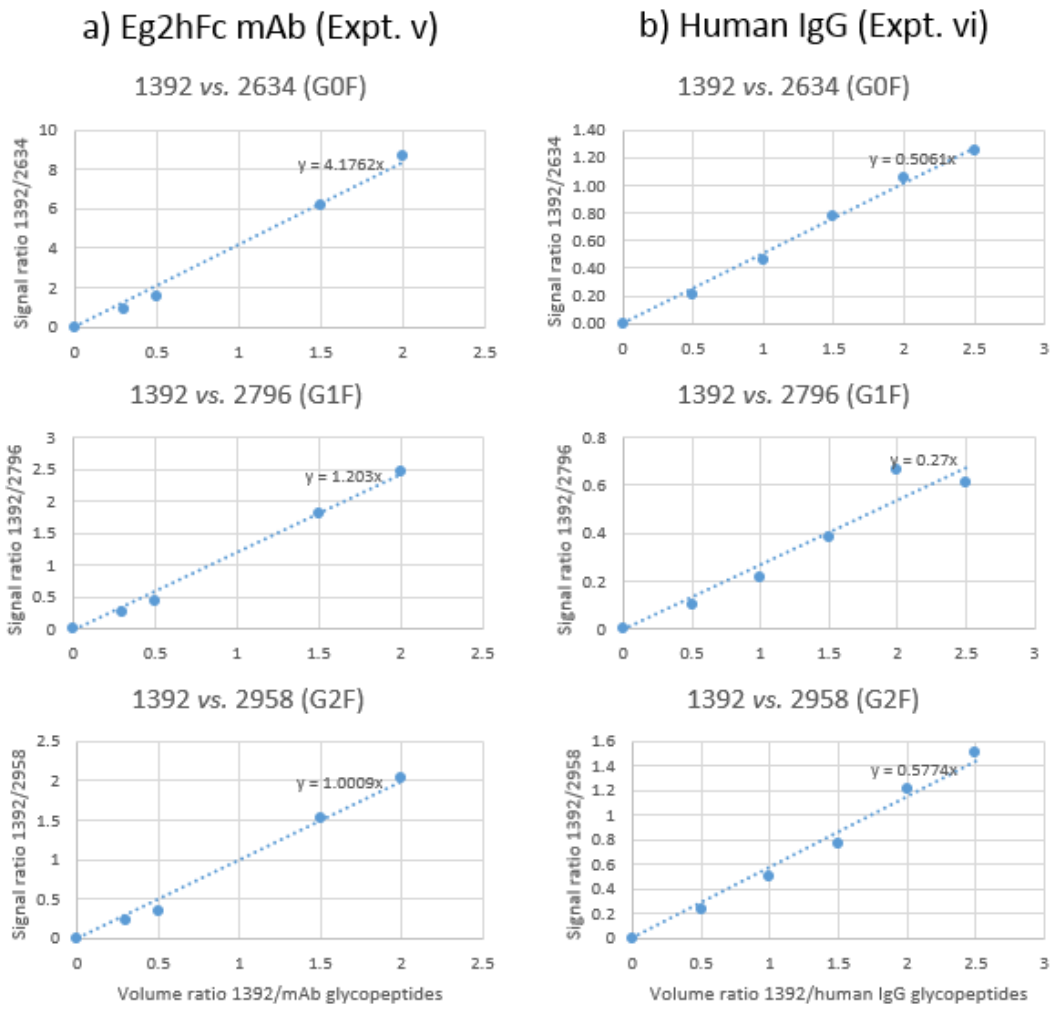

Figure 3.31. Attempts to use glycopeptide EEQYN(GlcNAc)STYR (1392) as internal standard for the dosage of solutions of tryptic glycopeptides from a) Eg2hFc mAb, (Expt. v) and b) human IgG, (Expt. vi). Concentration of standard: 5.75 mM for the mAb and 79.0 µM for human IgG.

Table 3.2. Calculated EEQYNSTYR glycoform concentrations of spiked solutions (before spiking) when peptide and glycopeptide internal standards were added.

Sample →	Eg2hFc mAb (Expt. v)	Eg2hFc mAb (Expt. vii)	Human IgG (Expt. vi)	Human IgG (Expt. viii)
Glycoform of EEQYNSTYR (*m/z*)	1392 standard	1189 standard	1392 standard	1189 standard
G0F (2634)	1.4 mM	12 mM	160 μM	450 μM
G1F (2796)	4.8 mM	48 mM	290 μM	820 μM
G2F (2958)	5.7 mM	67 mM	140 μM	340 μM
Total IgG1	12 mM	127 mM	0.58 mM	1.6 mM

Table 3.3. Method checking for 1392 *vs.* Eg2hFc mAb. Determination of relative slope^{-1} values and relative peak area values from mass spectra.

Vol ratio 1392/Eg2-hFc	G0F Signal ratio 1392/2634	G1F Signal ratio 1392/2796	G2F Signal ratio 1392/2958	
0	0	0	0	
0.3	0.92	0.26	0.22	
0.5	1.49	0.43	0.35	
1.5	6.16	1.81	1.53	
2	8.63	2.46	2.03	
	Slope^{-1}	Slope^{-1}	Slope^{-1}	Sum slope^{-1}
	0.239	0.831	0.999	2.070
	Relative slope^{-1} value	Relative slope^{-1} value	Relative slope^{-1} value	
	11.57%	40.16%	48.27%	100%
Vol ratio 1392/Eg2-hFc	Peak area	Peak area	Peak area	Sum of peak areas
0.3	3360	11810	14212	29382
0.5	13964	48455	58632	121051
1.5	9227	31417	34391	75035
2	34191	120448	150910	305549
Vol ratio 1392/Eg2-hFc	%Peak area	%Peak area	%Peak area	Sum
0.3	11.44	40.19	48.37	100
0.5	11.54	40.03	48.44	100
1.5	12.30	41.87	45.83	100
2	11.19	39.42	49.39	100
	Average %peak area	Average %peak area	Average %peak area	Sum
	11.62	40.38	48.01	100

The same experiment was repeated with 1392 *vs.* a glycopeptide mixture from a tryptic digest of commercial polyclonal human IgG (Experiment vi). Mass spectra are shown in Figure 3.32. Plotted results are shown in Figure 3.31b. The concentration of 1392 standard was 79.0 µM.

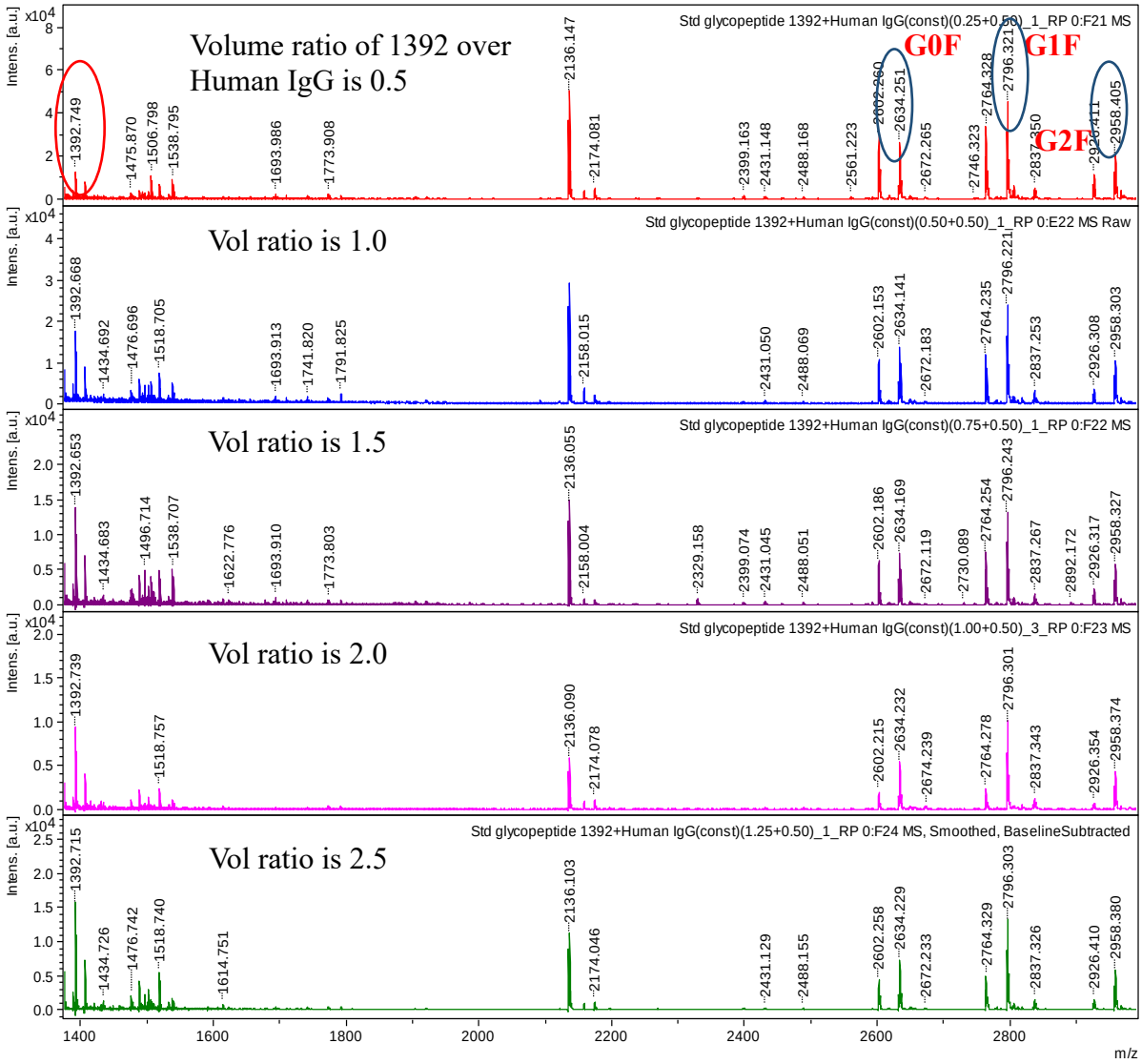

Figure 3.32. MALDI-ToF-MS spectra of glycopeptides from human IgG: spiking with glycopeptide standard EEQYN(GlcNAc)STYR (*m/z* 1392) for quantitation.

Calculated concentrations for the three glycoforms of interest are given in Table 3.2, column 4. The relative proportions of reverse slopes are 26.66, 49.97 and 23.37 %. These compare well with the relative abundances observed in the human IgG glycopeptide spectra, i.e. Figure 3.32

(26.09, 50.40 and 23.51%). Standard addition graphs are featured in Figure 3.33 and the method yielded the same values as the slopes method.

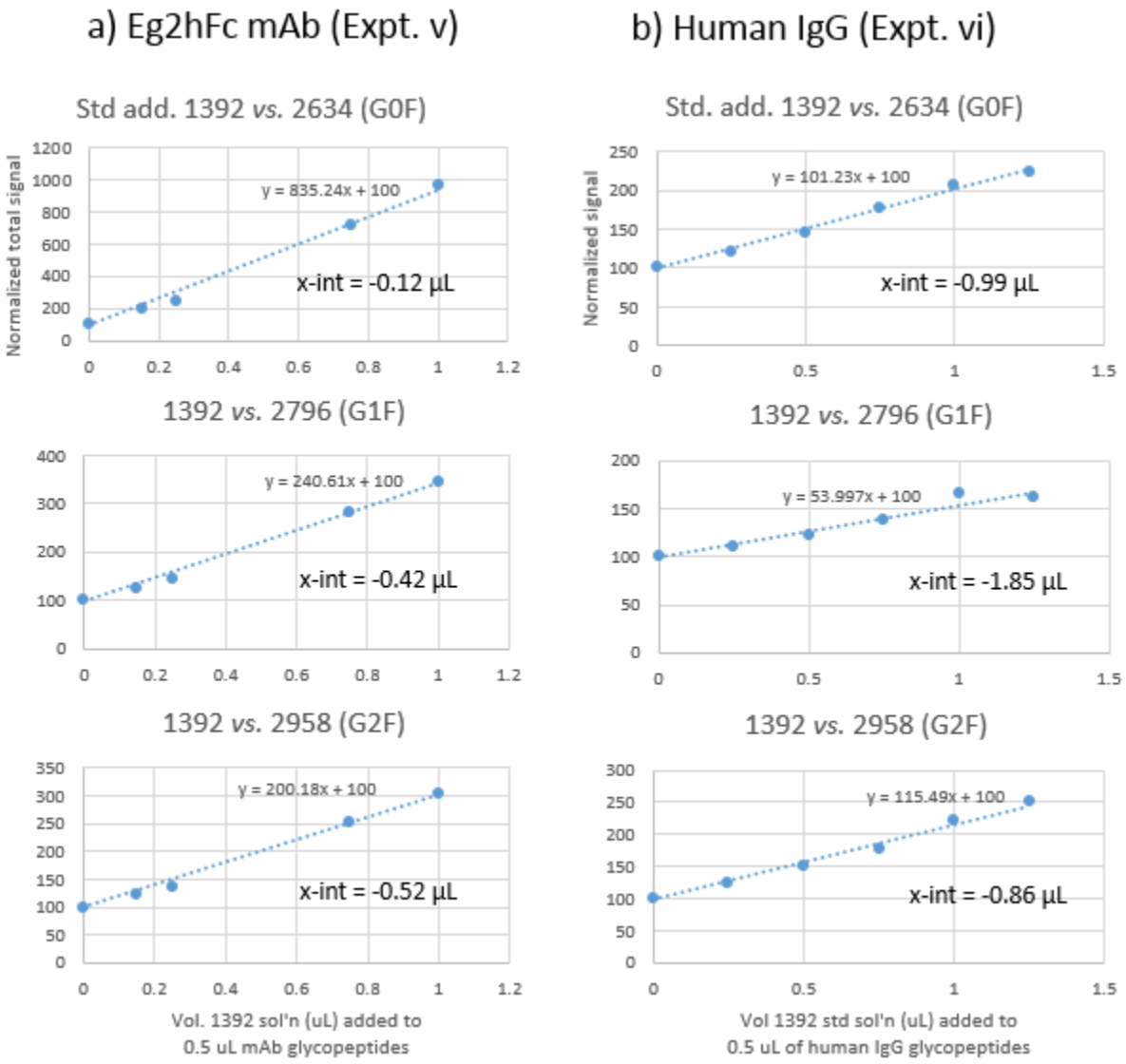

Figure 3.33. Results from Experiments v and vi (see Table 2.1) treated using standard additions method. The analytes (constant volume, 0.5µL) were the EEQNSTYR glycoforms G0F, G1F and G2F from a) Eg2-hFc mAb, b) human IgG. The standard (incremental volumes) was EEQYN(GlcNAc)STYR (1392). x-intercept values allow to calculate the moles of analyte present, which divided by 0.5µL yields the concentration.

The synthetic peptide EEQYNSTYR (*m/z* 1189 for $[M+H]^+$ ions) was also used as a potential internal standard in the dosage of Eg2-hFc mAb (Experiment vii) and human IgG

glycosylated analogs (Experiment viii). Figure 3.34 shows the Typical MALDI-MS spectra for 1189 *vs.* the three main glycoforms of fully glycosylated mAb.

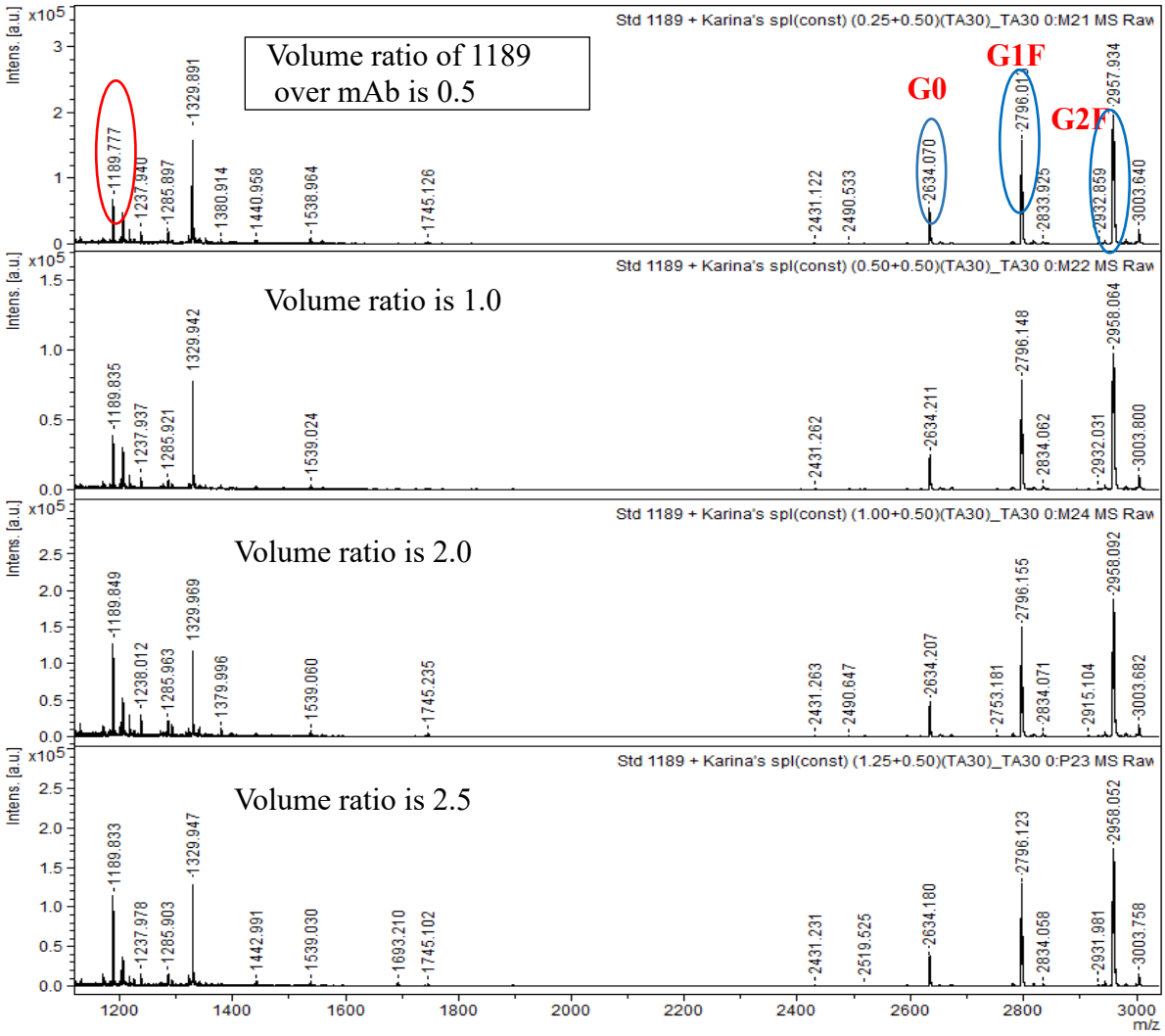

Figure 3.34. Typical MALDI-MS spectra of glycopeptides from fully glycosylated mAb: spiking with peptide standard (1189) for quantitation.

Figure 3.35 shows the plotted correlations between standard peptide EEQYNSTYR (*m/z* 1189) $[M+H]^+$ *vs.* fully glycosylated mAb (Experiment vii) and as well as human IgG (Experiment viii).

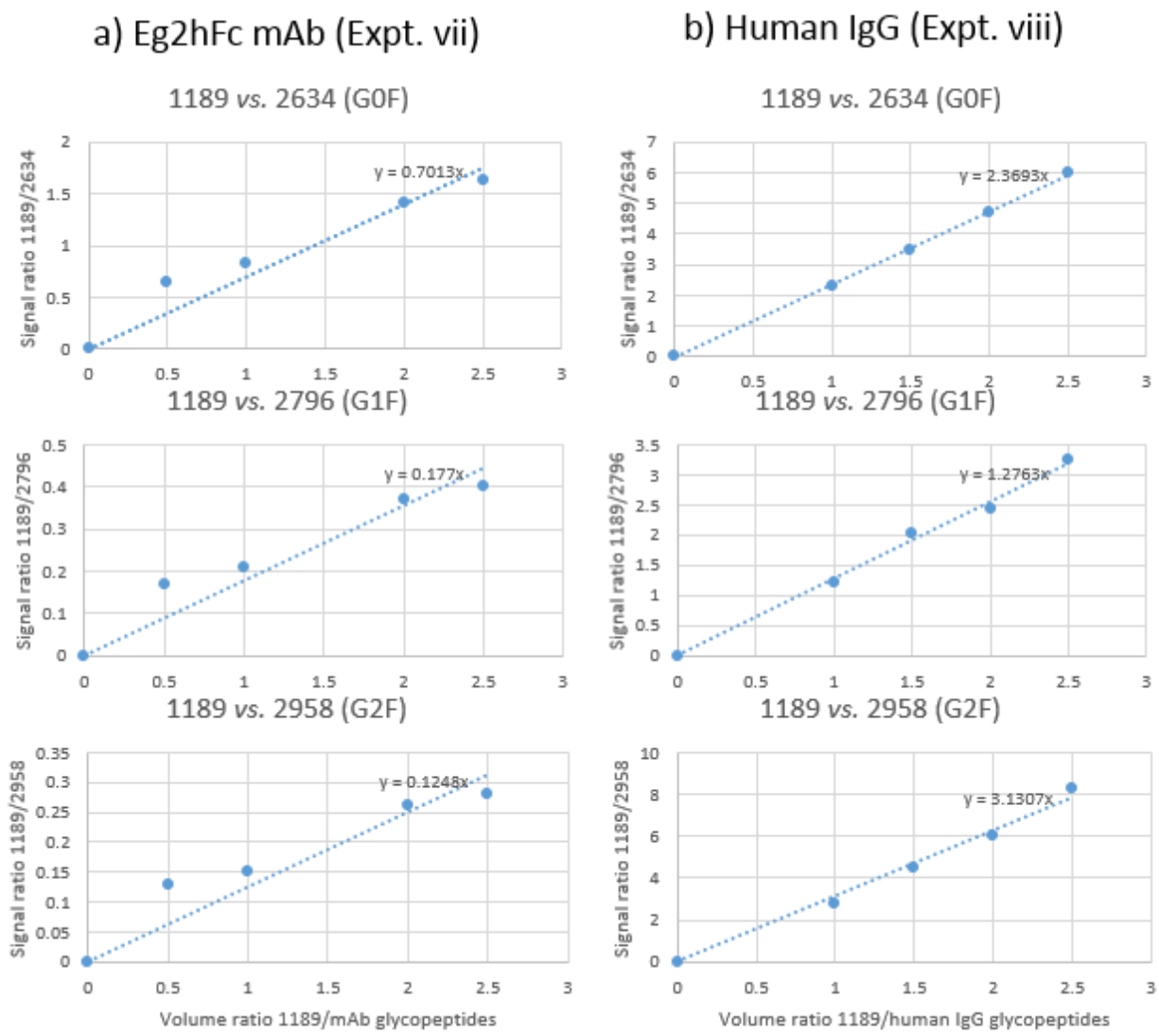

Figure 3.35. Attempts to use peptide EEQYNSTYR as internal standard for the dosage of solutions of tryptic glycopeptides from a) mAb and b) human IgG. Experiments vii and viii. Concentration of 1188: 8.41 mM for the mAb and 1.05 mM for human IgG.

Figure 3.35 shows the correlations. If a 1:1 response is assumed, using the slopes, the concentrations obtained are featured in Table 3.2, columns 3 and 5. Linearity was not satisfactory

for the mAb, and the y-origin was much above zero. The plot was forced through the (0,0) origin and slopes were obtained. The reverse of these slopes was 9.45, 37.44, 53.11% in proportion *vs.* 9.38, 37.43, 53.19% on average in the MALDI spectra for G0F, G1F and G2F (e.g. Figure 3.34). For IgG1 in polyclonal human IgG, the results were 27.68, 51.38, 20.94% (slopes) *vs* 26.12, 50.17, 23.73% (spectra, e.g. Figure 3.36).

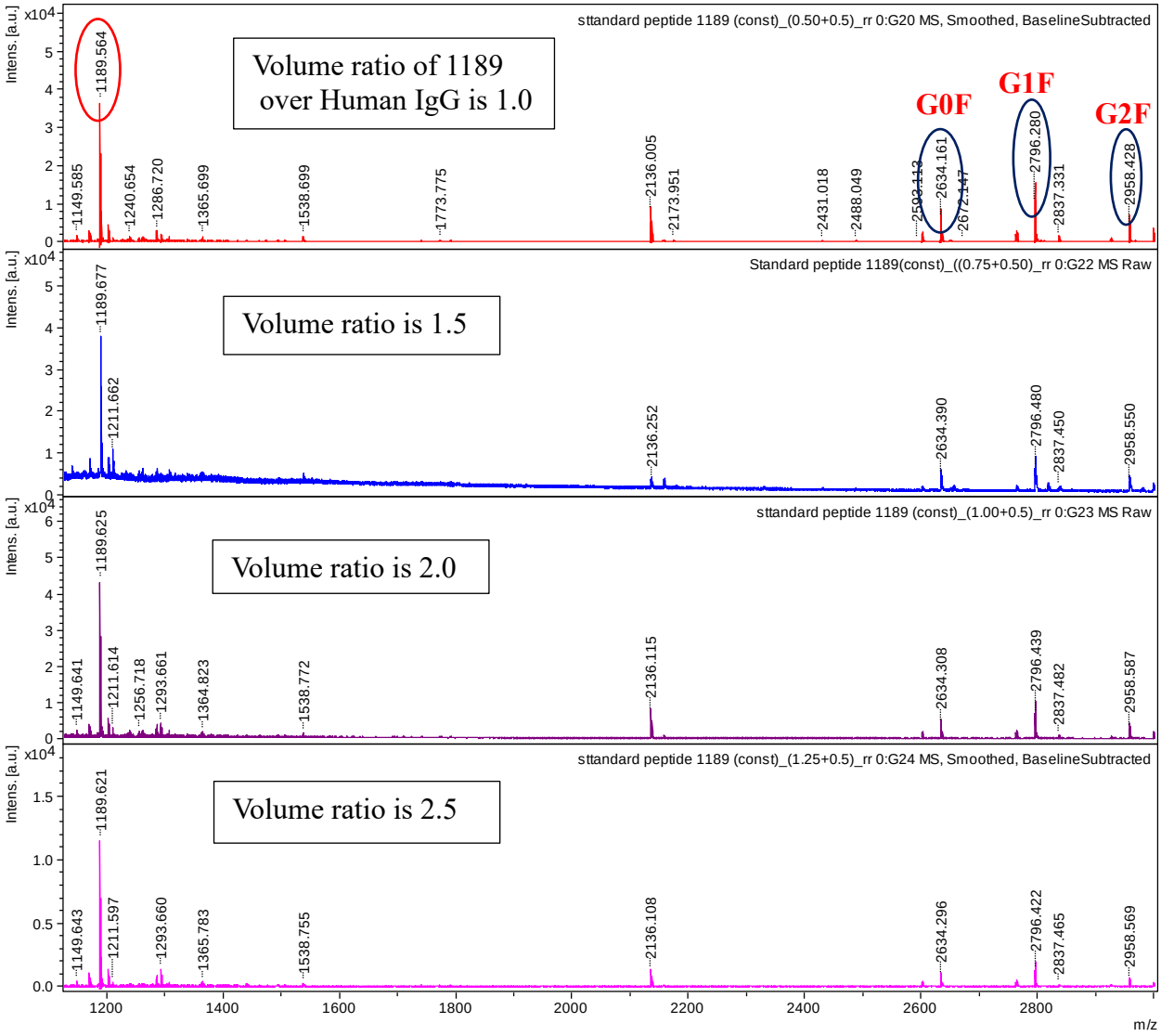

Figure 3.36. MALDI-MS spectra of tryptic glycopeptide fractions of Human IgG, spiking with peptide standard (*m/z* 1189) for quantitation.

The calculated mAb glycoform concentrations are reported in Table 3.2, column 3. These are one order of magnitude higher than those of column 2 with the glycopeptide standard. The column 3 values are too large to be realistic, according to Table 3.2, as they overshoot the user's estimated concentration. Also, values in column 5 are almost three times higher than those in column 4. Overall the 1189 peptide did not seem to yield as much signal as its 1392 counterpart.

Following these results, the MALDI-MS sensitivity of 1189 *vs.* 1392 was studied. In these experiments, equimolar solutions of 1189 and 1392 were spotted on target with incremental 1189 volumes over 1392 (constant). This was studied over two concentration ranges, ~850 µM [Figure 3.38 (left)] and ~100 mM (right). Figure 3.37 shows the mass spectra corresponding to one series (~100 mM).

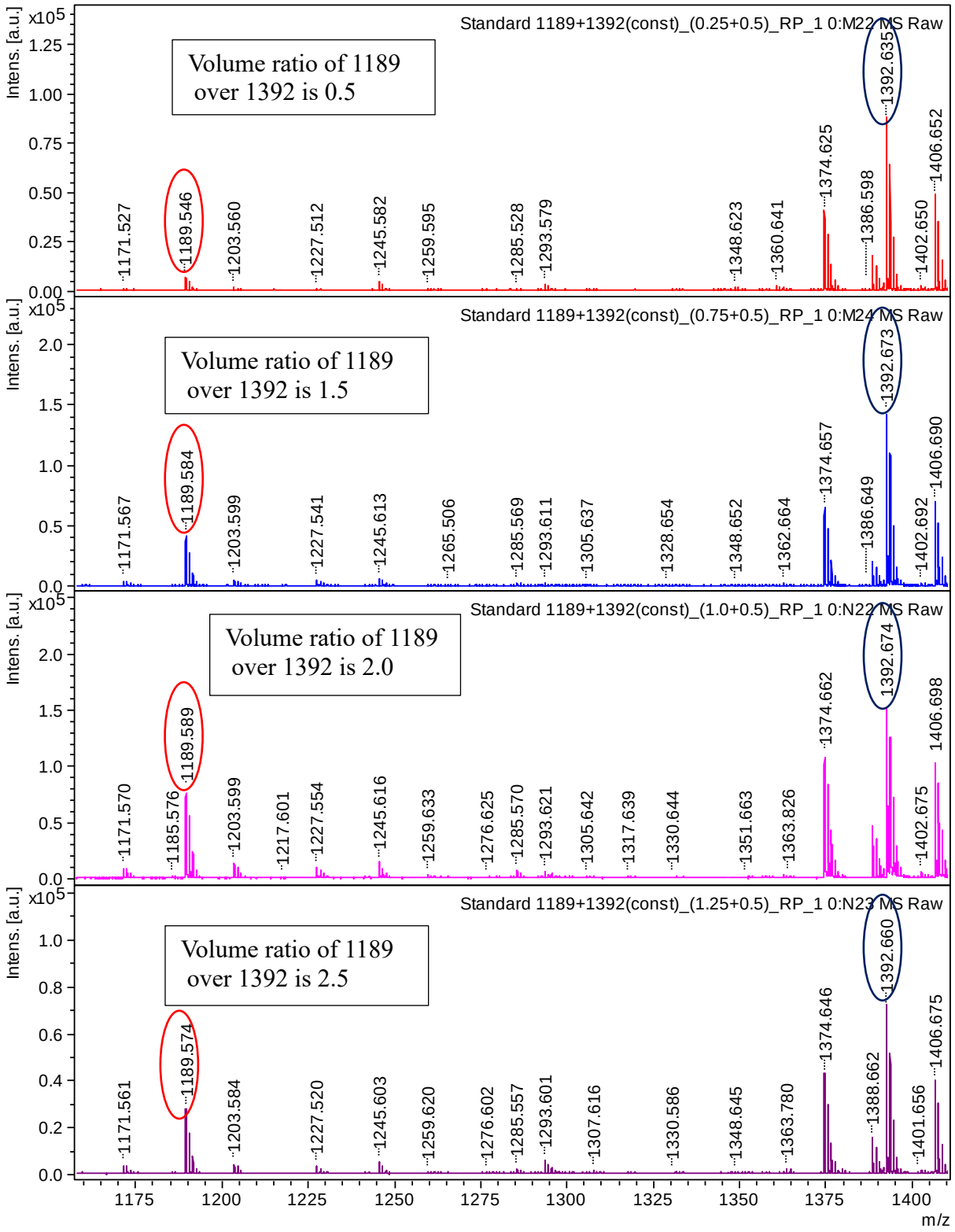

Figure 3.37. MALDI-ToF-MS spectra of mixtures of both synthesized internal standards EEQYNSTYR (*m/z* 1189 $[M+H]^+$) and EEQYN(GlcNAc)STYR (*m/z* 1392 $[M+H]^+$): equimolar solution (~100 mM) with incremental volumes of the 1189 solution *vs*. 1392.

Figure 3.38 was plotted and illustrates the feature that EEQYNSTYR yields inferior signals relative to EEQYN(GlcNAc)STYR. This was done over two concentration ranges, z~850 µM (left) and ~100 mM (right). At molar ratio 1, the signal ratios are lower than 1 and the general "slopes" are lower than 1. This means that more 1189 than 1392 standard must be added to the analyte to reach comparable signals, resulting in higher estimations of the unknown concentration with 1189 than with 1392.

Overall EEQYN(GlcNAc) (*m/z* 1392) was considered a better internal standard than EEQYNSTYR (*m/z* 1189) for the absolute quantitation of higher glycoforms of the peptide EEQYNSTYR because it yielded realistic antibody concentration and produce a linear relationship with the analyte.

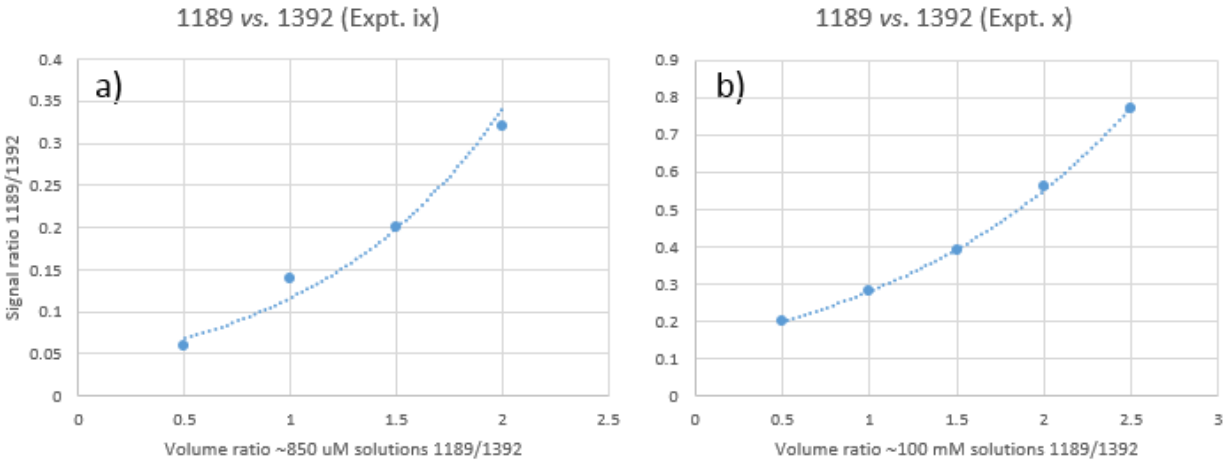

Figure 3.38. Mixture of equimolar solutions of EEQYNSTYR and EEQYN(GlcNAc)STYR on the MALDI target in different volume ratios and measurements of relative areas of $[M+H]^+$ peaks. Concentrations of 1189 and 1392: a) 875 and 841 µM (Experiment ix), b) 101 and 100 mM (Experiment x).

3.5. Absolute quantification of IgG2 Abs

The use of the same approach was attempted for the quantitation of IgG2 in samples containing only that subclass of human IgG and in a polyclonal human IgG glycopeptide samples (Experiments xi, xii).

Two internal standards were used for quantitation, synthetic peptide EEQFNSTFR *m/z* 1157) and glycopeptide EEQFN(GlcNAc)STFR (*m/z* 1360). Monoclonal IgG2 samples were HPLC fractions from a tryptic digest of human IgG where IgG2 had been found predominant.[125] Figure 3.39 shows typical MALDI-MS spectra of G0F, G1F and G2F glycoforms of EEQFNSTFR spiked with EEQFN(GlcNAc)STFR in a fraction containing only IgG2 *N*-glycopeptide (Experiment no: xi).

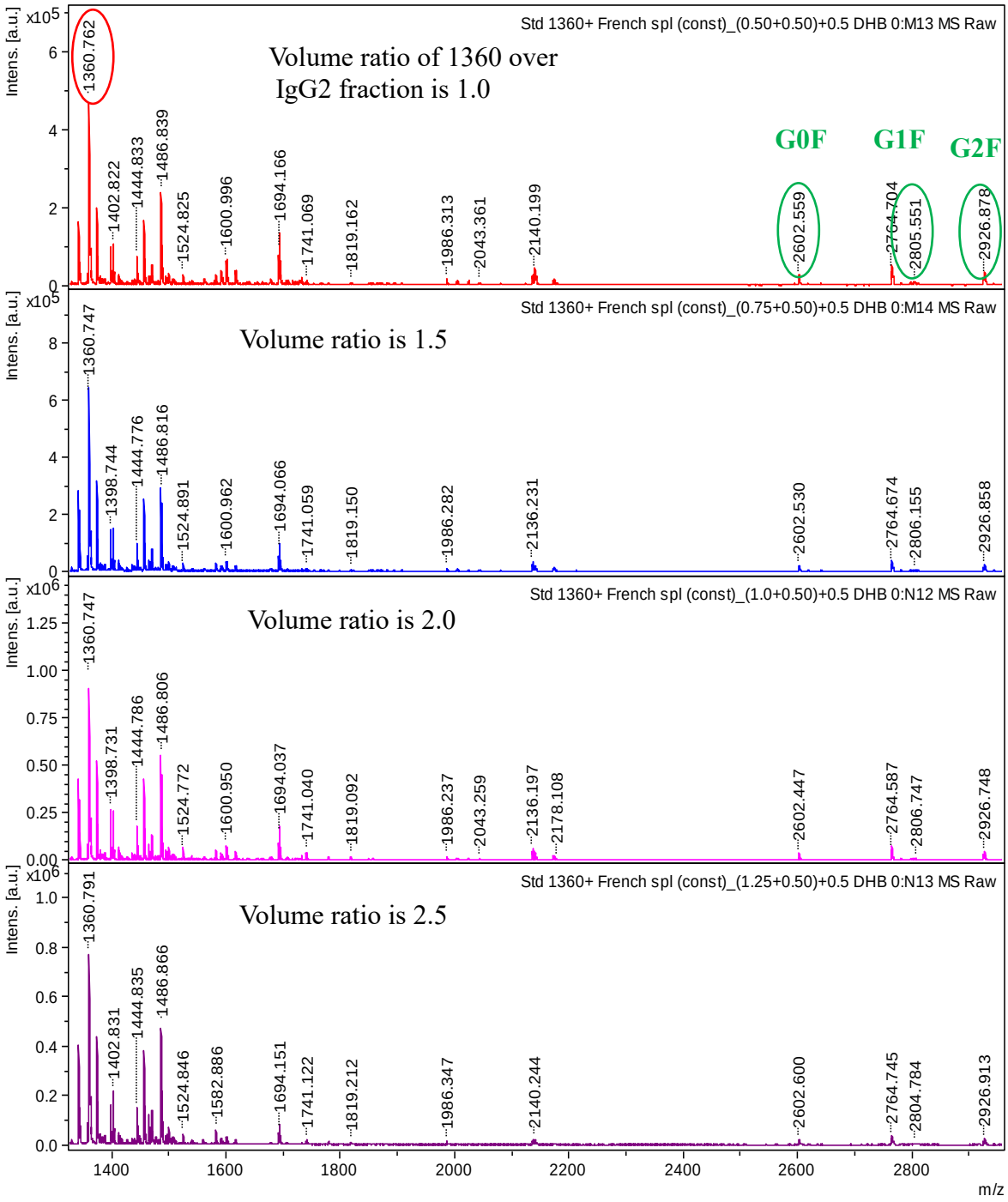

Figure 3.39. MALDI-ToF-MS spectra of only IgG2 fraction of tryptic glycopeptide from human IgG: spiking with glycopeptide standard (*m/z* 1360) for quantitation.

Similarly, G0F, G1F and G2F glycoforms of EEQFNSTFR from human IgG were quantified with EEQFN(GlcNAc)STFR. Figure 3.40 shows typical MALDI-MS spectra of this experiment (Experiment xii).

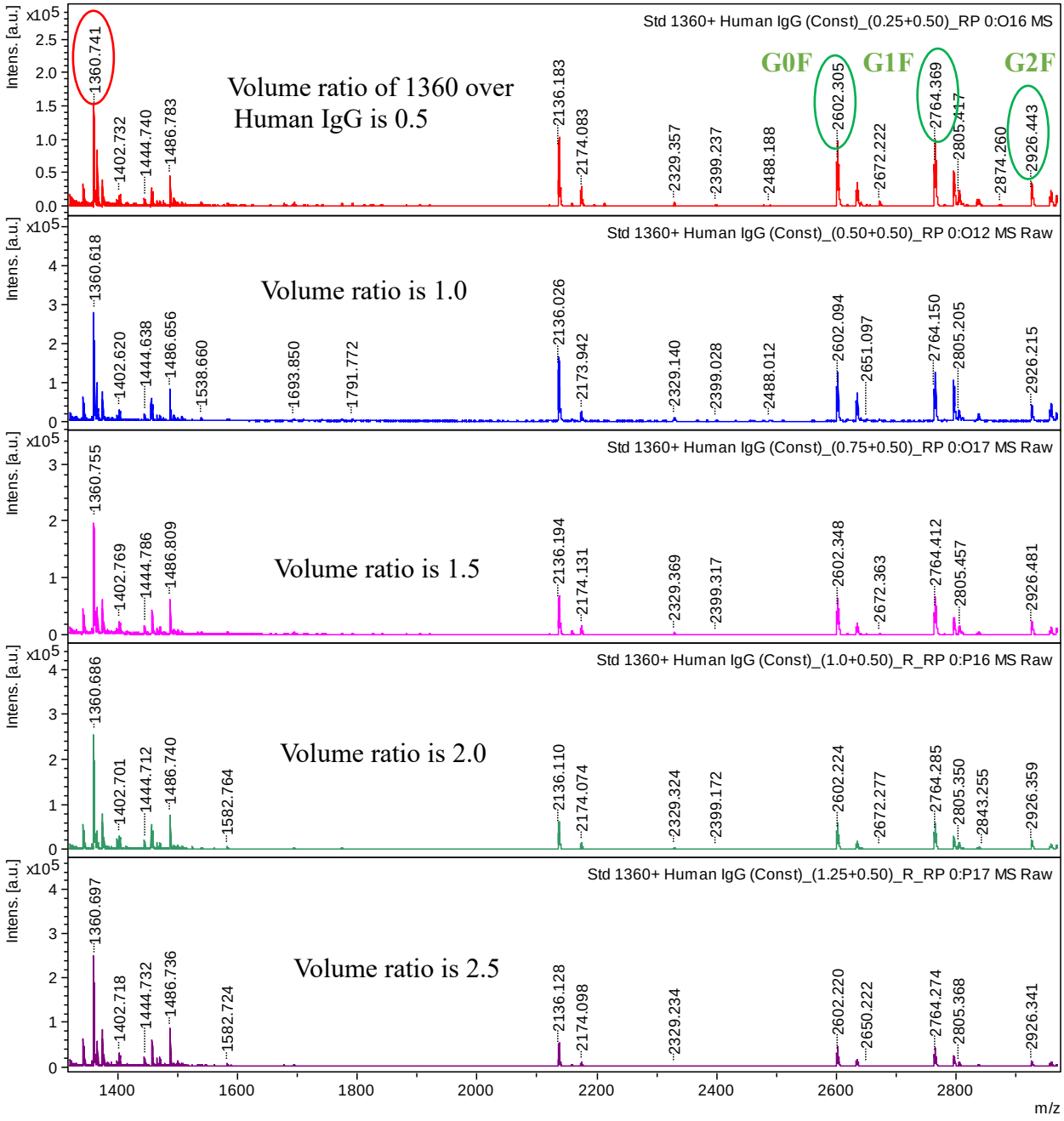

Figure 3.40. MALDI-ToF-MS spectra of glycopeptides from polyclonal human IgG: spiking with glycopeptide EEQFN(GlcNAc)STFR standard (1360) for quantitation. Volume ratios indicated on the spectra correspond to vol. 1360/vol. IgG glycopeptides (Experiment xii).

Figure 3.41 shows the plot obtained for the attempts in quantifying the G0F, G1F and G2F glycoforms of EEQFNSTFR with EEQFN(GlcNAc)STFR in a) a fraction containing only IgG2 *N*-glycopeptides (left), and b) in a sample of human IgG (right). The high slope values in (a) denote a very low concentration of IgG2 in the samples being tested. The reverse of the slopes reflected well the relative glycoform abundances observed in the spectra: 48.41, 41.26, 10.33 (slopes) *vs.*49.82, 39.51, and 10.67 (areas). The concentrations of IgG2 peptide glycoforms deposited on target were determined and reported in Table 3.4, column 2.

The graphs of Figure 3.41b represent the quantitation of IgG2 glycopeptides in a polyclonal human IgG sample, with concentrations in line with that of the standard (101 µM). The relative reverse slopes (42.36, 43.30, 14.34 %) matched the average peak areas in the mass spectra (42.03, 43.24,14.73%) suggesting even responses between the standard and analyte glycoforms. Concentrations of EEQFNSTFR glycoforms were calculated and reported in Table 3.4, column 4.

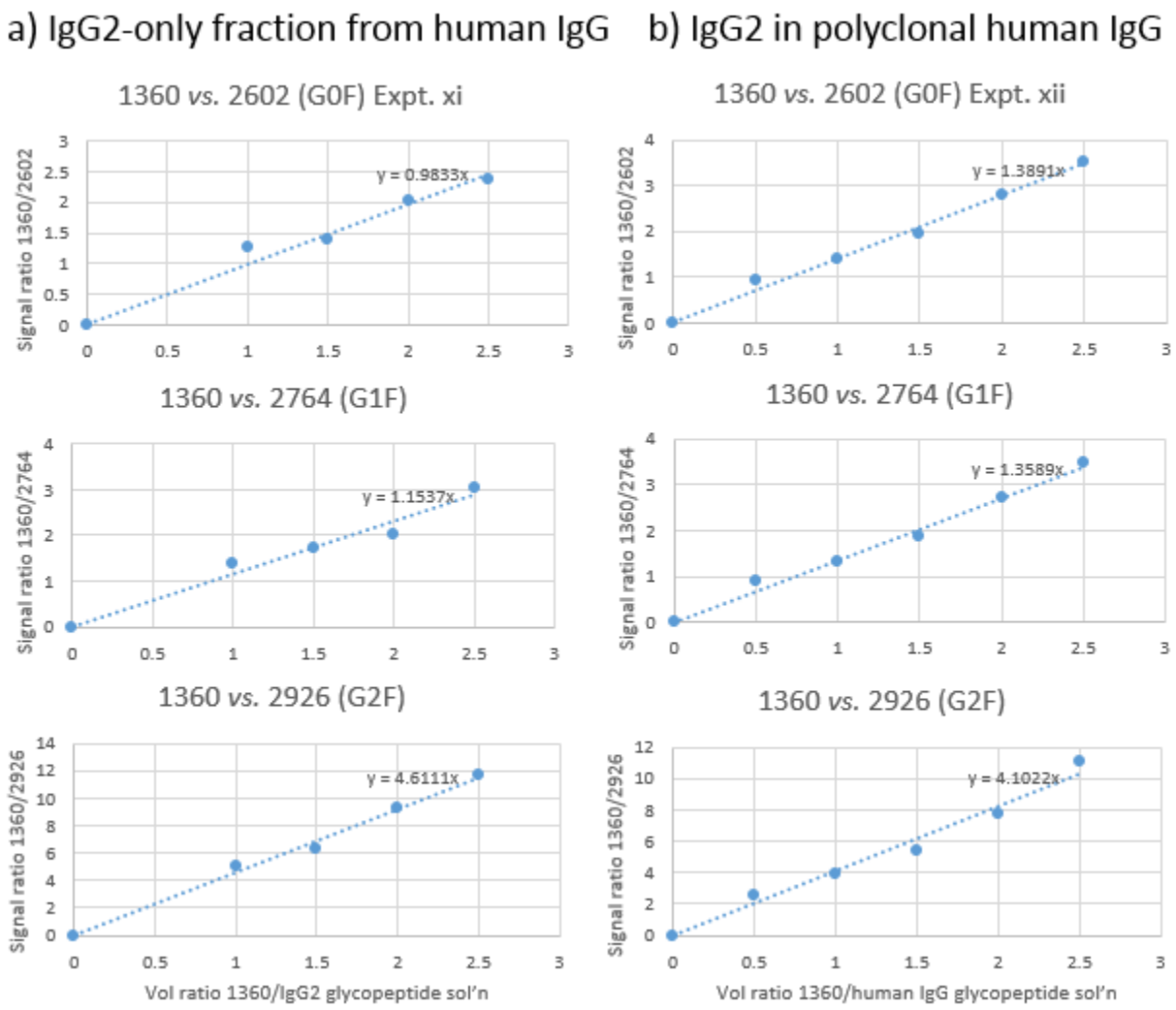

Figure 3.41. Attempts to use glycopeptide EEQFN(GlcNAc)STFR (1360) as internal standard for the dosage of solutions of tryptic glycopeptides from a) human IgG2 (Expt. xi) and b) IgG2 in polyclonal human IgG (Expt. xii). Concentration of standard: a) 0.052 mM and b) 101 μM.

Table 3.4. Calculated EEQFNSTFR glycoform concentrations of solutions to which peptide and glycopeptide internal standards were added. Note: both IgG2 fractions are not from the same human IgG sample and cannot be compared directly.

Sample →	IgG2 fraction Sample 1	IgG2 fraction Sample 2	Human IgG	Human IgG
Glycoform of EEQFNSTFR (*m/z*)	Glycopeptide standard (Expt. xi)	Peptide standard (Expt. xiii)	Glycopeptide standard (Expt. xii)	Peptide standard (Expt. xiv)
G0F (2602)	0.053 mM	0.20 mM	72 μM	1.5 mM
G1F (2764)	0.045 mM	0.26 mM	74 μM	1.6 mM
G2F (2926)	0.011 mM	0.093 mM	24 μM	0.52 mM
Total IgG2	0.11 mM	0.55 mM	0.17 mM	3.6 mM

The use of non-glycosylated synthetic EEQFNSTFR (1157) as internal standard was also investigated for the analysis of IgG2 peptide glycoforms (Exp. xiii-xiv). Results are presented in Figure 3.42 and sample spectra are shown in Figure 3.43. Figure 3.42a) corresponds to IgG2 fractions from human IgG (Expt. xiii), and reverse slope and peak area proportions showed relatively good matching values (36.68, 46.72, 16.60 for the slopes *vs* 35.99, 46.17 and 17.84 for peak areas). Glycopeptide concentrations are listed in Table 3.4, column 3.

For the analysis of IgG2 in the polyclonal human IgG samples (Expt. xiv), results are shown in Figure 3.42b). The reverse slopes (42.39, 43.22, 14.78%) *vs*. the relative peak areas (42.06, 43.07, 14.87%) offered a better match than in the case above. Glycoforms concentration for IgG2 EEQFNSTFR were calculated as indicated in Table 3.4, column 5. Once again for human IgG, the 1157 non-glycosylated standard exhibited less ionization efficiency than the 1360 glycosylated peptide, such that sample concentrations yielded by 1157 were much higher than the 1360. A total of 5.3 mM in glycopeptide concentration (see Table 2.1) was deemed too high for these Ab samples (see Table 2.1). The glycosylated peptide standard was decidedly a better internal standard for IgG2 than the non-glycosylated peptide.

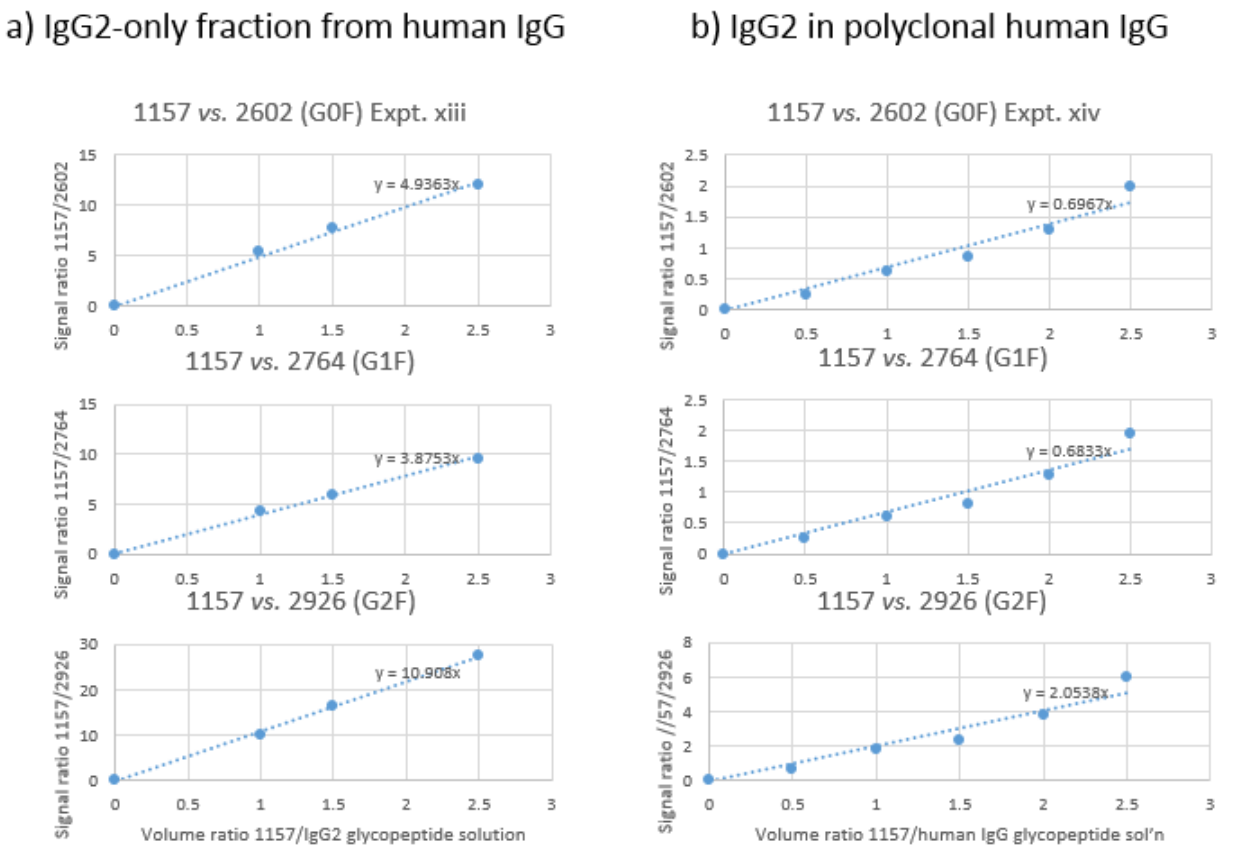

Figure 3.42 Attempts to use peptide EEQFNSTFR (1157) as internal standard for the dosage of solutions of tryptic glycopeptides from a) IgG2-only fractions and b) human IgG. Experiments xiii and xiv. Concentration of 1157; 1.01 mM for IgG2 and 1.07 mM for human IgG.

For human polyclonal IgG samples where glycoforms of both EEQYNSTYR (IgG1) and EEQFNSTFR (IgG2) are coexistent, Figure 3.33b and 3.41b suggest that the presence of another peptide subclass does not interfere significantly in the independent analysis of either IgG1 or IgG2 glycopeptides.

Figure 3.43 shows MALDI-MS spectra of tryptic glycopeptide fractions (only IgG2 fraction from human IgG), analyzed with internal standard EEQFNSTFR (*m/z* 1157) and Figure 3.44 shows the MALDI-MS spectra of glycopeptides from polyclonal human IgG: spiking with peptide EEQFNSTFR standard (*m/z* 1157) for quantitation.

.

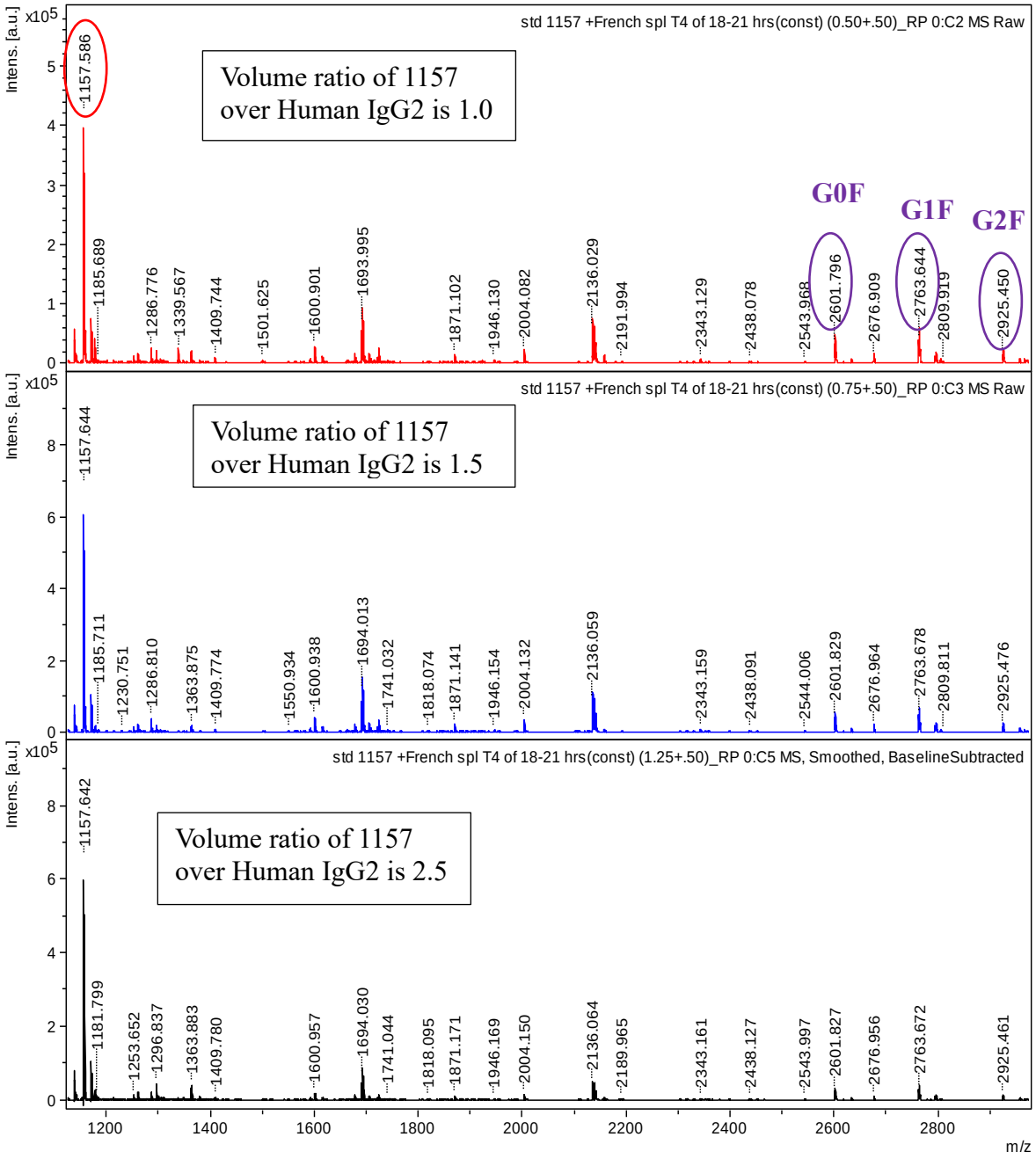

Figure 3.43. MALDI-ToF-MS mass spectra of tryptic glycopeptide fractions (IgG2 in polyclonal human IgG), analyzed with internal standard EEQFNSTFR (*m/z* 1157) (Experiment no: xiii).

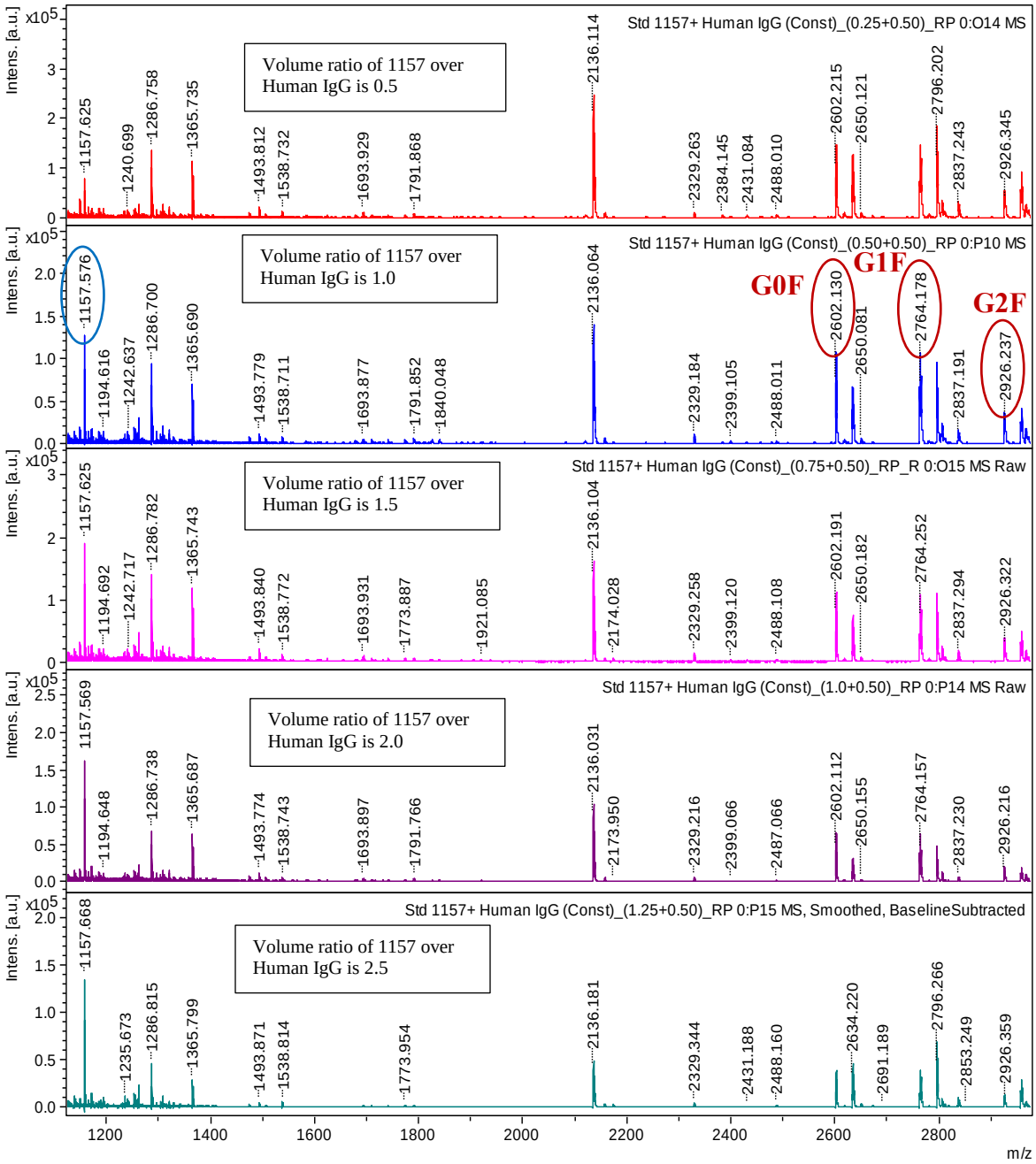

Figure 3.44. MALDI-ToF-MS spectra of glycopeptides from polyclonal human IgG: spiking with peptide EEQFNSTFR standard (1157) for quantitation (Experiment no: xiv).

The above results suggested that the glycosylated peptide standard was decidedly a better internal standard for IgG2 than the non-glycosylated peptides.

3.6. Comparison of IgG1 and IgG2 signals with (glyco)peptides are mixed on target

Intact human IgG1 and IgG2 have very similar molecular weights, i.e. 146 kDa on average.[40] These antibodies upon comparison have many analogies in their sequences, but also count many differences, as represented by 3.6.1 by the conserved gamma sequences of the heavy chains (UniprotKB - P01857(IGHG1_HUMAN), P01859 (IGHG2_HUMAN)). Figure 3.45 shows the conserved gamma sequences.

IgG1

```
        10         20         30         40         50
ASTKGPSVFP LAPSSKSTSG GTAALGCLVK DYFPEPVTVS WNSGALTSGV
        60         70         80         90        100
HTFPAVLQSS GLYSLSSVVT VPSSSLGTQT YICNVNHKPS NTKVDKKVEP
       110        120        130        140        150
KSCDKTHTCP PCPAPELLGG PSVFLFPPKP KDTLMISRTP EVTCVVVDVS
       160        170        180        190        200
HEDPEVKFNW YVDGVEVHNA KTKPREEQYN STYRVVSVLT VLHQDWLNGK
       210        220        230        240        250
EYKCKVSNKA LPAPIEKTIS KAKGQPREPQ VYTLPPSRDE LTKNQVSLTC
       260        270        280        290        300
LVKGFYPSDI AVEWESNGQP ENNYKTTPPV LDSDGSFFLY SKLTVDKSRW
       310        320        330
QQGNVFSCSV MHEALHNHYT QKSLSLSPGK
```

IgG2

```
        10         20         30         40         50
ASTKGPSVFP LAPCSRSTSE STAALGCLVK DYFPEPVTVS WNSGALTSGV
        60         70         80         90        100
HTFPAVLQSS GLYSLSSVVT VPSSNFGTQT YTCNVDHKPS NTKVDKTVER
       110        120        130        140        150
KCCVECPPCP APPVAGPSVF LFPPKPKDTL MISRTPEVTC VVVDVSHEDP
       160        170        180        190        200
EVQFNWYVDG VEVHNAKTKP REEQFNSTFR VVSVLTVVHQ DWLNGKEYKC
       210        220        230        240        250
KVSNKGLPAP IEKTISKTKG QPREPQVYTL PPSREEMTKN QVSLTCLVKG
       260        270        280        290        300
FYPSDISVEW ESNGQPENNY KTTPPMLDSD GSFFLYSKLT VDKSRWQQGN
       310        320
VFSCSVMHEA LHNHYTQKSL SLSPGK
```

Figure 3.45. Conserved gamma sequences of the heavy chains of human IgG1 and IgG2 (UniprotKB accession numbers P01857 and P01859). (*figure adapted from ref no. 125).*

It is difficult to measure the subclass components of intact polyclonal IgG directly by ESI-MS or MALDI-MS. Even for very high-resolution mass spectrometers, the variation of molecular weight due to sequences and possible glycosylation of the variable portions of each subclass renders the exercise laborious unless very specific IgGs are being investigated. Most studies on

mass measurement of intact antibodies have been conducted on monoclonal species. [126,127] The abundant ratios in healthy individuals should be around 60-71 (IgG1) to 19-31 (IgG2)[36] i.e. that the average IgG1/IgG2 ratio should be around 262% but it was interesting to observe that the signal due to IgG2 peptide was always predominant over that of the IgG1 peptide. These measurements were repeated by ESI-MS and the results confirmed the MALDI-MS observations. Table 3.5 gives an abundance ratio obtained by both ionization techniques from glycopeptides from tryptic digests of heathy human IgG1 enriched with EMD Proteoglycan^{TM} kit.

Table 3.5. Ion abundance ratios obtained for the Fc *N*-glycopeptides of IgG1/IgG2.

Sample (Proteoglycan^{TM}-enriched tryptic digest)	Ionization method	Signal Ratio EEQYNSTYR/EEQFNSTFR
Healthy serum IgG no. 1	MALDI	18%
Healthy serum IgG no. 2	MALDI	35%
Healthy serum IgG no. 3	MALDI	32%
Healthy serum IgG no. 4	MALDI	10%
Healthy serum IgG no. 5	MALDI	20%
Healthy serum IgG no. 6	MALDI	42%
Human IgG (Sigma)	MALDI (Figure 3.30, 3.32, 3.34 & 3.36))	165%
Human IgG (Sigma)	MALDI (Figure 3.43 & 3.44	91%
Human IgG (Sigma)	ESI (HPLC)	58%
Human IgG (Sigma)	ESI (HPLC) (no EMD)	53%

A few possible reasons will be investigated to explain these observations:

i) In MALDI and ESI-MS, the IgG2 peptide has better ionization efficiency than the IgG1peptide;

ii) Different solubilities in spotting solvents have an impact on ionization;

iii) IgG2 is more efficient in tryptic digestion than IgG1.

3.6.1. Relative ionization efficiencies of IgG1 and IgG2 glycopeptides as mixtures.

Relative sensitivity measurements were conducted on both synthetic glycopeptides under same solvent conditions (TA30) (30 % acetonitrile in water, 0.1% TFA). It was shown from Table 3.5 that in the glycopeptide analysis of human polyclonal antibodies by MALDI-TOF-MS, the presence of both IgG1 and IgG2 species on the same sample target cannot be quantified by a direct comparison of their molecular ion abundance. Figure 3.46a shows that relative abundances do not vary linearly with the increase of 1360 peptide amount while keeping the amount of the 1392 peptide constant. In this figure, the quasi-exponential curve suggests a greater MALDI-MS sensitivity for EEQFN(GlcNAc)STFR than EEQYN(GlcNAc)STYR through a competitive ionization mechanism, as aliquots of 1360 added are detrimental to the 1392 signal.

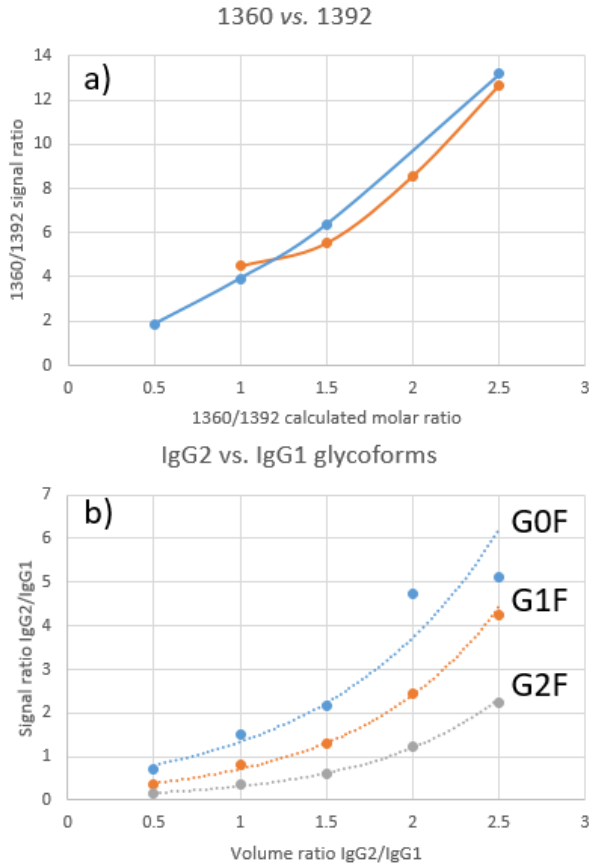

Figure 3.46. a) Variation of signal ratios *vs*. molar ratios for EEQFN(GlcNAc)/EEQYN(GlcNAc)STYR solution mixtures; b) variation of signal ratios according to volume ratios of IgG2/IgG1 glycopeptide solutions from IgG2 and IgG1 mAbs.

Figure 3.46a could potentially be used to create a "conversion factor" between the ionization efficiencies of EEQFNSTFR and EEQYNSTYR backbones to obtain more realistic molar abundances of IgG1 and IgG2 glycoforms in the mixture. For example, for sample no 6 in Table 3.5, the specrum showed a peak area ratio of 2.4 for IgG2/IgG1. Picking this ratio on the y axis of Figure 3.46a and projecting to the axis yields a ~ 0.7 IgG2/IgG1 molar ratio, which is closer to true values than 2.4, although still not representative of human IgG subclasses, which should be in the 0.3-0.4 range.[36]

In Figure 3.46b, two solutions of glycopeptides from unique subclasses, IgG1 and IgG2, were mixed in different volume ratios. Compiled signal ratios were calculated for each pair of

analogous glycoforms, e.g. EEQFN(G0F)STFR/EEQYN(G0F)STYR, and plotted against the volume ratios. The same trend as seen in Figure 3.46a was observed, and exponential fits best represented the plots. As exact concentrations were not known for IgG1 and IgG2 glycopeptide solutions used in this experiment, quantitation was not attenpted. Figure 3.47 shows the MALDI-MS spectra of EEQYN(GlcNAc)STYR (*m/z* 1392) and EEQFN(GlcNAc)STFR (*m/z* 1360) mixtures. In this experiment the amount of 1392 was kept constant while 1360 was spiked at different increasing volumes.

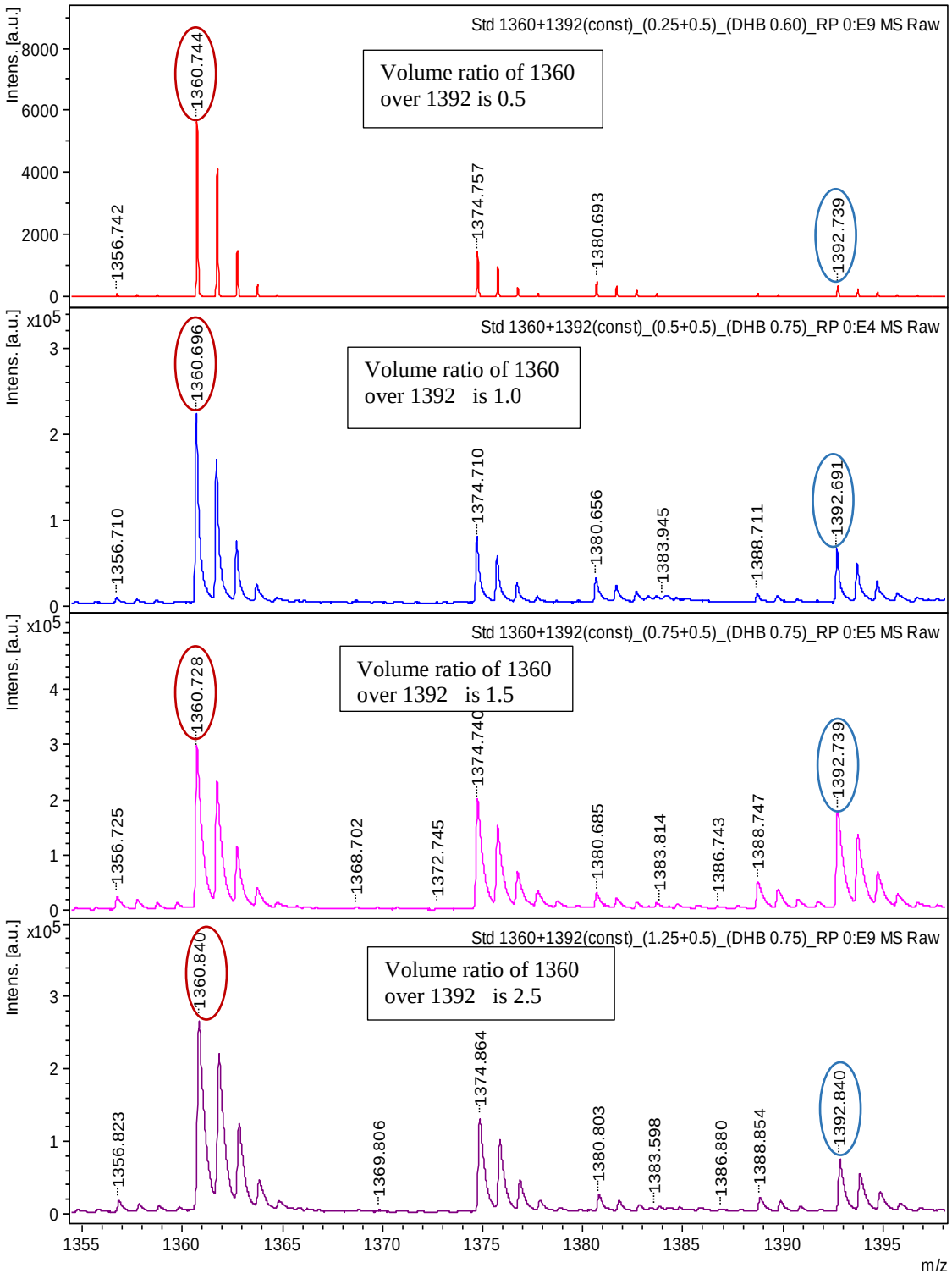

Figure 3.47. MALDI-ToF-MS spectra of both the standard glycopeptides EEQFN(GlcNAc)STFR (*m/z* 1360) and EEQYN(GlcNAc)STYR (*m/z* 1392) spotted simultaneously on the same target.

Figure 3.48 shows the spectra obtained during the experiment on variation of volume ratios with solutions of IgG2 and IgG1 mAbs.

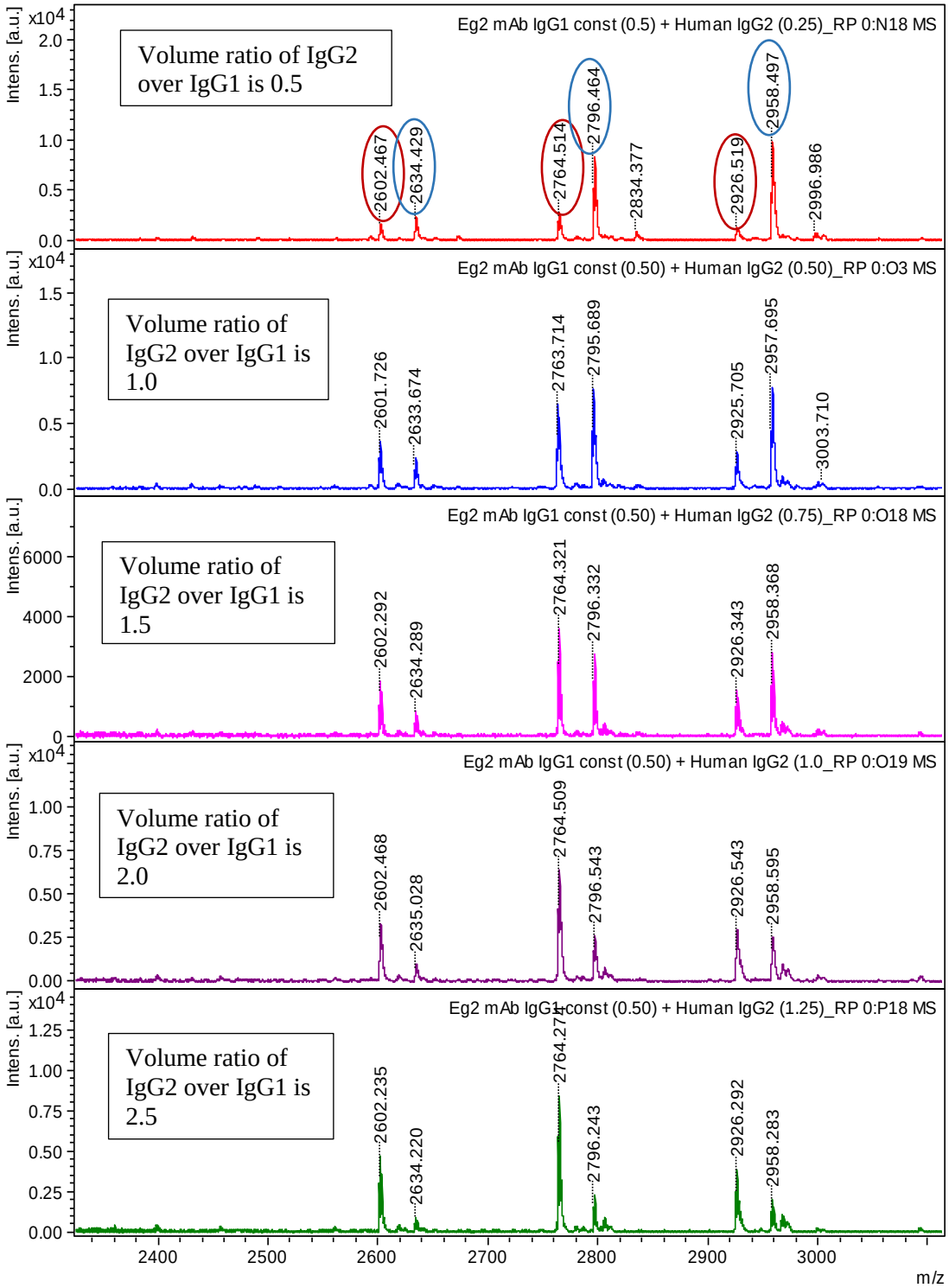

Figure 3.48. MALDI-MS spectra obtained for the variation of volume ratios of glycopeptide solutions from IgG2 and IgG1 mAbs.

Overall these experiments suggests that simultaneous quantitation of IgG1 and IgG2 glycoforms with both 1360 and 1392 standards on a MALDI target would be very difficult to achieve. It is preferable to perform the analysis of one subclass at a time using its related glycopeptide standard.

Quantitative analysis of both IgG1 and IgG2 glycoforms with their respective glycopeptide standards was nevertheless attempted with all compounds being present on target (Experiment xv). The analytes were human IgG glycopeptides. To a constant amount of analyte, both standards were added in identical increasing amounts. In each experiment, 0.5 µL of the analyte solution (human IgG) was spotted onto the target, and the volumes of both standard glycopeptide solutions (1360 and 1392) were added to match the ratios of 0.5, 1.0, 1.5 and 2.0. Plots were obtained for IgG1 and IgG2 species separately. Figure 3.49 shows the MALDI-MS spectra of both glycopeptide standards 1360 and 1392 when spiked into the same analyte.

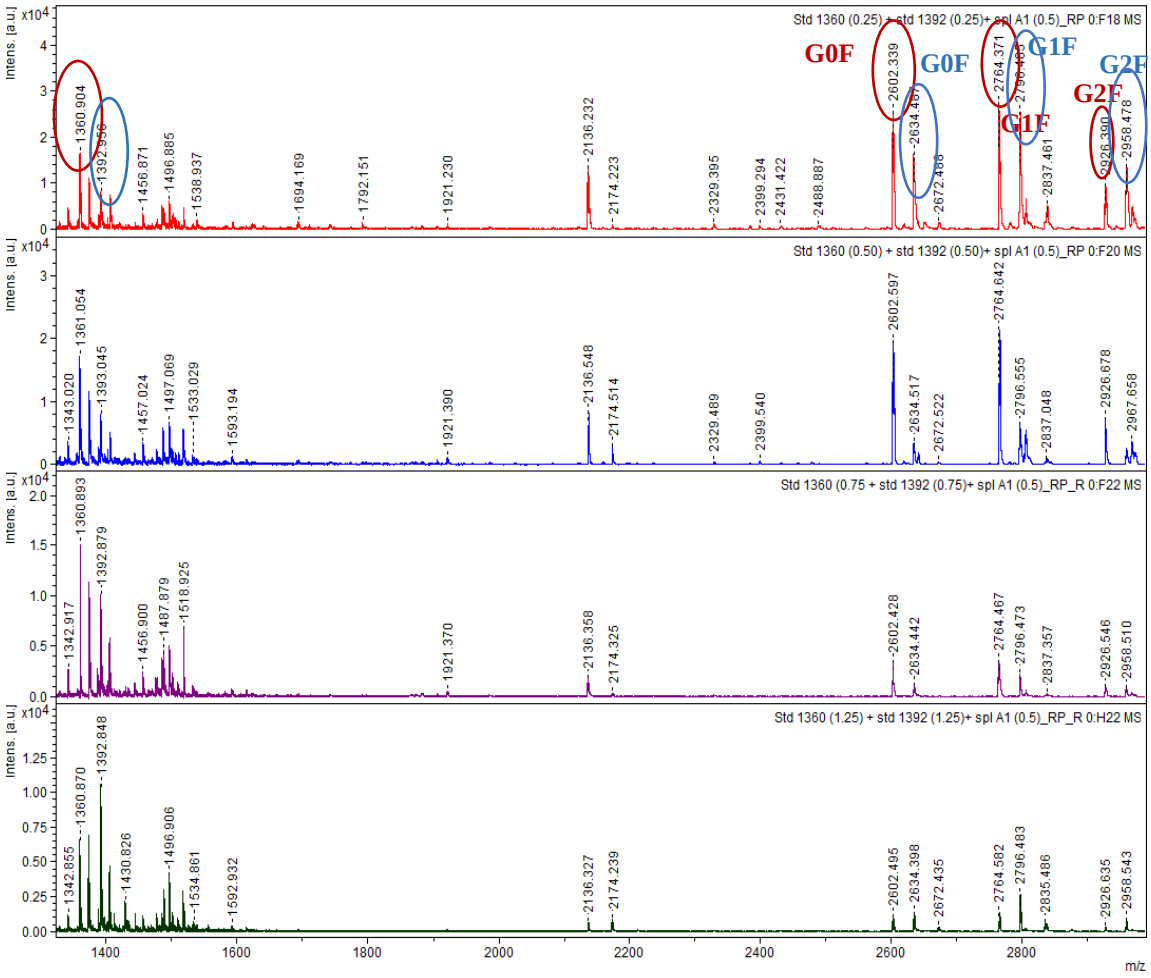

Figure 3.49. MALDI -ToF-MS spectra of both IgG1 and IgG2 glycoforms with their respective glycopeptide standards EEQYN(GlcNAc)STYR and EEQFN(GlcNAc)STFR.

Plots were obtained for IgG1 and IgG2 separately. The IgG1 plots (Figure 3.50a) Showed a linear relationship, although the intercept clearly did not go through zero. For IgG2 (Figure 3.50b) the situation was similar although less pronounced. Human IgG glycopeptides concentrations were calculated using the unmodified slopes (Figure 3.50 a-b) and also using slopes obtained by forcing the plot through the 0,0 origin as in all previous examples.

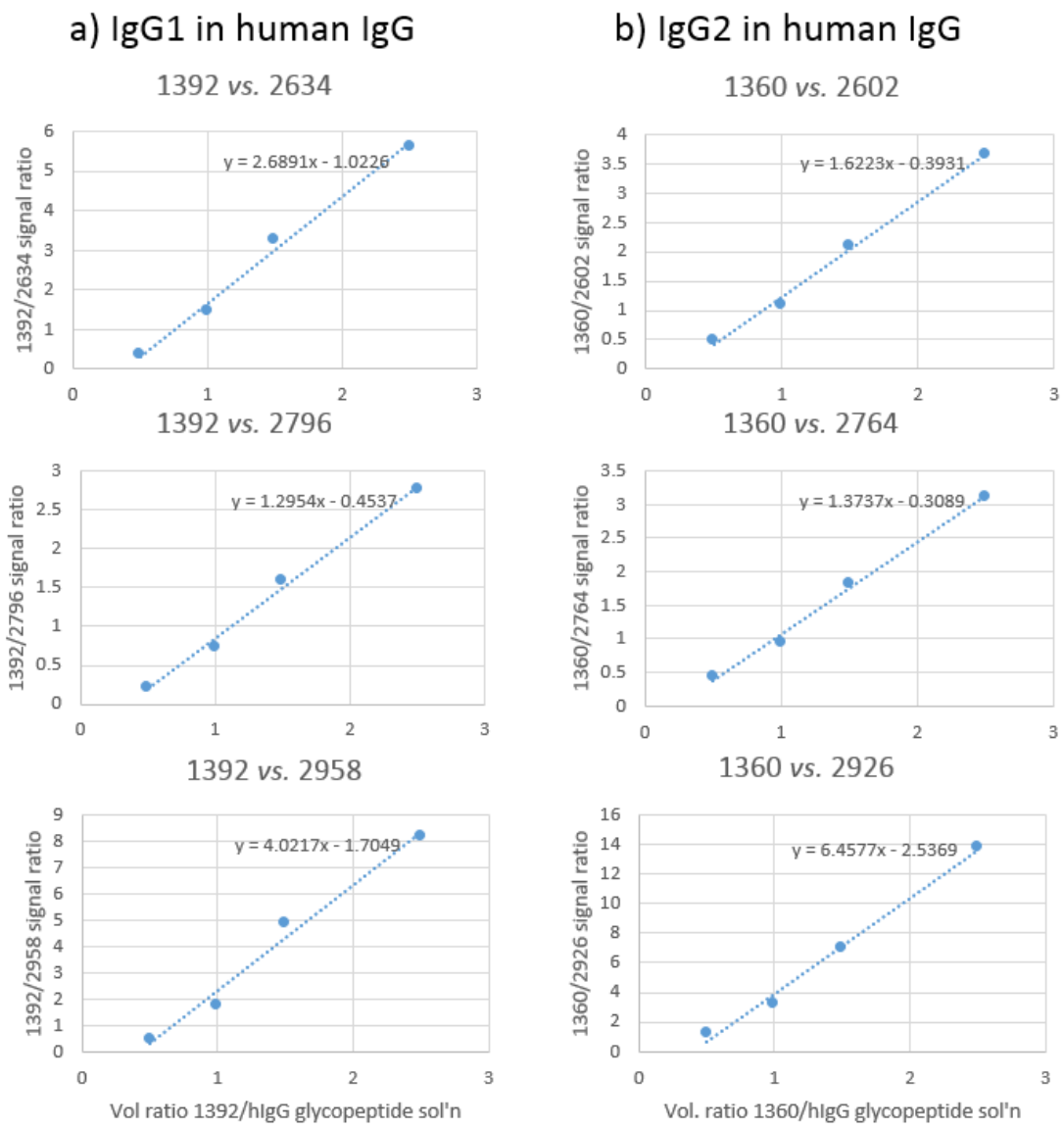

Figure 3.50. Simultaneous quantitation of IgG1 and IgG2 glycopeptides in human IgG with standard additions of EEQYN(GlcNAc)STYR (1392, IgG1, 0.95µM) and EEQFN(GlcNAc)STFR (1360, IgG2, 0.063 µM). Each spot analyzed contained 0.5 µM of human IgG glycopeptides. (Experiment xv).

Results of this experiment are shown in Table 3.5. These IgG2/IgG1 ratios (either 0.10/1.4 or 0.11/1.7) are below the predicted values of 0.3 to 0.4.[36] Thus, the method of using one internal standard at a time would be more reliable.

Table 3.6. Calculated EEQYNSTYR (IgG1) and EEQFNSTFR (IgG2) glycoform concentrations of a solution of internal standards EEQYN(GlcNAc)STYR and EEQFN(GlcNAc)STFR were added simultaneously at increasing volume ratios. Analytes: human IgG glycopeptides. (Experiment xv).

Glycoform	IgG1		IgG2	
	Calc. conc. (μM) (original slope)	Calc. conc. (μM) (forced through origin)	Calc. conc. (μM) (original slope)	Calc. conc. (μM) (forced through origin)
G0F	0.36	0.46	0.040	0.045
G1F	0.76	0.94	0.046	0.056
G2F	0.24	0.32	0.010	0.012
Total	1.4	1.7	0.10	0.11

3.6.2. Different solubilities of the peptides having an impact on ionization

Phenylalanine (F) as a single amino acid has a remarkably greater solubility in water than tyrosine (Y) (29.6 mg/mL *vs* 0.45 mg/mL) at 25°C. [128,129] This differences of solubility of single amino acids F and Y is likely to influence the relative solubilities of EEQFNSTFR vs EEQYNSTYR solubility effects of the two peptides were studied in the following experiments.

An equimolar mixture of EEQYNSTYR and EEQFNSTFR was prepared in water and spotted with DHB matrix onto the MALDI target.The mixture was then dried and analyzed by MALDI-ToF-MS (Figure 3.51a). Then a drop of water was added onto the dry sample, and pipetted out 90 sec later. The sample was dried again and reanalyzed: the spectrum showed a decrease in abundance of EEQYNSTYR relative to EEQFNSTFR (Figure 3.51b). The pipetted water drop was also deposited with DHB matrix and analyzed by MALDI, confirming the previous result: the *m/z* 1189 signal was higher than the *m/z* 1157 signal (Figure 3.51c). All these results suggests higher solubility for EEQYNSTYR *vs.* EEQFNSTFR, which goes against the relative solubilities of individual Y and F in water.

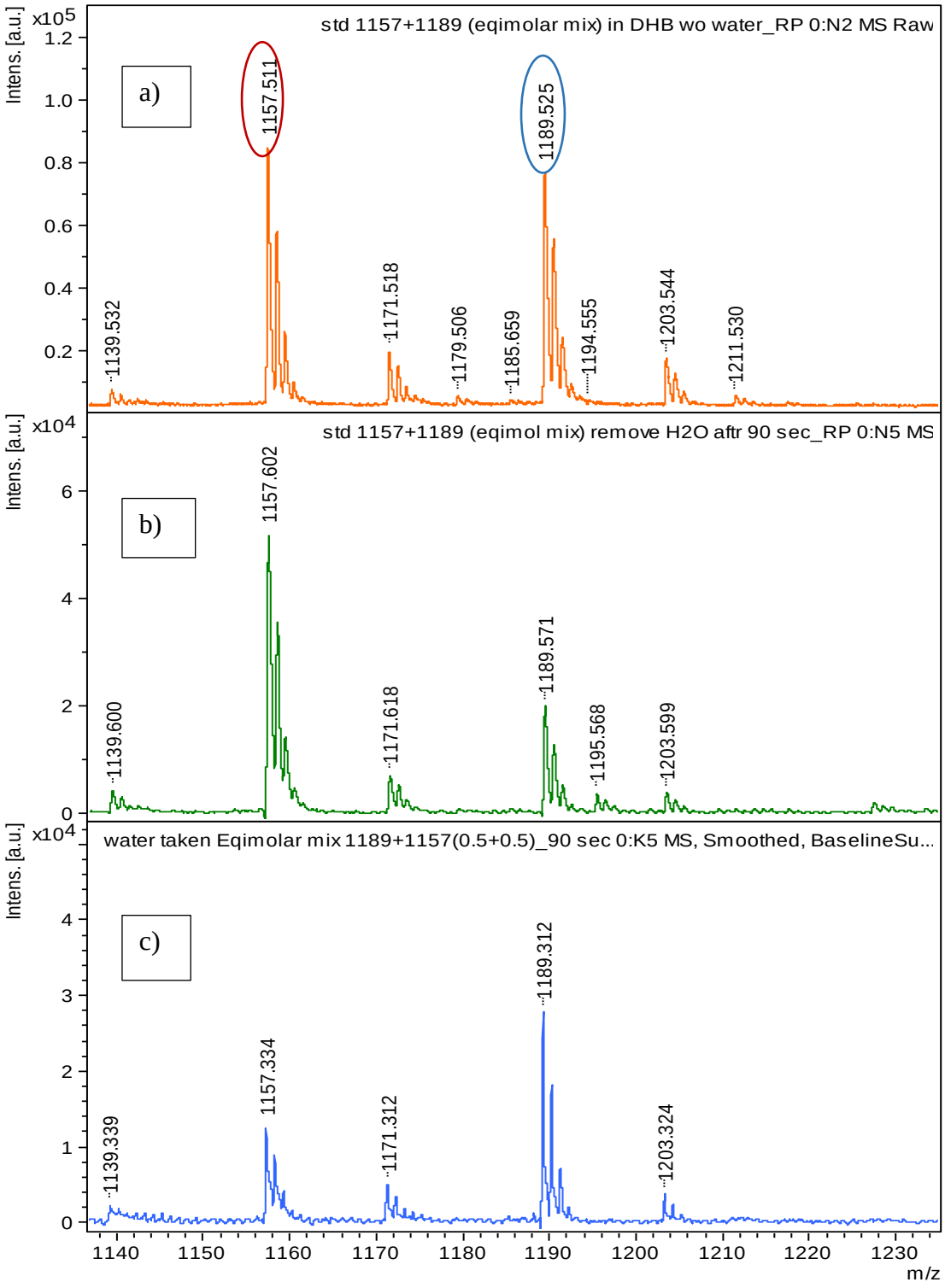

Figure 3.51. MALDI-ToF-MS spectra of a) an equimolar mixture of EEQFNSTFR (*m/z* 1157) and EEQYNSTYR (*m/z* 1189) dissolved and spotted in water; b) dried sample after adding a drop of water and pipetting it off 90s later; c) dried water withdrawn from the sample after 90s and spotted onto the target. In each case matrix used was DHB.

On the hydrophobicity scale,[130] EEQYNSTYR is more hydrophilic than EEQFNSTFR, such that in reverse-phase HPLC a larger percentage of acetonitrile in water is needed to elute EEQFNSTFR than EEQYNSTYR.[130] An equimolar solution of the synthetic peptides was prepared in water and in an aqueous acetonitrile solution. It was observed that relative ion abundances in MALDI-ToF-MS had some important variations (Figure 3.52). Figure 3.52a shows the spectrum obtained from the equimolar mixture in (a) water with 0.1% TFA and (b) in TA30. The most representative peak area ratios (*vs*. molar ratios) were obtained when the solution was prepared and spotted in water (0.1% TFA). It is interesting to observe that with the introduction of acetonitrile in b), EEQFNSTFR produced a stronger signal than EEQYNSTYR. The composition of 30% acetonitrile in water with 0.1% TFA (TA30) was used for most of this work, as it is the most common solvent normally used for sample preparation in our MALDI laboratory. Figure 3.52 shows MALDI-MS spectra of equimolar quantities of synthetic peptides dissolved and spotted used in different solvents.

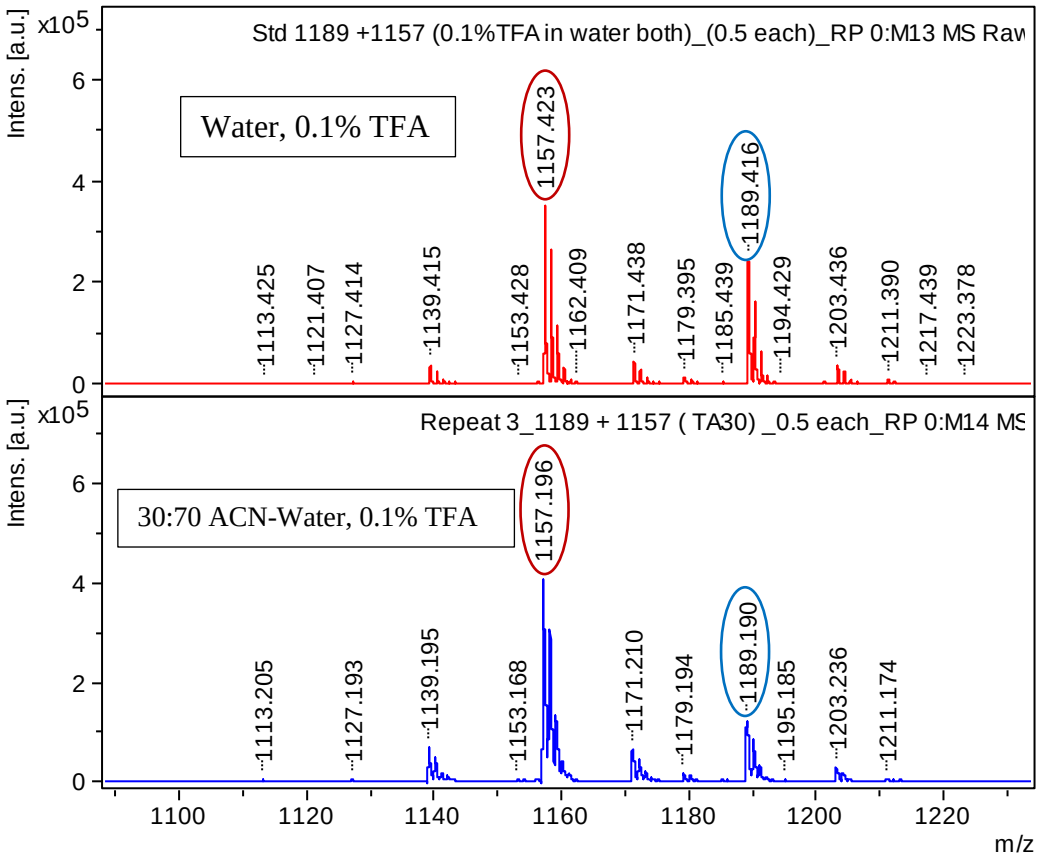

Figure 3.52. MALDI-MS spectra of equimolar quantities of synthetic peptides EEQFNSTFR (*m/z* 1157) and EEQYNSTYR (*m/z* 1189) acquired after dissolving and spotting using different aqueous solvents.The solvent used in b (TA30) was used for all of this work unless specified.

3.6.3. Digestion efficiency of IgG1 *vs* IgG2

In most MALDI spectra of human IgG glycopeptides (Table 3.6) there was a higher peak area proportion of EEQFNSTFR/EEQYNSTYR glycoforms irrespective if DTT reduction was used or not prior to tryptic digestion. Logically, the structure of intact IgG2 with two disulfide bonds in the hinge region should be more resistant to reduction than that of IgG1, which has one disulfide bond in that region. [125] The observation of more ions for the IgG2 peptide therefore goes against the predicted effect of this distinct feature of the antiodies. Another indication of reduction performance is the abundance of missed cleavage peptides TKPREEQFNSTFR and TKPREEQYNSTYR which helps to describe the above situation. Overall, there does not seem to be a detectable difference in the efficiency of digestion between IgG1 and IgG2.

3.7. Conclusion

Antibodies (Abs) are glycoproteins of prime importance in the immune system in which immunoglobulin G (IgG) is the most common representative of all. Glycoproteomic studies on human IgG are advantaged by different amino acid sequences of the heavy chain's tryptic *N*-glycopeptides EEQYNSTYR(IgG1), EEQFNSTFR(IgG2), EEQYSTFR(IgG3) and EEQFNSTYR(IgG4)[36]. It is thus possible to elaborate a quantitative method for IgG1 and IgG2 based on the synthetic glycopeptides with their respective sequences. It is well established that similar size peptides with different amino acid compositions or sequences yield different MS detection responses, therefore it is important that the amount of each different IgG *N*-glycopeptide be determined independently based on a synthetic peptide of same amino sequence and composition.

As many quantitative methods developed for glycopeptides are relative, the first objective of this work was to synthesize peptides and glycopeptides that are found in antibodies and that can serve as an internal standards. These (glyco)peptides correspond to the sequences of Fc tryptic fragments of human IgGs. They were used to perform absolute quantitative analyss of mAb and polyclonal samples, assuming that Fc glycosylation occurs in 100% of the molecules.

The next aim was to develop an absolute quantitation method for glycosylation and subclass analysis.The relative abundanes of subclasses can vary due to different health conditions (for example, monoclonal gammopathy), making quantitation necessary.

Overall the synthetic protocol shows that SPPS (solid phase peptide synthesis) of GlcNAc-glycosylated EEQYNSTYR and EEQFNSTFR is readily achievable using Fmoc peptide chemistry.

Spiking known amounts of these standards in tryptic digestion mixtures of human IgGs allowed to obtain absolute quantitation of IgG1 and IgG2 subclasses as well as the glycoforms of each subclass. In our experiments we have shown that MALDI-MS signals of $[M+H]^+$ ions of synthetic EEQYN(GlcNAc)STY*R varies proportionally with the amount deposited on target and, more importantly varies in the same fashion as $[M+H]^+$ signals of larger neutral glycoforms of the same peptide. It was possible to perform quantitation of one subclass of glycopeptides at a time, whether it was in a mAb or a polyclonal sample. IgG1 glycoforms of EEQYNSTYR were better quantified by the EEQYN(GlcNAc)STYR standard than by the bare peptide EEQNSTYR. Whether or not IgG2 was present in the sample did not seem to influence the linearity of the standard additions plots significantly with respect to IgG1. It was also possible to quantify IgG2 with EEQFN(GlcNAc)STFR.

Overall it was seen that EEQYN(GlcNAc)STYR and EEQFN(GlcNAc)STFR (glycopeptides) were better internal standards than EEQYNSTYR and EEQFNSTFR (peptides) for the absolute quantitaton of higher glycoforms of peptides, as concentration found were more coherent with values estimated from the sample preparation method.

The subclass abundance ratio in healthy individuals should be around 60-70% (IgG1) to 19-31 (IgG2) and the average IgG1/IgG2 ratio should be around 262% (Table 3.5). It was interesting to observe that when no real care was taken to notice exactly the solvent composition used for sample deposition, MALDI-ToF-MS spectra showed various trends (Table 3.2), where the signal due to the IgG2 peptide was always predominant over that of the IgG1 peptide. So the ionization efficiencies were studied for the two peptides EEQYNSTYR and EEQFNSTFR underdifferent sets of conditions.

For human IgG, the ratio of IgG2/IgG1 obtained using the quantitative method described in this work was within the predicted range in healthy persons. It was also shown that the IgG2

peptide backbone EEQFSTFR has a higer ionzation efficiency than EEQYNSTYR (IgG1), and that in the instance of a mixture the presence of the IgG2 peptide may have a competitive effect on the ionization of IgG1's and alter the analysis. Moreover it was shown that different solubilities of the peptides have a different impact on ionization.

It was also shown that the composition of the spotting solvent has a strong influence on the relative abundance of MALDI-MS signals for IgG2 *vs.* IgG1 peptides. This helps to explain some inconsistencies in the signals of human IgG glycoforms from difference subclasses observed in this work and in the literature.

This work highlights the importance of consistency in sample preparation for MALDI-ToF-MS analysis. The different ionization efficiencies of IgG1 and IgG2 glycopeptides directs them to be quantified preferentially one by one. Thus the method of using one internal standard at a time provided more reliability that the "all in one pot" method.

This work was limited to quantitation of IgG1 and IgG2 and their *N*-glycoforms, It will be important in the future to synthesize other peptides that are unique to IgG3 and IgG4 to allow their absolute quantitation and give the possibility to estimate relative glycoform concentrations in these subclasses. Differences in glycosylation among subclasses could help explaining their levels of inteaction with rceptors and complete binding factors.

Chapter-4. Future work

4.1. Future work

Mammals comprise a large variety of antibodies of which immunoglobulin G subtype is the most common.[40] Mammalian IgG is characterized by a diversity of subclasses ranging from one to at least eleven. [130,131] In humans, IgG1-4 have been well characterized and it has been established that their relative proportions influence the extent of important protein-protein interactions and of resulting biological implications.[40] The work of Butler et al. suggests similar implications for the relative abundances of the eleven pig IgG subclasses.[130] Our laboratory has already observed variable proportions of IgG6a *vs.* others in samples from different animals**.**[132,82] It will be important in a near future to develop a quantitative method for the eleven subclasses of pig Ig. A wide range of research is taking place with respect to porcine IgG, as pigs are important animal models for some human viral diseases[133] and for understanding the immune response to influenza[134,130] for instance. Swine are also important in xenotransplantation[135] and in generating humanized antibodies. [136] Future work to follow will focus on the quantification of porcine IgG subclasses. So far it has not been possible to separate these IgG subclasses by chromatography or electrophoresis, and an all inclusive method where tryptic peptides unique to each subclass is deemed appropriate. Examples of such tryptic peptides to be synthesized are given in Table 4.1. The only glycopeptide in this list is EAQFN(Glycan)STYR at the bottom, which is at this time thought to originate from IgG6a only. There are two Fc *N*-glycopeptides sequences in the eleven subclasses: EAQFNSTYR (IgG6a) and EEQFNSTYR (IgG1a-b, IgG2a-b, IgG4a-b).[132,82]

Table 4.1. Tryptic peptides that are unique to each porcine IgG subclass. Sequences in bold are to be synthesized in priority.

Peptide sequence	Unique to subtype(s)	m/z (M+H)+
TKPR	IgG5b	501.31
ATGPSR	IgG3	588.31
FSVDK	IgG2a-2b	595.31
FSVEK	IgG5b	609.32
AIGQSR	IgG1a-1b	631.35
VDLCVGK	IgG5b	733.39
DLLSPITR	IgG3	914.53
TYFLYSK	IgG5a	921.47
SIVTLTCLVK	IgG5a-5b	1076.64
TTPPQEDEDR	IgG5a	1187.52
TAPLVYPLAPCGR	IgG2b	1357.73
SNGQPEPENTYR	IgG1b	1391.62
EPQVYTLSPSAEELSR	IgG6a-6b	1805.89
VVSVLLIQHQDWLNGK	IgG4b	1849.03
STPPQEDEDGTYFLYSK	IgG6b	1976.88
EAQFNSTYR	IgG6a	1115.51 (+glycans)

The principle of the method is as explained in this thesis, except that most analysis will be carried out by spiking samples with non-glycosylated synthetic peptides. The only glycopeptide synthesized will be EAQFN(GlcNAc)STYR. One experiment will consist of determining if IgG6a is indeed the only subclass to include this sequence, then the following should hold: EPQVYTLSPSAEELSR = EAQFN(Glycan)STYR + STPPQEDEDGTYFLYSK, in terms of absolute quantities. Globally with the peptides of Table 4.1 spiked in tryptic digest fractionated samples, absolute quantities may be determined for each subclass. This approach should be tested using both MALDI and ESI MS detection techniques. Porcine IgG administered to graft patient as part of anti-rejection antibody cocktails may then be better characterized in terms of molecular contents.

References

1. Helenius, A.; Aebi, M. Intracellular functions of N-linked glycans. *Science,* **2001**, *291*, 2364-2369
2. Rudd, P. M.; Guile, G. R.; Kuster, B.; Harvey, D. J. et. al. Oligosaccharide sequencing technology. *Nature,* **1997**, *388*(6638), 205-207. doi: http://dx.doi.org/10.1038/40677
3. Bahl, O.P. (1992) *Glycoconjugates: Composition, structure, and function*. Allen, H.J, Kisailus, E.C (Ed.). New York: Marcel Dekker Inc. (pp. 1–12).
4. Oxford Glycosystems Ltd.; Tools for Glycobiology, Catalog and Technical Notes, Rosedale, NY (1992).
5. Burda, P.; Aebi, M. The dolichol pathway of N-linked glycosylation. *Biochimica et Biophysica Acta (BBA)-General Subjects,* **1992,** *1426*(2), 239-57. doi:10.1016/S0304-4156(98)00127-5.
6. Keesay, J. *Biochemic information*, Boehringers Mannheim Biochemicals, Indianapolis, IN
7. Tarentino, A.L.; Gómez, C. M.; Plummer, T. H. Deglycosylation of asparagine-linked glycans by peptide: N-glycosidase F. *Biochemistry*, **1985,** *24*(17), 4665-4671.
8. Lennarz, W. J. *Biochemistry*. **1987**, *26(23)*, 7205-7210.
9. Rothman, J. E. The golgi apparatus: two organelles in tandem. *Science,* **1981,** *213(4513),*1212-9.
10. Berg, J. M.; Tymoczko, J. L.; Stryer, L. (2002). *Biochemistry, 5th Edition,* New York: W H Freeman.
11. Voet, D.; Voet, J. G. (1990). *Biochemistry*, John Wiley and Sons Inc.
12. Steen, P. V. D.; Rudd, P. M.; Dwek, R. A.; Opdenakker, G. Concepts and Principles of O-Linked Glycosylation. *Crit Rev Biochem Mol Biol*. **1998,** *33,* 151-208
13. Mechref, Y.; Novotny, M. V. Structural investigations of glycoconjugates at high sensitivity. *Chem Rev,* **2002,** *102*(2), 321-69.

14. Walsh, G. Post-translational modifications of protein biopharmaceuticals. *Drug Discov Today*. **2010**, *15*(17-18), 773-80. doi: 10.1016/j.drudis.2010.06.009.

15. Stanley, P.; Schacter, H.; Taniguchi, N. (2009). N-Glycans. Varki, A.; Cummings, R.; Esko, J. D.; Freeze, H. H.; Stanley P, Bertozzi, C. R.; Hart, G.W.; Etzler, M. E.; (Ed.) *Essentials of Glycobiology* (2nd ed). Cold Spring Harbor (NY): Cold Spring Harbor Laboratory Press 2009.

16. Apweiler, R.; Hermjakob, H.; Sharon, N. On the frequency of protein glycosylation, as deduced from analysis of the SWISS-PROT database. *Biochim Biophys Acta*, **1999**, *1473(1)*,4-8. doi.org/10.1016/S0304-4165(99)00165-8

17. Solá, R. J.; Griebenow, K. Glycosylation of therapeutic proteins: an effective strategy to optimize efficacy. *BioDrugs.* **2010**, *24(1)*, 9-21. doi: 10.2165/11530550-000000000-00000.

18. Solá, R. J.; Griebenow. K. Effects of glycosylation on the stability of protein pharmaceuticals. *J Pharm Sci*, **2009**, *98(4)*, 1223-45. doi: 10.1002/jps.21504.

19. Ma, J.; Hart, G. W. Protein O-GlcNAcylation in diabetes and diabetic complications. *Expert Rev Proteomics.* **2013**, *10(4)*, 365-80. doi: 10.1586/14789450.2013.820536.

20. Xiao, Y.; Lee, T.; Latham, M. P.; Warner, L. R.; Tanimoto, A.; Pardi, A.; Ahn, N. G. Phosphorylation releases constraints to domain motion in ERK2. *Proc Natl Acad Sci USA*, **2014**, *111(7)*, 2506-11. doi: 10.1073/pnas.1318899111.

21. Hakomori, S. Glycosylation defining cancer malignancy: new wine in an old bottle. *Proc Natl Acad Sci USA*, **2002**, *99(16)*, 10231-3. doi: 10.1073/pnas.172380699.

22. Kameyama, A. Nakaya, S.; Ito, H.; Kikichi, N.; Angata, T.; Makamura, M. et al. Strategy for Simulation of CID Spectra of N-Linked Oligosaccharides toward Glycomics. *J. Proteome Res*, **2006**, *5(4)*, 808–814. doi: 10.1021/pr0503937

23. Chapman, N. R.; Barratt, C. L. The role of carbohydrate in sperm-ZP3 adhesion. *Mol Hum Reprod.* **1996**, *2(10)*, 767-74.

24. Shur, B. D.; Hall, N. G. A role for mouse sperm surface galactosyltransferase in sperm binding to the egg zona pellucida. *J Cell Biol,* **1982**, *95(2 Pt 1),* 574-579. doi: 10.1083/jcb.95.2.574

25. Varki, A. (1993). Biological roles of oligosaccharides: all of the theories are correct. *Glycobiology, 3(2),* 97-130.

26. Gabel, C.A.; Foster, S.A. Lysosomal enzyme trafficking in mannose 6-phosphate receptor-positive mouse L-cells: demonstration of a steady state accumulation of phosphorylated acid hydrolases. *J Cell Biol*. **1986**, *102,* 943-50.

27. Herzog, V.; Neumüller, W.; Holzmann, B. Thyroglobulin, the major and obligatory exportable protein of thyroid follicle cells, carries the lysosomal recognition marker mannose-6-phosphate. *EMBO J.* 1987, *6,* 555-560.

28. Yamamoto, K.; Tsuji T.; Tarutani, O.; Osawa, T. Phosphorylated high mannose-type and hybrid-type oligosaccharide chains of human thyroglobulin isolated from malignant thyroid tissue. *Biochimica et Biophysica Acta.* **1985**, 838, 84-91.

29. Lowe, J. B.; Marth, J. D. A genetic approach to Mammalian glycan function. *Annu Rev Biochem,* **2003,** *72,* 643-91.

30. Marklová, E.; Albahri, Z. Screening and diagnosis of congenital disorders of glycosylation. *Clin Chim Acta,* **2007**, *385(1-2),* 6-20.

31. Dwek, R. A.; Lellouch, A. C.; Wormald, M. R. Glycobiology: 'the function of sugar in the IgG molecule'. *Journal of Anatomy*, **1995**, *187*, 279–292.

32. Kobata A. Structures and functions of the sugar chains of glycoproteins. *Eur J Biochem,* **1992**, *209*(2), 483-501.

33. Malhotra, R.; Wormald, M. R.; Rudd, P. M.; Fischer, P. B.; Dwek, R. A.; Sim, R. B. Glycosylation changes of IgG associated with rheumatoid arthritis can activate complement via the mannose-binding protein. *Nat Med.* **1995**, *1*, 237-43.

34. Parekh, R. B.; Dwek, R. A.; Sutton, B. J.; et al. Association of rheumatoid arthritis and primary osteoarthritis with changes in the glycosylation pattern of total serum IgG. *Nature.* **1985**, *316*, 452-457.

35. Zauner, G.; Selman, M. H.; Bondt, A.; Rombouts, Y.; Blank, D.; Deelder, A. M. et al. Glycoproteomic analysis of antibodies. *Mol Cell Proteomics.* **2013**, *12*, 856-65.

36. Hamilton, R. G. Human IgG subclass measurements in the clinical laboratory. *Clin Chem*, **1987**, *33(10)*, 1707-25.

37. Ballieux, R. E.; Bernier, G. M.; Tominaga, K.; Putnam, F. W. GAMMA GLOBULIN ANTIGENIC TYPES DEFINED BY HEAVY CHAIN DETERMINANTS. *Science*, **1964,** *145 (3628)*,168-70.

38. Terry, W. D.; Fahey, J. L. SUBCLASSES OF HUMAN GAMMA-2-GLOBULIN BASED ON DIFFERENCES IN THE HEAVY POLYPEPTIDE CHAINS. *Science.* **1964**, *146(3642)*, 400-1.

39. Schur, P. H. IgG subclasses. A historical perspective. *Monogr Allergy*, **1988,** *23*, 1-11.

40. Vidarsson, G.; Dekkers, G.; Rispens, T. IgG subclasses and allotypes: from structure to effector functions. *Front Immunol*, **2014,** *5*, 520. doi: 10.3389/fimmu.2014.00520

41. Jefferis, R.; Kumararatne, D. S. Selective IgG subclass deficiency: quantification and clinical relevance. *Clin Expl Immunol*, **1990**, *81(3)*, 357–367.

42. French, M. A.; Harrison, G. Serum IgG subclass concentrations in healthy adults: a study using monoclonal antisera. *Clin Exp Immunol.* 1984, *56(2)*, 473–475.

43. French, M. Serum IgG subclasses in normal adults. *Monogr Allergy.* 1986, *19*, 100-107.

44. Hayes, J. M, Cosgrave, E. F.; Struwe, W. B.; Wormald, M.; Davey, G. P, Jefferis, R. et al. Glycosylation and Fc receptors. *Curr Top Microbiol Immunol.* 2014, *382*, 165-199.

45. Idusogie, E. E.; Presta, L. G.; Gazzano-santoro, H.; Totpal, K.; Wong, P. Y.; Ultsch, M.; et al. Mapping of the C1q binding site on rituxan, a chimeric antibody with a human IgG1 Fc. *J Immunol.* **2000**, *164(8)*, 4178-84.

46. Deisenhofer, J. Crystallographic refinement and atomic models of a human Fc fragment and its complex with fragment B of protein A from Staphylococcus aureus at 2.9- and 2.8-A resolution. *Biochemistry.* **1981**, *20(9)*, 2361-2370.

47. Feige, M. J.; Nath, S.; Catharino, S. R.; Weinfurtner, D.; Steinbacher, S.; Buchner, J. Structure of the murine unglycosylated IgG1 Fc fragment. *J Mol Biol.* **2009**, *391(3)*, 599-608.

48. Parekh, R. B.; Dwek, R. A.; Sutton, B. J.; et al. Association of rheumatoid arthritis and primary osteoarthritis with changes in the glycosylation pattern of total serum IgG. *Nature.* **1985**, *316*, 452-457.

49. Van zeben, D.; Rook, G. A.; Hazes, J. M.; Zwinderman, A. H.; Zhang, Y.; Ghelani, S. et al. Early agalactosylation of IgG is associated with a more progressive disease course in patients with rheumatoid arthritis: results of a follow-up study. *Br J Rheumatol.* **1994**, *33(1)*, 36-43.

50**.** Wood, J. S. Characterization of the N-Glycosylation Pattern of Antibodies by Complementary Use of ESI and MALDI Mass Spectrometry; Technical Note from Bioscience Technology, **2013**; Available from http://www.biosciencetechnology.com/articles/2013/11/characterization-n- (accessed 10 August 2017)

51. Malpiedi, L. P.; Díaz, C. A.; Nerli, B. B.; Pessoa A. Jr. Single-chain antibody fragments: Purification methodologies. *Process Biochem.* **2014**, *32*, 992-1000.

52. Herrington-Symes, A. R.; Farys1, M.; Khalili1, H.; Brocchini1, S. Antibody fragments: Prolonging circulation half-life special issue-antibody research. *Adv. Biosci. Biotech.* **2013**, *4*, 689-698. doi: 10.4236/abb.2013.45090

53. Walsh, G. Biopharmaceutical benchmarks 2014. *Nat Biotechnol.* **2014**, *32(10)*, 992-1000.

54. Zhang, J.; Liu, X.; Bell, A.; To, R.; Baral, T. N.; Azizi, A. et al. Transient expression and purification of chimeric heavy chain antibodies. *Protein Expr Purif.* **2009**, *65*, 77-82.

55. Spearman, M.; Bodnar, E.; Perreault, H.; Butler, M. Glycosylation analysis of chinese hamster ovary produced glycoproteins. *Pharma Bioproc.* **2014**, *2*, 449-468

56. Sola, R. J.; Griebenow, K. Glycosylation of therapeutic proteins: an effective strategy to optimize efficacy. *Biodrugs.* **2010,** *24*, 9-21.

57. Rodriguez, J.; Spearman, M.; Huzel, N.; Butler, M. Enhanced production of monomeric interferon-beta by CHO cells through the control of culture conditions. *Biotechnol Prog.* **2005**, *21*, 22-30.

58. Ferrara, C.; Grau, S.; Jager, C.; Sondermann, P.; Brunker, P.; Waldhauer, I, et al. Unique carbohydrate-carbohydrate interactions are required for high affinity binding between FcγRIII and antibodies lacking core fucose. *Proc Natl Acad Sci, USA.* **2011,** *108*, 12669-74

59. Raymond, C.; Robotham, A.; Kelly, J.; Lattová, E.; Perreault, H.; Durocher, Y. Production of highly sialylated monoclonal antibodies. in *Glycosylation.* Stefana Petrescu (ed.), InTech. **2012**, 397

60. Garnock-Jones, K. P. 1.; Keating, G. M.; Scott, L. J. Trastuzumab: A review of its use as adjuvant treatment in human epidermal growth factor receptor 2 (HER2)-positive early breast cancer. *Drugs.* **2010**, *70*, 215-239. doi: 10.2165/11203700-000000000-00000.

61. Ferrante, A.; Beard, L. J.; Feldman, R. G. IgG subclass distribution of antibodies to bacterial and viral antigens. *Pediatr Infect Dis J.* **1990**, *9*, 516-524.

62. Dolscheid-pommerich, R. C.; Beinert, S.; Eichhorn, L.; Conrad, R.; Stoffel-wagner, B.; Zur, B. IgG subclass distribution in patients with monoclonal gammopathy. *Clin Chim Acta.* **2015,** *444,* 167-169.

63. Schneider, S.; Potter, S. N-Glycan Analysis of mAbs and Other Glycoproteins with UHPLC and Fluorescence Detection. Technical note from Agilent Technologies Inc. **2005**.

64. Jain, M.; Venkatraman, G.; Batra, S. K. Optimization of radioimmunotherapy of solid tumors: biological impediments and their modulation. *Clin Cancer Res.* **2007**, *13,* 1374-1382.

65. Adams, G. P.; Schier, R.; Mccall, A. M, Crawford, R. S.; Wolf, E. J.; Weiner, L. M. et al. Prolonged in vivo tumour retention of a human diabody targeting the extracellular domain of human HER2/neu. *Br J Cancer.* **1998**, *77*, 1405-1412.

66. Goel, A.; Colcher, D.; Baranowska-kortylewicz, J.; Augustine, S.; Booth, B. J.; Pavlinkova, G. et al. Genetically engineered tetravalent single-chain Fv of the pancarcinoma monoclonal antibody CC49: improved biodistribution and potential for therapeutic application. *Cancer Res.* **2000**, *60*, 6964-6971.

67. Hu, S.; Shively, L.; Raubitschek, A.; Sherman, M.; Williams, L. E.; Wong, J. Y. et al. Minibody: A novel engineered anti-carcinoembryonic antigen antibody fragment (single-chain Fv-CH3) which exhibits rapid, high-level targeting of xenografts. *Cancer Res.* **1996**, *56*, 3055-3061.

68. Pavlinkova, G.; Beresford, G. W.; Booth, B. J.; Batra, S. K.; Colcher, D. Pharmacokinetics and biodistribution of engineered single-chain antibody constructs of MAb CC49 in colon carcinoma xenografts. *J Nucl Med.* **1999**, *40,* 1536-46.

69. Kenanova, V.; Olafsen, T.; Crow, D. M.; Sundaresan, G.; Subbarayan, M.; Carter, N. H. et al. Tailoring the pharmacokinetics and positron emission tomography imaging properties of anti-carcinoembryonic antigen single-chain Fv-Fc antibody fragments. *Cancer Res.* **2005**, *65*, 622-631.

70. Kenanova, V.; Olafsen, T.; Williams, L. E.; Ruel, N. H.; Longmate, J.; Yazaki, P. J. et al. Radioiodinated versus radiometal-labeled anti-carcinoembryonic antigen single-chain Fv-Fc antibody fragments: optimal pharmacokinetics for therapy. *Cancer Res.* **2007**, *67*, 718-726.

71. Hamers-casterman, C.; Atarhouch, T.; Muyldermans, S.; Robinson, G.; Hamers, C.; Songa, E. B. et al. Naturally occurring antibodies devoid of light chains. *Nature.* **1993**, *363*, 446-8.

72. Saerens, D.; Kinne, J.; Bosmans, E.; Wernery, U.; Muyldermans, S.; Conrath, K. Single domain antibodies derived from dromedary lymph node and peripheral blood lymphocytes sensing conformational variants of prostate-specific antigen. *J Biol Chem.* **2004**, *279*, 51965-51972.

73. Reusch, D.; Haberger, M.; Falck, D.; Peter, B.; Maier, B.; Gassner, J. et al. Comparison of methods for the analysis of therapeutic immunoglobulin G Fc-glycosylation profiles-Part 2: Mass spectrometric methods. *MAbs.* **2015**, *7(4)*, 732-742. doi: 10.1080/19420862.2015.1045173.

74. Planinc, A.; Dejaegher, B.; Heyden, Y. V.; Viaene, J.; Van Praet, S.; Rappez, F. et al. LC-MS analysis combined with principal component analysis and soft independent modelling by class analogy for a better detection of changes in N-glycosylation profiles of therapeutic glycoproteins. *Anal Bioanal Chem.* **2017**, *409(2)*, 477-485. doi: 10.1007/s00216-016-9683-9.

75. Trimble, R. B.; Maley, F. Optimizing hydrolysis of N-linked high-mannose oligosaccharides by endo-beta-N-acetylglucosaminidase H. *Anal Biochem.* **1984**, *141(2)*, 515-522.

76. Takahashi, N.; Nishibe, H. Some characteristics of a new glycopeptidase acting on aspartylglycosylamine linkages. *J Biochem.* **1978**, *84(6)*,1467-73.

77. Ishihara, H.; Takahashi, N.; Ito, J.; Takeuchi, E.; Tejima, S. Either high-mannose-type or hybrid-type oligosaccharide is linked to the same asparagine residue in ovalbumin. *Biochim Biophys Acta.* **1981**, *669(2)*, 216-21.

78. Maley, F.; Trimble, R. B.; Tarentino, A. L.; Plummer, T. H. Characterization of glycoproteins and their associated oligosaccharides through the use of endoglycosidases. *Anal Biochem.* **1989**, *180(2)*, 195-204.

79. Kolarich, D.; Altmann, F. N-Glycan analysis by matrix-assisted laser desorption/ionization mass spectrometry of electrophoretically separated nonmammalian proteins: application to peanut allergen Ara h 1 and olive pollen allergen Ole e 1. *Anal Biochem.* **2000**, *285(1)*, 64-75.

80. Triguero, A.; Cabrera, G.; Royle, L.; Harvey, D. J.; Rudd, P. M.; Dwek, R. A. et al. Chemical and enzymatic N-glycan release comparison for N-glycan profiling of monoclonal antibodies expressed in plants. *Anal Biochem.* **2010**, *400(2)*, 173-83.

81. Zauner, G.; Selman, M. H.; Bondt, A.; Blank, D.; Deelder, A. M. et al. Glycoproteomic analysis of antibodies. *Mol Cell Proteomics.* **2013**, *12(4)*, 856-865.

82. Komatsu, E.; Buist, M.; Roy, R.; Gomes de Oliveira, A. G.; Bodnar, E.; Salama, A. et al. Characterization of immunoglobulins through analysis of N-glycopeptides by MALDI-TOF MS. Methods. **2016**, *104*, 170-181.

83. Wuhrer, M.; Stam, J. C.; Van de geijn, F. E.; Koeleman, C. A.; Verrips, C. T.; Dolhain, R. J. et al. Glycosylation profiling of immunoglobulin G (IgG) subclasses from human serum. Proteomics. **2007**, 7(22), 4070-4081.

84. Merrifield, R. B. Solid Phase Peptide Synthesis. I. The Synthesis of a Tetrapeptide. *J. Am. Chem. Soc.* **1963**, *85(14)*, 2149–2154. doi: 10.1021/ja00897a025

85. Schnölzer, M.; Alewood, P.; Jones, A.; Alewood, D.; Kent, S. B. In situ neutralization in Boc-chemistry solid phase peptide synthesis. Rapid, high yield assembly of difficult sequences. *Int J Pept Protein Res*. **1992**, *40(3-4)*, 180-93.

86. Carpino, L. A.; Han, Y. G. 9-Fluorenylmethoxycarbonyl function, a new base-sensitive amino-protecting group. *J. Am. Chem. Soc.* **1970**, *92 (19)*, 5748–5749. doi: 10.1021/ja00722a043

87. Stavenhagen, K.; Hinneburg, H.; Thaysen-andersen, M.; Hartmann, L.; Varón Silva, D.; Fuchser, J, et al. Quantitative mapping of glycoprotein micro-heterogeneity and macro-heterogeneity: an evaluation of mass spectrometry signal strengths using synthetic peptides and glycopeptides. *J Mass Spectrom.* **2013**, *48(6)*, 627-39. doi: 10.1002/jms.3210.

88. Kurogochi, M.; Amano, J. Relative quantitation of glycopeptides based on stable isotope labeling using MALDI-TOF MS. *Molecules.* **2014**, *19(7)*, 9944-9961.

89. Jansen, B. C.; Falck, D.; de Haan, N.; Hipgrave Ederveen, A. L.; Razdorov, G.; Lauc, G. et al. LaCyTools: A Targeted Liquid Chromatography-Mass Spectrometry Data Processing Package for Relative Quantitation of Glycopeptides. *J. Proteome Res.* **2016**, *15(7)*, 2198-2210.

doi: 10.1021/acs.jproteome.6b00171.

90. Yuan, W.; Sanda, M.; Wu, J.; Koomen, J.; Goldman, R. Quantitative analysis of immunoglobulin subclasses and subclass specific glycosylation by LC-MS-MRM in liver disease. *J Proteomics.* **2015**, *116*, 24-33. doi: 10.1016/j.jprot.2014.12.020.

91. Remily-Wood, E. R.; Benson, K.; Baz, R. C.; Chen, Y. A.; Hussein, M.; Hartley-Brown, M. A. et. al. Quantification of Peptides from Immunoglobulin Constant and Variable Regions by Liquid Chromatography-Multiple Reaction Monitoring Mass Spectrometry for Assessment of Multiple Myeloma Patients. *Proteomics. Clinical Applications*, **2014**, *8*, 783–795. doi:10.1002/prca. 201300077

92. Pan, S.; Chen, R.; Aebersold, R.; Brentnall, T. A. Mass spectrometry based glycoproteomics--from a proteomics perspective. Mol Cell Proteomics. 2011, 10(1), R110.003251. doi: 10.1074/mcp. R110.003251.

93. Dell, A.; Reason, J. A.; Khoo, K.; Panico, M., McDowell, R. A.; Morris, H. R. Mass spectrometry of carbohydrate-containing biopolymers. *Methods Enzymmol.* **1994**, *230*, 108-132

94. Karas, M.; Hillenkamp, F. Laser desorption ionization of proteins with molecular masses exceeding 10,000 daltons. *Anal Chem.* **1988**, *60(20)*, 2299-301.

95. Mamyrin, B. A.; Karataev, V. I, Shmikk, D. V.; Zagulin, V. A. The mass-reflectron, a new nonmagnetic time-of-flight mass spectrometer with high resolution. *Journ. Phys. JETP*, **1973**, *37(1)*, 82

96. https://www.abrf.org/ABRFNews/1997/June1997/jun97lennon.html

97. Xia, B.; Feasley, C. L.; Sachdev, G. P.; Smith, D. F.; Cummings, R. D. Glycan reductive isotope labeling for quantitative glycomics. *Anal Biochem.* **2009**, *387(2),* 162-70. doi: 10.1016/j.ab. 2009.01.028.

98. Roepstorff, P.; Fohlman, J. Proposal for a common nomenclature for sequence ions in mass spectra of peptides. *Biomed Mass Spectrom.* **1984**, *11(11),* 601.

99. Biemann, K. Appendix 5. Nomenclature for peptide fragment ions (positive ions). *Meth Enzymol.* 1990, *193,* 886-867.

100. Biemann, K. Contributions of mass spectrometry to peptide and protein structure. *Biomed Environ Mass Spectrom.* **1988**, *16(1-12),* 99-111.

101. Stimson, E.; Hope, J.; Chong, A.; Burlingame, A. L. Site-specific characterization of the N-linked glycans of murine prion protein by high-performance liquid chromatography/electrospray mass spectrometry and exoglycosidase digestions. *Biochemistry.* **1999**, *38(15),* 4885-4895.

102. Harazono, A.; Kawasaki, N.; Itoh, S.; Hashii, N.; Ishii-Watabe, A.; Kawanishi, T. et al. Site-specific N-glycosylation analysis of human plasma ceruloplasmin using liquid chromatography with electrospray ionization tandem mass spectrometry. *Anal Biochem.* **2006**, *348(2),* 259-68.

103. Nimtz, M.; Conradt, H. S.; Mann, K. LacdiNAc (GalNAcbeta1-4GlcNAc) is a major motif in N-glycan structures of the chicken eggshell protein ovocleidin-116. *Biochim Biophys Acta.* **2004**, *1675(1-3*), 71-80.

104. Henriksson, H.; Denman, S. E.; Campuzano, I. D.; Ademark, P.; Master, E. R.; Teeri, T. T. et al. N-linked glycosylation of native and recombinant cauliflower xyloglucan endotransglycosylase 16A. *Biochem J.* **2003**, *375(1),* 61-73.

105. Nemeth, J. F.; Hochgesang, G. P.; Marnett, L. J.; Caprioli, R. M.; Hochensang, G. P. Characterization of the glycosylation sites in cyclooxygenase-2 using mass spectrometry. *Biochemistry*. **2001**, *40(10)*, 3109-16.

106. Hui, J. P.; White, T. C.; Thibault, P. Identification of glycan structure and glycosylation sites in cellobiohydrolase II and endoglucanases I and II from Trichoderma reesei. *Glycobiology*. **2002**, *12(12)*, 837-49.

107. Zeng, R.; Xu, Q.; Shao, X. X.; Wang, K. Y.; Xia, Q. C. Characterization and analysis of a novel glycoprotein from snake venom using liquid chromatography-electrospray mass spectrometry and Edman degradation. *Eur J Biochem.* **1999**, *266(2)*, 352-8.

108. Batamenab, K. P.; Whitea, R. L.; Yaguchic, M.; Thibaultb, P. Characterization of protein glycoforms by capillary-zone electrophoresis–nanoelectrospray mass spectrometry. *J. Chromatpgraph.* **1998**, *794 (1-2)*, 327-344.

109. Zhu, X.; Borchers, C.; Bienstock, R. J.; Tomer, K. B. Mass spectrometric characterization of the glycosylation pattern of HIV-gp120 expressed in CHO cells. *Biochemistry*. **2000**, *39(37)*, 11194-11204.

110. Krokhin, O.; Ens, W.; Standing, K. G.; Wilkins, J.; Perreault, H. Site-specific N-glycosylation analysis: matrix-assisted laser desorption/ionization quadrupole-quadrupole time-of-flight tandem mass spectral signatures for recognition and identification of glycopeptides. *Rapid Commun. Mass Spectrom*,**2004**, *18*, 2020–2030. doi:10.1002/rcm.1585.

111. http://www.biology.arizona.edu/immunology/tutorials/immunology/humoral.html

112. http://www.sigmaaldrich.com

113. http://www.chemsynthesis.com

114. https://www.promega.ca/-/media/files/resources/protocols/technical-bulletins/101/trypsin-gold-mass-spectrometry-grade-protocol.pdf

115. https://chemtips.wordpress.com/tag/chloranil/

116. http://www.sigmaaldrich.com/catalog/product/aldrich

117. Amblard, M.; Fehrentz, J. A.; Martinez, J.; Subra, G. Methods and protocols of modern solid phase peptide synthesis. *Mol Biotechnol.* **2006**, *33(3)*, 239-54.

118. Pratt, M. R.; Bertozzi, C. R. Chemoselective ligation applied to the synthesis of a biantennary N-linked glycoform of CD52. *J Am Chem Soc.* **2003**, *125(20)*, 6149-59. (6)

119. Madadkar, P.; Sadavarte, R.; Butler, M.; Durocher, Y.; Ghosh, R. Preparative separation of monoclonal antibody aggregates by cation-exchange laterally-fed membrane chromatography. *J Chromatogr B Analyt Technol Biomed Life Sci.* **2017**, *1055-1056*, 158-164.

120. Bodnar, E.; Nascimento, T.; Girard, L.; Komatsu, E.; Lopez, P.; Gomes de Oliveira, A.et al. An integrated approach to analyze EG2-hFc monoclonal antibody N-glycosylation by MALDI-MS. *Can J Chem.* **2015**, *93*, 754-763.

121. Villacrés, C.; Tayi, V. S.; Lattová, E.; Perreault, H.; Butler, M. Low glucose depletes glycan precursors, reduces site occupancy and galactosylation of a monoclonal antibody in CHO cell culture. *Biotechnol J.* **2015**, *10(7)*, 1051-1066. doi: 10.1002/biot.201400662.

122. https://www.anaspec.com/html/peptidenotes.html

123. http://www.sigmaaldrich.com/technical documents/articles/biology/glycobiology /endoglycosidases.html

124. www.uniprotkb.com

125. Jacobs, J. F, Wevers, R. A., Lefeber, D. J., van Secherpenzeel, M. (2016). Fast, robust and high-resolution glycosylation profiling of intact monoclonal IgG antibodies using nanoLC-chip-QTOF. *Clin Chim Acta, International Journal of Clinical Chemistry, 461:*90-97. doi: 10.1016/j.cca.2016.07.015

126. Han, M., Rock, B. M., Pearson, J. T., Rock, D. A. (2016). Intact mass analysis of monoclonal antibodies by capillary electrophoresis-Mass spectrometry. *J Chromatogr B Analyt Technol Biomed Life Sci. 1011:*24-32. doi: 10.1016/j.jchromb.2015.12.045.

127. http://www.sigmaaldrich.com/content/dam/sigma-aldrich/does/sigma-aldrich/productinformation%20sheet/%20t3754%20pis.pdf

128. http://www.sigmaaldrich.com/content/dam/sigma-aldrich/does/sigma-aldrich/productinformation%20sheet/%20t2126%20pis.pdf

129. Krokhin, O.V. Sequence-specific retention calculator. Algorithm for peptide retention prediction in ion-pair RP-HPLC: application to 300- and 100-A pore size C18 sorbents. *Analytical chemistry*, **2006,** *78*, 7785-7795

130. Butler, J. E.; Wertz, N.; Deschacht, N.; Kacskovics, I. Porcine IgG: structure, genetics, and evolution. *Immunogenetics*. **2009**, *61(3)*, 209-230. doi: 10.1007/s00251-008-0336-9.

131. Butler, J. E. Immunoglobulin gene organization and the mechanism of repertoire development. *Scand J Immunol.* **1997**, *45(5)*, 455-462.

132. Lopez, P.G.; Girard, L.; Buist, M.; de Oliveira A. G.; Bodnar, E.; Salama, A. et al.

Characterization of N-glycosylation and amino acid sequence features of immunoglobulins from swine. Glycoconj J. **2016**, *33(1)*, 79-91. doi: 10.1007/s10719-015-9637-z.

133. Lorusso, A.; Vincent, A. L.; Gramer, M. R.; Lager, K. M.; & Ciacci-Zanella, J. R. Contemporary epidemiology of north American lineage triple reassortant influenza A viruses in pigs. *Curr. Top. Microbiol Immunol.* **2013**, *370*, 113-131. doi: 10.1007/82-2011-196

134. Vincent, A.L.; Lager, K. M.; Ma, W.; Lekcharoensuk, P.; Gramer, M. R.; Loiacono, C. et al. Evaluation of hemagglutinin subtype 1 swine influenza viruses from the United States. *Vet Microbiol.* **2006**, *118(3-4)*, 212-22.

135. Auchincloss, H.; Sachs, D. H. Xenogeneic transplantation. *Annu Rev Immunol.***1998**, *16*, 433-470.

136. Waltz, E. Polyclonal antibodies step out of the shadows. *Nat Biotechnol.* **2006**, *24(10)*,1181.

137. http://nptel.ac.in/courses/102103044/module2/lec11/6.html

138. Berg, M. J.; Blaise, A. C. Structure-Based Thermodynamics Analysis of a Coupled Metal Binding-Protein Folding Reaction Involving a Zinc Finger Peptide. *Biochem.* **2002,** *41* (50), 15068-15073. doi: 10.1021/bi026621h

139. Dass, C. *Principles and practice of biological mass spectrometry.* Wiley: New York, 2001; Vol. 27, pp 416.

140. http://www.uniprot.org/help/carbohyd

141. Dumoulin, M.; Conrath, K.; Van, M. A. et al. Single-domain antibody fragments with high conformational stability. *Protein Science.* **2002**, *11(3)*, 500-515. doi: 10.1110/ps.34602

142. Harmsen, M. M.; Van Solt, C. B.; Van Zijderveld-van Bemmel, A. M.; Niewold, T. A.; Van Zijderveld, F. G. Selection and optimization of proteolytically stable llama single-domain antibody fragments for oral immunotherapy. *Appl. Microbiol. Biotechnol.* **2006**, Vol.72(3), pp 544-551.